

# Radiative charmless $B_{(s)} \rightarrow V\gamma$ and $B_{(s)} \rightarrow A\gamma$ decays in pQCD approach

Wei Wang<sup>a</sup>, Run-Hui Li<sup>b,a</sup> and Cai-Dian Lü<sup>a</sup>

<sup>a</sup> *Institute of High Energy Physics, P.O. Box 918(4) Beijing 100049, P.R. China*

<sup>b</sup> *Department of Physics, Shandong University, Jinan 250100, P.R. China*

<sup>c</sup> *Graduate University of Chinese Academy of Sciences, Beijing 100049, P.R. China*

We study the radiative charmless  $B_{(s)} \rightarrow V(A)\gamma$  decays in perturbative QCD (pQCD) approach to the leading order in  $\alpha_s$  (here  $V$  and  $A$  denotes vector mesons and two kinds of axial-vector mesons:  $^3P_1$  and  $^1P_1$  states, respectively.). Our predictions of branching ratios are consistent with the current available experimental data. We update all  $B_{(s)} \rightarrow V$  form factors and give the predictions for  $B \rightarrow A$  form factors using the recent hadronic inputs. In addition to the dominant factorizable spectator diagrams, which is form factor like, we also calculate the so-called “power suppressed” annihilation type diagrams, the gluonic penguin, charming penguin, and two photon diagrams. These diagrams give the main contributions to direct CP asymmetries, mixing-induced CP asymmetry variables, the isospin asymmetry and U-spin asymmetry variables. Unlike the branching ratios, these ratios or observables possess higher theoretical precision in our pQCD calculation, since they do not depend on the input hadronic parameters too much. Most of the results still need experimental tests in the on-going and forthcoming experiments.

## I. INTRODUCTION

Present studies on  $B$  decays are mainly concentrated on the precise test of standard model (SM) and the search for signals of possible new physics. Radiative processes  $b \rightarrow s\gamma$  and  $b \rightarrow d\gamma$  are among the most ideal probes and thus have received considerable efforts [1]. In the standard model, these processes are induced by the flavor-changing-neutral-current transitions which are purely loop effects. Such decays are rare and the measurement of parameters in these channels, especially the CP asymmetry variables, may shed light on detailed information on the flavor structure of the electroweak interactions. This predictive power relies on the accuracy of both the experimental side and the theoretical side. Thanks to the technique of operator-product-expansion, remarkable theoretical progress has been made in the SM to the next-to-next-to-leading order accuracy [2]. Compared with experimental results [3], the theoretical prediction is consistent with but  $1.2\sigma$  below the experimental data [4]. This consistence could certainly provide a rather stringent constraint on non-standard model scenarios.

Compared with inclusive processes, the exclusive processes  $B \rightarrow V\gamma$  is more tractable on the experimental side, but more difficult on the theoretical side. Theoretical predictions are often hampered by our ability to calculate the decay amplitude  $\langle V\gamma|O_i|B\rangle$ , where  $O_i$  is a magnetic moment or a four-quark operator. We have to use some non-perturbative hadronic quantities to describe the bound state effects. In the heavy-quark limit, the non-perturbative contributions can be organized in a universal and channel-independent manner. Factorization analysis, the separation of the short-distance and long-distance dynamics, can give many important predictions.

The dominant contribution to the radiative decay amplitudes is proportional to the transition form factor. Different treatments on the dynamics in form factor  $F^{B \rightarrow V}$  result in different explicit approaches. There are many approaches such as Lattice QCD (LQCD) [5], light-front quark model (LFQM) [6, 7] and light-cone sum rules (LCSR) [8]. Recently three commonly-accepted approaches are developed to study exclusive  $B$  decays: QCD factorization (QCDF) [9], soft collinear effective theory (SCET) [10] and perturbative QCD approach [11]. In pQCD approach, the recoiling meson moves on the light-cone and a large momentum transfer is required. Keeping quarks' transverse momentum, pQCD approach is free of endpoint divergence and the Sudakov formalism makes it more self-consistent. It has been successfully applied to various decay channels and quite recently this approach is accessing to next-to-leading order accuracy [12]. A bigger advantage is that we can really do the form factor calculation and the quantitative annihilation type diagram calculation in this approach. The importance of annihilation diagrams are already tested in the predictions of

direct CP asymmetries in  $B^0 \rightarrow \pi^+\pi^-$ ,  $K^+\pi^-$  decays [11, 13] and in the explanation of  $B \rightarrow \phi K^*$  polarization problem [14, 15]. These “power suppressed” contributions are the main source of isospin symmetry breaking (or SU(3) breaking) effects in radiative decays  $B \rightarrow V\gamma$  [16, 17].

Some of charmless  $B \rightarrow V\gamma$  decay channels have been studied in pQCD approach [16, 17, 18] separately. According to the transition at the quark level, all the 10 decay channels can be divided into three different groups:  $b \rightarrow s$ ,  $b \rightarrow d$  and purely annihilation type. The two  $B \rightarrow K^*\gamma$  modes ( $b \rightarrow s$  process) have been well measured experimentally. The agreement of pQCD approach results and experimental data [3] is very encouraging. In this paper, we study all those channels including the corresponding  $B_s$  decays in a comprehensive way. The input hadronic parameters will be chosen the same as that in Ref. [19]. We also updated all the  $B \rightarrow V$  decay form factors in pQCD approach [20]. Despite branching ratios and CP asymmetry parameters which heavily depend on the input parameters, we also study some ratios characterizing the isospin and SU(3) breaking effects, where most of the uncertainties cancel. Experimental measurements of these quantities will prove a good test of our theory, since different method gives different prediction. With the ongoing  $B$  factories BaBar and Belle, the  $B$ -Physics program on CDF and the onset of the LHC experiments, as well as the Super B-factories being contemplated for the future, we expect a wealth of data involving these decays.

Although experimentalists have already measured one channel of the  $B \rightarrow A\gamma$  decays [21], there are not many discussions on the theoretical side. The pQCD study on  $B \rightarrow V\gamma$  can be straightforward extended to radiative processes involving higher resonants such as  $K_1(1270)$ ,  $K_1(1400)$ . In the quark model, the quantum numbers  $J^{PC}$  for the orbitally excited axial-vector mesons are  $1^{++}$  or  $1^{+-}$ , depending on different spins of the two quarks. In SU(3) limit, these mesons can not mix with each other; but since the  $s$  quark is heavier than  $u, d$  quarks,  $K_1(1270)$  and  $K_1(1400)$  are not purely  $1^3P_1$  or  $1^1P_1$  states. These two mesons are believed to be mixtures of  $K_{1A}$  and  $K_{1B}$ , where  $K_{1A}$  and  $K_{1B}$  are  $3P_1$  and  $1P_1$  states, respectively. In general, the mixing angle can be determined by experimental data. But unfortunately, there is not too much data on the mixing of these mesons which leaves the mixing angle much free. Analogous to  $\eta$  and  $\eta'$ , the flavor-singlet and flavor-octet axial-vector meson can also mix with each other. Using those hadronic parameters determined in  $B \rightarrow V\gamma$  decays, the production of  $A\gamma$  in  $B$  decays could provide a unique insight to these mysterious axial-vector mesons.

This paper is organized as follows: In section II, we briefly review pQCD approach with the operator basis used subsequently. Some input quantities which enter pQCD approach, wave function of the  $B$ -meson, distribution amplitudes for light vector mesons, and for light axial-vector

mesons and input values of the various mesonic decay constants, are also given here. In section III, we give the factorization formulae and the numerical results for  $B \rightarrow V$  and  $B \rightarrow A$  form factors. Section IV contains the calculation of  $B \rightarrow V\gamma$  decays, making explicit the contributions from the electromagnetic dipole operator, the chromo-magnetic moment operator, some higher order ( $\mathcal{O}(\alpha_s)$ ) corrections from tree operators, the contribution from two-photon diagrams, the tree operator annihilation diagrams and penguin operator annihilation diagrams. Numerical results for the charge-conjugated averages of decay branching ratios are given in comparison with the corresponding numerical results obtained in QCDF approach and SCET, as well as the available experimental data. We also give direct CP-asymmetries, time-dependent CP asymmetries  $S_f$  and observables  $H_f$  (for  $B_s$  system) in the time-dependent decay rates in this section. In section V, we study  $B \rightarrow A\gamma$  decays by predicting branching ratios and direct CP asymmetries. Our summary is given in the last section. Some functions are relegated to the appendix: appendix A contains the various functions that enter the factorization formulae in the pQCD approach; appendix B and C give the analytic formulae for the  $B \rightarrow V\gamma$  and  $B \rightarrow A\gamma$  decays used in numerical calculations, respectively.

## II. FORMALISM OF PQCD APPROACH

### A. Notations and conventions

We specify the weak effective Hamiltonian which describes  $b \rightarrow D$  ( $D = d, s$ ) transitions [22]:

$$\mathcal{H}_{eff} = \frac{G_F}{\sqrt{2}} \left\{ \sum_{q=u,c} V_{qb} V_{qD}^* [C_1(\mu) O_1^q(\mu) + C_2(\mu) O_2^q(\mu)] - V_{tb} V_{tD}^* \left[ \sum_{i=3}^{10,7\gamma,8g} C_i(\mu) O_i(\mu) \right] \right\} + \text{H.c.}, \quad (1)$$

where  $V_{qb(D)}$  and  $V_{tb(D)}$  are Cabibbo-Kobayashi-Maskawa (CKM) matrix elements. Functions  $O_i$  ( $i = 1, \dots, 10, 7\gamma, 8g$ ) are local four-quark operators or the moment type operators:

- current-current (tree) operators

$$O_1^q = (\bar{q}_\alpha b_\beta)_{V-A} (\bar{D}_\beta q_\alpha)_{V-A}, \quad O_2^q = (\bar{q}_\alpha b_\alpha)_{V-A} (\bar{D}_\beta q_\beta)_{V-A}, \quad (2)$$

- QCD penguin operators

$$O_3 = (\bar{D}_\alpha b_\alpha)_{V-A} \sum_{q'} (\bar{q}'_\beta q'_\beta)_{V-A}, \quad O_4 = (\bar{D}_\beta b_\alpha)_{V-A} \sum_{q'} (\bar{q}'_\alpha q'_\beta)_{V-A}, \quad (3)$$

$$O_5 = (\bar{D}_\alpha b_\alpha)_{V-A} \sum_{q'} (\bar{q}'_\beta q'_\beta)_{V+A}, \quad O_6 = (\bar{D}_\beta b_\alpha)_{V-A} \sum_{q'} (\bar{q}'_\alpha q'_\beta)_{V+A}, \quad (4)$$

- electro-weak penguin operators

$$O_7 = \frac{3}{2}(\bar{D}_\alpha b_\alpha)_{V-A} \sum_{q'} e_{q'} (\bar{q}'_\beta q'_\beta)_{V+A}, \quad O_8 = \frac{3}{2}(\bar{D}_\beta b_\alpha)_{V-A} \sum_{q'} e_{q'} (\bar{q}'_\alpha q'_\beta)_{V+A}, \quad (5)$$

$$O_9 = \frac{3}{2}(\bar{D}_\alpha b_\alpha)_{V-A} \sum_{q'} e_{q'} (\bar{q}'_\beta q'_\beta)_{V-A}, \quad O_{10} = \frac{3}{2}(\bar{D}_\beta b_\alpha)_{V-A} \sum_{q'} e_{q'} (\bar{q}'_\alpha q'_\beta)_{V-A}, \quad (6)$$

- magnetic moment operators

$$O_{7\gamma} = -\frac{e}{4\pi^2} \bar{D}_\alpha \sigma^{\mu\nu} (m_D P_L + m_b P_R) b_\alpha F_{\mu\nu}, \quad O_{8g} = -\frac{g}{4\pi^2} \bar{D}_\alpha \sigma^{\mu\nu} (m_D P_L + m_b P_R) T_{\alpha\beta}^a b_\beta G_{\mu\nu}^a \quad (7)$$

where  $\alpha$  and  $\beta$  are color indices and  $q'$  are the active quarks at the scale  $m_b$ , i.e.  $q' = (u, d, s, c, b)$ . The left handed current is defined as  $(\bar{q}'_\alpha q'_\beta)_{V-A} = \bar{q}'_\alpha \gamma_\nu (1 - \gamma_5) q'_\beta$  and the right handed current  $(\bar{q}'_\alpha q'_\beta)_{V+A} = \bar{q}'_\alpha \gamma_\nu (1 + \gamma_5) q'_\beta$ . The projection operators are defined as  $P_L = (1 - \gamma_5)/2$  and  $P_R = (1 + \gamma_5)/2$ . The combinations  $a_i$  of Wilson coefficients are defined as usual [23]:

$$a_1 = C_2 + C_1/3, \quad a_2 = C_1 + C_2/3, \quad a_3 = C_3 + C_4/3, \quad a_4 = C_4 + C_3/3, \quad a_5 = C_5 + C_6/3, \\ a_6 = C_6 + C_5/3, \quad a_7 = C_7 + C_8/3, \quad a_8 = C_8 + C_7/3, \quad a_9 = C_9 + C_{10}/3, \quad a_{10} = C_{10} + C_9/3. \quad (8)$$

For the explicit formulae, we will consider  $\bar{B}$  meson decays and use light-cone coordinates to describe the momentum:

$$p = (p^+, p^-, \vec{p}_T) = \left( \frac{p^0 + p^3}{\sqrt{2}}, \frac{p^0 - p^3}{\sqrt{2}}, \vec{p}_T \right). \quad (9)$$

where  $\vec{p}_T = (p^1, p^2)$ . In the  $\bar{B}$  meson rest frame, momenta of  $\bar{B}$  meson, vector (axial-vector) meson and the photon are chosen as:

$$P_1 = \frac{m_B}{\sqrt{2}}(1, 1, \vec{0}_T), \quad P_2 = \frac{m_B}{\sqrt{2}}(0, 1, \vec{0}_T), \quad P_\gamma = \frac{m_B}{\sqrt{2}}(1, 0, \vec{0}_T), \quad (10)$$

where the vector (axial-vector) is mainly moving on the minus direction  $n_-$  and the photon is moving on the plus direction  $n_+$ . Longitudinal momenta fractions of the spectator anti-quarks in  $\bar{B}$  and final state meson are chosen as  $x_1 = k_1^+/P_1^+$  and  $x_2 = k_2^-/P_2^-$ .<sup>1</sup> Including the transverse components, the momenta of these spectator antiquarks are expressed by:

$$k_1 = \left( \frac{m_B}{\sqrt{2}} x_1, 0, \vec{k}_{1T} \right), \quad k_2 = \left( 0, \frac{m_B}{\sqrt{2}} x_2, \vec{k}_{2T} \right), \quad (11)$$

---

<sup>1</sup> One should be cautious that in the discussion of light cone distribution amplitudes (LCDAs) for the vectors and axial-vectors,  $x$  is defined as the momentum fraction of the positive quark which is different with our definition here.

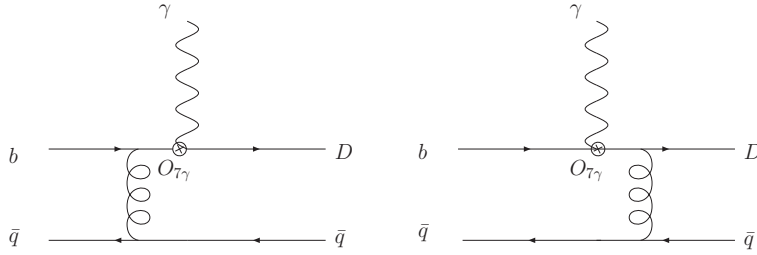


FIG. 1: Feynman diagrams of the electromagnetic penguin operator  $O_{\tau\gamma}$

then the  $b$  and  $D(=s, d)$  quark momenta are  $p_b = P_1 - k_1$  and  $p_D = P_2 - k_2$ . For convenience, we can define the following useful ratio variables:

$$r_b = \frac{m_b}{m_B}, \quad r_D = \frac{m_D}{m_B}, \quad r_V = \frac{m_V}{m_B}, \quad r_A = \frac{m_A}{m_B}, \quad (12)$$

where  $m_D$  and  $m_{V(A)}$  are masses for the  $d(s)$  quark and the vector (axial-vector) meson, respectively. In the calculation of decay amplitudes, we will only keep terms of leading order in  $r_V$  but we will consider the corrections together with kinematic corrections in the phase space as in Eq. (87).

According to the Lorentz structure, decay amplitudes from various operators can be generally decomposed into scalar and pseudoscalar components as:

$$\mathcal{M} = (\epsilon_\gamma^* \cdot \epsilon_V^*) \mathcal{M}^S + i \epsilon_{\mu\nu\alpha\beta} \epsilon_\gamma^{*\mu} \epsilon_V^{*\nu} n_+^\alpha n_-^\beta \mathcal{M}^P, \quad (13)$$

and where we adopt the convention  $\epsilon^{0123} = +1$ . In order to study mixing-induced CP asymmetries, it is convenient to separate different chiralities in the amplitudes. If the emitted photon is left-handed, the relationship between the scalar  $\mathcal{M}^S$  and pseudoscalar component  $\mathcal{M}^P$  is required as

$$\mathcal{M}^S = -\mathcal{M}^P \equiv \frac{1}{2} \mathcal{M}^L, \quad (14)$$

while the condition

$$\mathcal{M}^S = \mathcal{M}^P \equiv \frac{1}{2} \mathcal{M}^R, \quad (15)$$

is required for the right-handed photon.

## B. A brief review of pQCD approach

The basic idea of pQCD approach is that it takes into account the intrinsic transverse momentum of valence quarks. The decay amplitude, taking the first diagram in Fig. 1 as an example, can

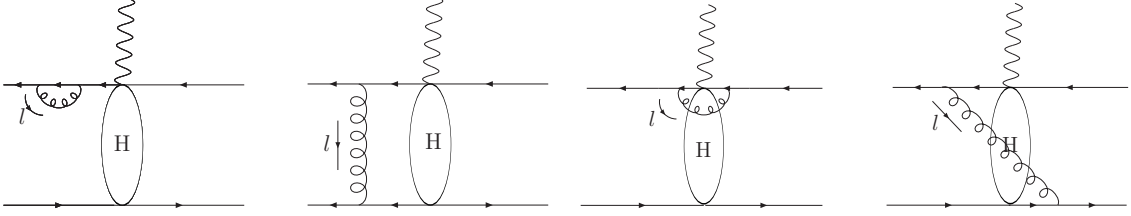


FIG. 2:  $O(\alpha_s)$  corrections to the hard scattering kernel  $H$ .

be expressed as a convolution of wave functions  $\phi_B$ ,  $\phi_V$  and hard scattering kernel  $T_H$  by both longitudinal and transverse momenta:

$$\mathcal{M} = \int_0^1 dx_1 dx_2 \int \frac{d^2 \vec{k}_{1T}}{(2\pi^2)} \frac{d^2 \vec{k}_{2T}}{(2\pi^2)} \phi_B(x_1, \vec{k}_{1T}, p_1, t) T_H(x_1, x_2, \vec{k}_{1T}, \vec{k}_{2T}, t) \phi_V(x_2, \vec{k}_{2T}, p_2, t). \quad (16)$$

Usually it is convenient to compute the amplitude in coordinate space. Through Fourier transformation, the above equation can be expressed by:

$$\mathcal{M} = \int_0^1 dx_1 dx_2 \int d^2 \vec{b}_1 d^2 \vec{b}_2 \phi_B(x_1, \vec{b}_1, p_1, t) T_H(x_1, x_2, \vec{b}_1, \vec{b}_2, t) \phi_V(x_2, \vec{b}_2, p_2, t). \quad (17)$$

This derivation is mainly concentrated on tree level diagrams, but actually we have to take into account some loop effects which can give sizable corrections. The  $\mathcal{O}(\alpha_s)$  radiative corrections to hard scattering process  $H$  are depicted in Fig. 2. In general, individual higher order diagrams may suffer from two types of infrared divergences: soft and collinear. Soft divergence comes from the region of a loop momentum where all its momentum components vanish:

$$l^\mu = (l^+, l^-, \vec{l}_T) = (\Lambda, \Lambda, \vec{\Lambda}), \quad (18)$$

where  $\Lambda$  is the typical scale for hadronization. Collinear divergence originates from the gluon momentum region which is parallel to the massless quark momentum,

$$l^\mu = (l^+, l^-, \vec{l}_T) \sim (m_B, \Lambda^2/m_B, \vec{\Lambda}). \quad (19)$$

In both cases, the loop integration corresponds to  $\int d^4 l/l^4 \sim \log \Lambda$ , thus logarithmic divergences are generated. It has been shown order by order in perturbation theory that these divergences can be separated from the hard kernel and absorbed into meson wave functions using eikonal approximation [24]. But when soft and collinear momentum overlap, there will be double logarithm divergences in the first two diagrams of Fig. 2. These large double logarithm can be resummed into the Sudakov factor whose explicit form is given in Appendix A.

Furthermore, there are also another type of double logarithm which comes from the loop correction for the weak decay vertex correction. The left diagram in Fig. 1 gives an amplitude proportional

to  $1/(x_2^2 x_1)$ . In the threshold region with  $x_2 \rightarrow 0$  [(to be precise,  $x_2 \sim O(\Lambda_{QCD}/m_B)$ ), additional soft divergences are associated with the internal quark at higher orders. The QCD loop corrections to the electro-weak vertex can produce the double logarithm  $\alpha_s \ln^2 x_2$  and resummation of this type of double logarithms lead to the Sudakov factor  $S_t(x_2)$ . Similarly, resummation of  $\alpha_s \ln^2 x_1$  due to loop corrections in the other diagram leads to the Sudakov factor  $S_t(x_1)$ . These double logarithm can also be factored out from the hard part and grouped into the quark jet function. Resummation of the double logarithms results in the threshold factor [25]. This factor decreases faster than any other power of  $x$  as  $x \rightarrow 0$ , which modifies the behavior in the endpoint region to make pQCD approach more self-consistent. For simplicity, this factor has been parameterized in a form which is independent on channels, twists and flavors [26].

Combing all the elements together, we can get the typical factorization formulae in pQCD approach:

$$\begin{aligned} \mathcal{M} = & \int_0^1 dx_1 dx_2 \int d^2 \vec{b}_1 d^2 \vec{b}_2 (2\pi)^2 \phi_B(x_1, \vec{b}_1, p_1, t) \\ & \times T_H(x_1, x_2, Q, \vec{b}_1, \vec{b}_2, t) \phi_V(x_2, \vec{b}_2, p_2, t) S_t(x_2) \exp[-S_B(t) - S_2(t)]. \end{aligned} \quad (20)$$

### C. Wave functions of $B$ mesons

In order to calculate the analytic formulas of decay amplitudes, we will use light cone wave functions  $\Phi_{M,\alpha\beta}$  decomposed in terms of the spin structure. In general,  $\Phi_{M,\alpha\beta}$  with Dirac indices  $\alpha, \beta$  can be decomposed into 16 independent components,  $1_{\alpha\beta}, \gamma_5_{\alpha\beta}, \gamma_{\alpha\beta}^\mu, (\gamma^\mu \gamma_5)_{\alpha\beta}, \sigma_{\alpha\beta}^{\mu\nu}$ . If the considered meson is the  $B$  meson, a heavy pseudo-scalar meson, the  $B$  meson light-cone matrix element can be decomposed [27, 28, 29] by:

$$\begin{aligned} & \int d^4 z e^{ik_1 \cdot z} \langle 0 | b_\beta(0) \bar{D}_\alpha(z) | \bar{B}(P_B) \rangle \\ & = \frac{i}{\sqrt{2N_c}} \left\{ (P_B + m_B) \gamma_5 \left[ \phi_B(k_1) - \frac{\not{n} - \not{v}}{\sqrt{2}} \bar{\phi}_B(k_1) \right] \right\}_{\beta\alpha}, \end{aligned} \quad (21)$$

where  $N_c = 3$  is the color factor.  $n$  and  $v$  are two light-like vectors:  $n^2 = v^2 = 0$ . From equation (21), one can see that there are two Lorentz structures in the  $B$  meson distribution amplitudes. They obey the following normalization conditions:

$$\int \frac{d^4 k_1}{(2\pi)^4} \phi_B(k_1) = \frac{f_B}{2\sqrt{2N_c}}, \quad \int \frac{d^4 k_1}{(2\pi)^4} \bar{\phi}_B(k_1) = 0. \quad (22)$$

In general, one should consider these two Lorentz structures in the calculations of  $B$  meson decays. However, it is found that the contribution of  $\bar{\phi}_B$  is numerically small [20], thus its contribution can be safely neglected. With this approximation, we only retain the first term in the



square bracket from the full Lorentz structure in Eq. (21):

$$\Phi_B = \frac{i}{\sqrt{2N_c}} (\not{P}_B + m_B) \gamma_5 \phi_B(k_1). \quad (23)$$

In the following calculation, we will see that the hard part is always independent of one of the  $k_1^+$  and/or  $k_1^-$ . The  $B$  meson wave function is then a function of the variables  $k_1^-$  (or  $k_1^+$ ) and  $k_1$  only,

$$\phi_B(k_1^-, \vec{k}_{1T}) = \int \frac{dk_1^+}{2\pi} \phi_B(k_1^+, k_1^-, \vec{k}_{1T}). \quad (24)$$

In the  $b$ -space, the  $B$  meson's wave function can be expressed by

$$\Phi_B(x, b) = \frac{i}{\sqrt{2N_c}} [\not{P}_B \gamma_5 + m_B \gamma_5] \phi_B(x, b), \quad (25)$$

where  $b$  is the conjugate space coordinate of the transverse momentum  $k_T$ .

In this study, we use the following phenomenological wave function:

$$\phi_B(x, b) = N_B x^2 (1-x)^2 \exp \left[ -\frac{m_B^2 x^2}{2\omega_b^2} - \frac{1}{2} (\omega_b b)^2 \right], \quad (26)$$

with  $N_B$  the normalization factor. In recent years, a lot of studies have been performed for  $B_d^0$  and  $B^\pm$  decays in pQCD approach. The parameter  $\omega_b = (0.40 \pm 0.05)$  GeV has been fixed using the rich experimental data on  $B_d^0$  and  $B^\pm$  meson decays. In the SU(3) symmetry limit, this parameter should be the same in  $B_s$  decays. Considering a small SU(3) breaking,  $s$  quark momentum fraction should be a little larger than that of  $u$  or  $d$  quark in the lighter  $B$  mesons, since  $s$  quark is heavier than  $u$  or  $d$  quark. We will use  $\omega_b = (0.50 \pm 0.05)$  GeV in this paper for the  $B_s$  decays [19].

#### D. Light-cone distribution amplitudes of light vector mesons

Decay constants for vector mesons are defined by:

$$\langle 0 | \bar{q}_1 \gamma_\mu q_2 | V(p, \epsilon) \rangle = f_V m_V \epsilon_\mu, \quad \langle 0 | \bar{q}_1 \sigma_{\mu\nu} q_2 | V(p, \epsilon) \rangle = i f_V^T (\epsilon_\mu p_\nu - \epsilon_\nu p_\mu). \quad (27)$$

The longitudinal decay constants of charged vector mesons can be extracted from the data on  $\tau^- \rightarrow (\rho^-, K^{*-}) \nu_\tau$  [30]. Neutral vector meson's longitudinal decay constant can be determined by its electronic decay width through  $V^0 \rightarrow e^+ e^-$ <sup>2</sup> and results are given in Table I. Transverse decay constants are mainly explored by QCD sum rules [31] that are also collected in Table I.

<sup>2</sup> There is a recent study on extracting vectors' decay constants from experimental data, which has taken into account the effects of  $\rho^0$ - $\omega$  and  $\omega$ - $\phi$  mixing [31]. Since we do not consider the mixing for the decay amplitudes in our calculation, we will not use those values for self-consistence.

TABLE I: Input values of the decay constants for the vector mesons (in MeV)

$f_\rho$	$f_\rho^T$	$f_\omega$	$f_\omega^T$	$f_{K^*}$	$f_{K^*}^T$	$f_\phi$	$f_\phi^T$
$209 \pm 2$	$165 \pm 9$	$195 \pm 3$	$151 \pm 9$	$217 \pm 5$	$185 \pm 10$	$231 \pm 4$	$186 \pm 9$

We choose the vector meson momentum  $P$  with  $P^2 = m_V^2$ , which is mainly on the plus direction. The polarization vectors  $\epsilon$ , satisfying  $P \cdot \epsilon = 0$ , include one longitudinal polarization vector  $\epsilon_L$  and two transverse polarization vectors  $\epsilon_T$ . The vector meson distribution amplitudes up to twist-3 are defined by:

$$\begin{aligned} \langle V(P, \epsilon_L^*) | \bar{q}_{2\beta}(z) q_{1\alpha}(0) | 0 \rangle &= \frac{1}{\sqrt{2N_c}} \int_0^1 dx e^{ixP \cdot z} [m_V \not{\epsilon}_L^* \phi_V(x) + \not{\epsilon}_L^* \not{P} \phi_V^t(x) + m_V \phi_V^s(x)]_{\alpha\beta}, \\ \langle V(P, \epsilon_T^*) | \bar{q}_{2\beta}(z) q_{1\alpha}(0) | 0 \rangle &= \frac{1}{\sqrt{2N_c}} \int_0^1 dx e^{ixP \cdot z} [m_V \not{\epsilon}_T^* \phi_V^v(x) + \not{\epsilon}_T^* \not{P} \phi_V^T(x) \\ &\quad + m_V i \epsilon_{\mu\nu\rho\sigma} \gamma_5 \gamma^\mu \epsilon_T^{*\nu} n^\rho v^\sigma \phi_V^a(x)]_{\alpha\beta}, \end{aligned} \quad (28)$$

for the longitudinal polarization and transverse polarization, respectively. Here  $x$  is the momentum fraction associated with the  $q_2$  quark.  $n$  is the moving direction of the vector meson and  $v$  is the opposite direction. These distribution amplitudes can be related to the ones used in QCD sum rules by:

$$\begin{aligned} \phi_V(x) &= \frac{f_V}{2\sqrt{2N_c}} \phi_{||}(x), \quad \phi_V^t(x) = \frac{f_V^T}{2\sqrt{2N_c}} h_{||}^{(t)}(x), \\ \phi_V^s(x) &= \frac{f_V^T}{4\sqrt{2N_c}} \frac{d}{dx} h_{||}^{(s)}(x), \quad \phi_V^T(x) = \frac{f_V^T}{2\sqrt{2N_c}} \phi_\perp(x), \\ \phi_V^v(x) &= \frac{f_V}{2\sqrt{2N_c}} g_\perp^{(v)}(x), \quad \phi_V^a(x) = \frac{f_V}{8\sqrt{2N_c}} \frac{d}{dx} g_\perp^{(a)}(x). \end{aligned} \quad (29)$$

The twist-2 distribution amplitudes can be expanded in terms of Gegenbauer polynomials  $C_n^{3/2}$  with the coefficients called Gegenbauer moments  $a_n$ :

$$\phi_{||,\perp}(x) = 6x(1-x) \left[ 1 + \sum_{n=1}^{\infty} a_n^{||,\perp} C_n^{3/2}(t) \right], \quad (30)$$

where  $t = 2x - 1$ . The Gegenbauer moments  $a_n^{||,\perp}$  are mainly determined by the technique of QCD sum rules. Here we quote the recent numerical results [32, 33, 34, 35] as

$$a_1^{||}(K^*) = 0.03 \pm 0.02, \quad a_1^\perp(K^*) = 0.04 \pm 0.03, \quad (31)$$

$$a_2^{||}(\rho) = a_2^{||}(\omega) = 0.15 \pm 0.07, \quad a_2^\perp(\rho) = a_2^\perp(\omega) = 0.14 \pm 0.06, \quad (32)$$

$$a_2^{||}(K^*) = 0.11 \pm 0.09, \quad a_2^\perp(K^*) = 0.10 \pm 0.08, \quad (33)$$

$$a_2^{||}(\phi) = 0.18 \pm 0.08, \quad a_2^\perp(\phi) = 0.14 \pm 0.07, \quad (34)$$

TABLE II: Input values of the decay constants (absolute values) for the axial-vector mesons (in MeV). The transverse decays constants for  $^1P_1$  are evaluated at  $\mu = 1$  GeV.

$f_{a_1(1260)}$	$f_{f_1(1^3P_1)}$	$f_{f_8(1^3P_1)}$	$f_{K_{1A}}$	$f_{b_1(1235)}^T$	$f_{h_1(1^1P_1)}^T$	$f_{h_8(1^1P_1)}^T$	$f_{K_{1B}}^T$
$238 \pm 10$	$245 \pm 13$	$239 \pm 13$	$250 \pm 13$	$180 \pm 8$	$180 \pm 12$	$190 \pm 10$	$190 \pm 10$

where the values are taken at  $\mu = 1$  GeV.

Using equation of motion, two-particle twist-3 distribution amplitudes are related to twist-2 LCDAs and three-particle twist-3 distribution amplitudes. But in some  $B \rightarrow VV$  decays, there exists the so-called polarization problem. It has been suggested that using asymptotic LCDAs can resolve this problem in pQCD approach. Thus to be self-consistent, we should also use the same form to calculate radiative decays. As in Ref. [19], we use the asymptotic form for twist-3 LCDAs:

$$h_{\parallel}^{(t)}(x) = 3t^2, \quad h_{\parallel}^{(s)}(x) = 6x(1-x), \quad (35)$$

$$g_{\perp}^{(a)}(x) = 6x(1-x), \quad g_{\perp}^{(v)}(x) = \frac{3}{4}(1+t^2). \quad (36)$$

### E. Light-cone distribution amplitudes of axial-vectors

Longitudinal and transverse decay constants for axial-vectors are defined by:

$$\langle A(P, \epsilon) | \bar{q}_2 \gamma_{\mu} \gamma_5 q_1 | 0 \rangle = i f_A m_A \epsilon_{\mu}^*, \quad \langle A(P, \epsilon) | \bar{q}_2 \sigma_{\mu\nu} \gamma_5 q_1 | 0 \rangle = f_A^T (\epsilon_{\mu}^* P_{\nu} - \epsilon_{\nu}^* P_{\mu}). \quad (37)$$

In SU(2) limit, due to G-parity, the longitudinal (transverse) decay constants vanish for the non-strange  $^1P_1$  [ $^3P_1$ ] states. This will affect the normalization for the corresponding distribution amplitudes which will be discussed in the following. For convenience, we take  $f_{3P_1} \equiv f$  [ $f_{1P_1}^T (\mu = 1 \text{ GeV}) \equiv f$ ] as the ‘‘normalization constant’’. The numbers of axial vector meson decay constants shown in table II are taken from Ref. [36, 37].

Distribution amplitudes for axial-vectors with quantum numbers  $J^{PC} = 1^{++}$  or  $1^{+-}$  are defined by:

$$\begin{aligned} \langle A(P, \epsilon_L^*) | \bar{q}_{2\beta}(z) q_{1\alpha}(0) | 0 \rangle &= \frac{-i}{\sqrt{2N_c}} \int_0^1 dx e^{ixp \cdot z} [m_A \not{\epsilon}_L^* \gamma_5 \phi_A(x) - \not{\epsilon}_L^* \not{P} \gamma_5 \phi_A^t(x) - m_A \gamma_5 \phi_A^s(x)]_{\alpha\beta}, \\ \langle A(P, \epsilon_T^*) | \bar{q}_{2\beta}(z) q_{1\alpha}(0) | 0 \rangle &= \frac{-i}{\sqrt{2N_c}} \int_0^1 dx e^{ixp \cdot z} [m_A \not{\epsilon}_T^* \gamma_5 \phi_A^v(x) - \not{\epsilon}_T^* \not{P} \gamma_5 \phi_A^T(x) \\ &\quad - m_A i \epsilon_{\mu\nu\rho\sigma} \gamma^{\mu} \epsilon_T^{*\nu} n^{\rho} v^{\sigma} \phi_A^a(x)]_{\alpha\beta}. \end{aligned} \quad (38)$$

Besides the factor  $-i\gamma_5$  from the right hand, axial-vector mesons’ distribution amplitudes can be

related to the vector ones by making the following replacement:

$$\begin{aligned}\phi_V &\rightarrow \phi_A, \quad \phi_V^t \rightarrow -\phi_A^t, \quad \phi_V^s \rightarrow -\phi_A^s, \\ \phi_V^T &\rightarrow -\phi_A^T, \quad \phi_V^v \rightarrow \phi_A^v, \quad \phi_V^a \rightarrow \phi_A^a.\end{aligned}\tag{39}$$

These distribution amplitudes can be related to the ones calculated in QCD sum rules by:

$$\begin{aligned}\phi_A(x) &= \frac{f}{2\sqrt{2N_c}}\phi_{||}(x), \quad \phi_A^t(x) = \frac{f}{2\sqrt{2N_c}}h_{||}^{(t)}(x), \\ \phi_A^s(x) &= \frac{f}{4\sqrt{2N_c}}\frac{d}{dx}h_{||}^{(s)}(x), \quad \phi_A^T(x) = \frac{f}{2\sqrt{2N_c}}\phi_{\perp}(x), \\ \phi_A^v(x) &= \frac{f}{2\sqrt{2N_c}}g_{\perp}^{(v)}(x), \quad \phi_A^a(x) = \frac{f}{8\sqrt{2N_c}}\frac{d}{dx}g_{\perp}^{(a)}(x),\end{aligned}\tag{40}$$

where we use  $f$  as the ‘‘normalization’’ constant for both longitudinal polarized and transversely polarized mesons.

In SU(2) limit, due to G-parity,  $\phi_{||}$ ,  $g_{\perp}^{(a)}$  and  $g_{\perp}^{(v)}$  are symmetric [antisymmetric] under the replacement  $x \leftrightarrow 1 - x$  for non-strange  $1^3P_1$  [ $1^1P_1$ ] states, whereas  $\phi_{\perp}$ ,  $h_{||}^{(t)}$ , and  $h_{||}^{(s)}$  are antisymmetric [symmetric]. In the above, we have taken  $f_{3P_1}^T = f_{3P_1} = f$  [ $f_{1P_1} = f_{1P_1}^T$  ( $\mu = 1$  GeV) =  $f$ ], thus we have

$$\langle 1^3P_1(P, \epsilon) | \bar{q}_1 \sigma_{\mu\nu} \gamma_5 q_2 | 0 \rangle = f_{3P_1}^T a_0^{\perp, 3P_1} (\epsilon_{\mu}^* P_{\nu} - \epsilon_{\nu}^* P_{\mu}),\tag{41}$$

$$\langle 1^1P_1(P, \epsilon) | \bar{q}_1 \gamma_{\mu} \gamma_5 q_2 | 0 \rangle = i f_{1P_1} a_0^{\parallel, 1P_1} m_{1P_1} \epsilon_{\mu}^*,\tag{42}$$

where  $a_0^{\perp, 3P_1}$  and  $a_0^{\parallel, 1P_1}$  are the Gegenbauer zeroth moments. That can give the following normalization for the distribution amplitudes:

$$\int_0^1 dx \phi_{\perp}(x) = a_0^{\perp} \left[ \int_0^1 dx \phi_{||}(x) = a_0^{\parallel} \right],\tag{43}$$

for the  $1^3P_1$  [ $1^1P_1$ ] states. The zeroth Gegenbauer moments  $a_0^{\perp, 3P_1}$  and  $a_0^{\parallel, 1P_1}$ , characterizing the degree of the flavor SU(3) symmetry breaking, are non-zero for only strange mesons. We normalize the distribution amplitude  $\phi_{||}$  of the  $1^3P_1$  states as

$$\int_0^1 dx \phi_{||}(x) = 1.\tag{44}$$

For convenience, we formally define  $a_0^{\parallel} = 1$  for the  $1^3P_1$  states so that we can use Eq. (43) as the normalization condition. Similarly, we also define  $a_0^{\perp} = 1$  for  $1^1P_1$  states so that  $\phi_{\perp}(x)$  has a correct normalization.

TABLE III: Gegenbauer moments of  $\phi_{\perp}$  and  $\phi_{\parallel}$  for  $1^3P_1$  and  $1^1P_1$  mesons evaluated in Ref. [37], where the values are taken at  $\mu = 1$  GeV.

$a_2^{\parallel, a_1(1260)}$	$a_2^{\parallel, f_1^{3P_1}}$	$a_2^{\parallel, f_8^{3P_1}}$	$a_2^{\parallel, K_{1A}}$	$a_1^{\parallel, K_{1A}}$	
$-0.02 \pm 0.02$	$-0.04 \pm 0.03$	$-0.07 \pm 0.04$	$-0.05 \pm 0.03$	$0.00 \pm 0.26$	
$a_1^{\perp, a_1(1260)}$	$a_1^{\perp, f_1^{3P_1}}$	$a_1^{\perp, f_8^{3P_1}}$	$a_1^{\perp, K_{1A}}$	$a_0^{\perp, K_{1A}}$	$a_2^{\perp, K_{1A}}$
$-1.04 \pm 0.34$	$-1.06 \pm 0.36$	$-1.11 \pm 0.31$	$-1.08 \pm 0.48$	$0.08 \pm 0.09$	$0.02 \pm 0.20$
$a_1^{\parallel, b_1(1235)}$	$a_1^{\parallel, h_1^{1P_1}}$	$a_1^{\parallel, h_8^{1P_1}}$	$a_1^{\parallel, K_{1B}}$	$a_0^{\parallel, K_{1B}}$	$a_2^{\parallel, K_{1B}}$
$-1.95 \pm 0.35$	$-2.00 \pm 0.35$	$-1.95 \pm 0.35$	$-1.95 \pm 0.45$	$0.14 \pm 0.15$	$0.02 \pm 0.10$
$a_2^{\perp, b_1(1235)}$	$a_2^{\perp, h_1^{1P_1}}$	$a_2^{\perp, h_8^{1P_1}}$	$a_2^{\perp, K_{1B}}$	$a_1^{\perp, K_{1B}}$	
$0.03 \pm 0.19$	$0.18 \pm 0.22$	$0.14 \pm 0.22$	$-0.02 \pm 0.22$	$0.17 \pm 0.22$	

Up to conformal spin 6, twist-2 distribution amplitudes for axial-vector mesons can be expanded as:

$$\phi_{\parallel}(x) = 6x\bar{x} \left[ a_0^{\parallel} + 3a_1^{\parallel} t + a_2^{\parallel} \frac{3}{2}(5t^2 - 1) \right], \quad (45)$$

$$\phi_{\perp}(x) = 6x\bar{x} \left[ a_0^{\perp} + 3a_1^{\perp} t + a_2^{\perp} \frac{3}{2}(5t^2 - 1) \right], \quad (46)$$

where the Gegenbauer moments are calculated in Refs. [36, 37] shown in table III. From the results in table III, we can see that there are large uncertainties in Gegenbauer moments which can inevitably induce large uncertainties to branching ratios and CP asymmetries. We hope the uncertainties could be reduced in future studies in order to make more precise predictions.

As for twist-3 LCDAs, we use the following form:

$$g_{\perp}^{(v)}(x) = \frac{3}{4}a_0^{\parallel}(1+t^2) + \frac{3}{2}a_1^{\parallel}t^3, \quad g_{\perp}^{(a)}(x) = 6x\bar{x}(a_0^{\parallel} + a_1^{\parallel}t), \quad (47)$$

$$h_{\parallel}^{(t)}(x) = 3a_0^{\perp}t^2 + \frac{3}{2}a_1^{\perp}t(3t^2 - 1), \quad h_{\parallel}^{(s)}(x) = 6x\bar{x}(a_0^{\perp} + a_1^{\perp}t). \quad (48)$$

### III. $B \rightarrow V$ AND $B \rightarrow A$ FORM FACTORS

$\bar{B} \rightarrow V$  form factors are defined under the conventional form as follows:

$$\begin{aligned}
\langle V(P_2, \epsilon^*) | \bar{q} \gamma^\mu b | \bar{B}(P_1) \rangle &= -\frac{2V(q^2)}{m_B + m_V} \epsilon^{\mu\nu\rho\sigma} \epsilon_\nu^* P_{1\rho} P_{2\sigma}, \\
\langle V(P_2, \epsilon^*) | \bar{q} \gamma^\mu \gamma_5 b | \bar{B}(P_1) \rangle &= 2im_V A_0(q^2) \frac{\epsilon^* \cdot q}{q^2} q^\mu + i(m_B + m_V) A_1(q^2) \left[ \epsilon_\mu^* - \frac{\epsilon^* \cdot q}{q^2} q^\mu \right] \\
&\quad - iA_2(q^2) \frac{\epsilon^* \cdot q}{m_B + m_V} \left[ (P_1 + P_2)^\mu - \frac{m_B^2 - m_V^2}{q^2} q^\mu \right], \\
\langle V(P_2, \epsilon^*) | \bar{q} \sigma^{\mu\nu} q_\nu b | \bar{B}(P_1) \rangle &= -2iT_1(q^2) \epsilon^{\mu\nu\rho\sigma} \epsilon_\nu^* P_{1\rho} P_{2\sigma}, \\
\langle V(P_2, \epsilon^*) | \bar{q} \sigma^{\mu\nu} \gamma_5 q_\nu b | \bar{B}(P_1) \rangle &= T_2(q^2) [(m_B^2 - m_V^2) \epsilon^{*\mu} - (\epsilon^* \cdot q)(P_1 + P_2)^\mu] \\
&\quad + T_3(q^2) (\epsilon^* \cdot q) \left[ q^\mu - \frac{q^2}{m_B^2 - m_V^2} (P_1 + P_2)^\mu \right], \tag{49}
\end{aligned}$$

where  $q = P_1 - P_2$  and the relation  $2m_V A_0(0) = (m_B + m_V) A_1(0) - (m_B - m_V) A_2(0)$  is obtained in order to cancel the pole at  $q^2 = 0$ .

In pQCD approach, the factorization formulae for these form factors at maximally recoiling ( $q^2 = 0$ ) are expressed by:

$$\begin{aligned}
V &= 8\pi C_F m_B (m_B + m_V) \int_0^1 dx_1 dx_2 \int_0^\infty b_1 db_1 b_2 db_2 \phi_B(x_1, b_1) \\
&\quad \times \left\{ E_e(t_a) h_e(x_1 x_2, x_2, b_1, b_2) \left[ \phi_V^T(x_2) + (2 + x_2) r_V \phi_V^a(x_2) - r_V x_2 \phi_V^v(x_2) \right] \right. \\
&\quad \left. + E'_e(t'_a) h_e(x_1 x_2, x_1, b_2, b_1) r_V \left[ \phi_V^a(x_2) + \phi_V^v(x_2) \right] \right\}, \tag{50}
\end{aligned}$$

$$\begin{aligned}
A_0 &= 8\pi C_F m_B^2 \int_0^1 dx_1 dx_2 \int_0^\infty b_1 db_1 b_2 db_2 \phi_B(x_1, b_1) \\
&\quad \times \left\{ E_e(t_a) h_e(x_1 x_2, x_2, b_1, b_2) \left[ (1 + x_2) \phi_V(x_2) + (1 - 2x_2) r_V (\phi_V^s(x_2) + \phi_V^t(x_2)) \right] \right. \\
&\quad \left. + 2r_V E'_e(t'_a) h_e(x_1 x_2, x_1, b_2, b_1) \phi_V^s(x_2) \right\}, \tag{51}
\end{aligned}$$

$$\begin{aligned}
A_1 &= 8\pi C_F m_B (m_B - m_V) \int_0^1 dx_1 dx_2 \int_0^\infty b_1 db_1 b_2 db_2 \phi_B(x_1, b_1) \\
&\quad \times \left\{ E_e(t_a) h_e(x_1 x_2, x_2, b_1, b_2) \left[ \phi_V^T(x_2) + (2 + x_2) r_V \phi_V^v(x_2) - r_V x_2 \phi_V^a(x_2) \right] \right. \\
&\quad \left. + E'_e(t'_a) h_e(x_1 x_2, x_1, b_2, b_1) r_V \left[ \phi_V^a(x_2) + \phi_V^v(x_2) \right] \right\}, \tag{52}
\end{aligned}$$

$$A_2 = \frac{1}{m_B - m_V} \left[ (m_B + m_V) A_1 - 2m_V A_0 \right], \tag{53}$$

$$\begin{aligned}
T_1 &= T_2 \\
&= 8\pi C_F m_B^2 \int_0^1 dx_1 dx_2 \int_0^\infty b_1 db_1 b_2 db_2 \phi_B(x_1, b_1) \\
&\quad \times \left\{ E_e(t_a) h_e(x_1 x_2, x_2, b_1, b_2) \left[ (1+x_2) \phi_V^T(x_2) + (1-2x_2) r_V (\phi_V^v(x_2) + \phi_V^a(x_2)) \right] \right. \\
&\quad \left. + E'_e(t'_a) h_e(x_1 x_2, x_1, b_2, b_1) r_V (\phi_V^v(x_2) + \phi_V^a(x_2)) \right\}, \tag{54}
\end{aligned}$$

$$\begin{aligned}
T_3 &= T_2 - 16\pi C_F m_B^2 r_V \int_0^1 dx_1 dx_2 \int_0^\infty b_1 db_1 b_2 db_2 \phi_B(x_1, b_1) \\
&\quad \times \left\{ E_e(t_a) h_e(x_1 x_2, x_2, b_1, b_2) \left[ \phi_V(x_2) + 2r_V \phi_V^t(x_2) + r_V x_2 (\phi_V^t(x_2) - \phi_V^s(x_2)) \right] \right. \\
&\quad \left. + 2r_V E'_e(t'_a) h_e(x_1 x_2, x_1, b_2, b_1) \phi_V^s(x_2) \right\}, \tag{55}
\end{aligned}$$

with  $C_F = 4/3$ . The definitions of functions  $E_i$ , the factorization scales  $t_i$  and hard functions  $h_i$ , are given in Appendix A.

With the above expressions for form factors, we obtain the numerical results that are collected in table IV. When evaluating the form factor  $A_0$ , we used  $2m_V A_0(0) = (m_B + m_V) A_1(0) - (m_B - m_V) A_2(0)$  and assume  $A_1$  and  $A_2$  are linearly correlated to estimate the uncertainties. The first error comes from decay constants of  $B_{(s)}$  meson and shape parameters  $\omega_b$ ; while the second one is from hard scale  $t$  and  $\Lambda_{QCD}$ . In the calculation,  $f_B = (0.19 \pm 0.02)$  GeV,  $\omega_B = (0.40 \pm 0.05)$  GeV (for  $B^\pm$  and  $B_d^0$  mesons) and  $f_{B_s} = (0.23 \pm 0.02)$  GeV,  $\omega_{B_s} = (0.50 \pm 0.05)$  GeV (for  $B_s^0$  meson) have been used. It is clear that these hadronic parameters give the dominant theoretical uncertainties. They quantify the SU(3)-symmetry breaking effects in the form factors in pQCD approach. To make a comparison, we also collect the results using other approaches [5, 6, 8, 39, 40]. From table IV, we can see that most of our results are consistent with others within theoretical errors.

Likewise,  $\bar{B} \rightarrow A$  form factors are defined by:

$$\begin{aligned}
\langle A(P_2, \epsilon^*) | \bar{q} \gamma^\mu \gamma_5 b | \bar{B}(P_1) \rangle &= -\frac{2iA(q^2)}{m_B - m_A} \epsilon^{\mu\nu\rho\sigma} \epsilon_\nu^* P_{1\rho} P_{2\sigma}, \\
\langle A(P_2, \epsilon^*) | \bar{q} \gamma^\mu b | \bar{B}(P_1) \rangle &= -2m_V V_0(q^2) \frac{\epsilon^* \cdot q}{q^2} q^\mu - (m_B - m_A) V_1(q^2) \left[ \epsilon_\mu^* - \frac{\epsilon^* \cdot q}{q^2} q^\mu \right] \\
&\quad + V_2(q^2) \frac{\epsilon^* \cdot q}{m_B - m_A} \left[ (P_1 + P_2)^\mu - \frac{m_B^2 - m_A^2}{q^2} q^\mu \right], \\
\langle A(P_2, \epsilon^*) | \bar{q} \sigma^{\mu\nu} \gamma_5 q_\nu b | \bar{B}(P_1) \rangle &= -2T_1(q^2) \epsilon^{\mu\nu\rho\sigma} \epsilon_\nu^* P_{1\rho} P_{2\sigma}, \\
\langle A(P_2, \epsilon^*) | \bar{q} \sigma^{\mu\nu} q_\nu b | \bar{B}(P_1) \rangle &= -iT_2(q^2) [(m_B^2 - m_A^2) \epsilon^{*\mu} - (\epsilon^* \cdot q)(P_1 + P_2)^\mu] \\
&\quad - iT_3(q^2) (\epsilon^* \cdot q) \left[ q^\mu - \frac{q^2}{m_B^2 - m_A^2} (P_1 + P_2)^\mu \right], \tag{56}
\end{aligned}$$

with a factor  $-i$  different from  $B \rightarrow V$  and the factor  $m_B + m_V$  ( $m_B - m_V$ ) is replaced by  $m_B - m_A$  ( $m_B + m_A$ ). Similar with  $B \rightarrow V$  form factors, the relation  $2m_A V_0 = (m_B - m_A) V_1 - (m_B + m_A) V_2$

TABLE IV:  $B \rightarrow V$  form factors at maximally recoil, i.e.  $q^2 = 0$ . The first error comes from decay constants of  $B$  mesons and shape parameters  $\omega_b$ ; while the second one is from hard scale  $t$  and  $\Lambda_{QCD}$ .

		$B \rightarrow \rho$	$B \rightarrow K^*$	$B \rightarrow \omega$	$B_s \rightarrow K^*$	$B_s \rightarrow \phi$
LFQM[6]	$V$	0.27	0.31			
	$A_0$	0.28	0.31			
	$A_1$	0.22	0.26			
	$A_2$	0.20	0.24			
LCSR[8]	$V$	0.323	0.411	0.293	0.311	0.434
	$A_0$	0.303	0.374	0.281	0.360	0.474
	$A_1$	0.242	0.292	0.219	0.233	0.311
	$A_2$	0.221	0.259	0.198	0.181	0.234
	$T_2$	0.267	0.333	0.242	0.260	0.349
LQCD[5]	$V$	0.35				
	$A_0$	0.30				
	$A_1$	0.27				
	$A_2$	0.26				
[39]	$T_1$		0.24			
SCET LCQM[40]	$V$	0.298	0.339	0.275	0.323	0.329
	$A_0$	0.260	0.283	0.240	0.279	0.279
	$A_1$	0.227	0.248	0.209	0.228	0.232
	$A_2$	0.215	0.233	0.198	0.204	0.210
	$T_1 = T_2$	0.260	0.290	0.239	0.271	0.276
	$T_3$	0.184	0.194	0.168	0.165	0.170
This work	$V$	$0.21^{+0.05+0.00}_{-0.04-0.00}$	$0.25^{+0.05+0.00}_{-0.05-0.00}$	$0.20^{+0.04+0.00}_{-0.04-0.00}$	$0.21^{+0.04+0.00}_{-0.03-0.01}$	$0.25^{+0.05+0.00}_{-0.04-0.01}$
	$A_0$	$0.25^{+0.05+0.00}_{-0.05-0.01}$	$0.30^{+0.06+0.00}_{-0.05-0.01}$	$0.24^{+0.05+0.00}_{-0.04-0.01}$	$0.26^{+0.05+0.00}_{-0.04-0.01}$	$0.30^{+0.05+0.00}_{-0.05-0.01}$
	$A_1$	$0.17^{+0.04+0.00}_{-0.03-0.00}$	$0.19^{+0.04+0.00}_{-0.03-0.00}$	$0.15^{+0.03+0.00}_{-0.03-0.00}$	$0.16^{+0.03+0.00}_{-0.02-0.01}$	$0.18^{+0.03+0.00}_{-0.03-0.01}$
	$A_2$	$0.13^{+0.03+0.00}_{-0.02-0.00}$	$0.14^{+0.03+0.00}_{-0.03-0.00}$	$0.13^{+0.03+0.00}_{-0.02-0.00}$	$0.12^{+0.02+0.00}_{-0.02-0.01}$	$0.13^{+0.02+0.00}_{-0.02-0.01}$
	$T_1 = T_2$	$0.20^{+0.04+0.00}_{-0.04-0.00}$	$0.23^{+0.05+0.00}_{-0.04-0.00}$	$0.18^{+0.04+0.00}_{-0.03-0.00}$	$0.19^{+0.04+0.00}_{-0.03-0.01}$	$0.22^{+0.04+0.00}_{-0.04-0.01}$
	$T_3$	$0.13^{+0.03+0.00}_{-0.02-0.00}$	$0.13^{+0.03+0.00}_{-0.02-0.00}$	$0.12^{+0.03+0.00}_{-0.02-0.00}$	$0.11^{+0.02+0.00}_{-0.02-0.01}$	$0.12^{+0.02+0.00}_{-0.02-0.01}$

is obtained at  $q^2 = 0$ . In pQCD approach,  $B \rightarrow A$  form factors' formulas can be derived from the corresponding  $B \rightarrow V$  form factor formulas in eq.(50-55) using the replacement in Eq. (39) with the proper change of the momentum fraction.

In the following, we will use  $a_1$  to denote  $a_1(1260)$ ,  $b_1$  to denote  $b_1(1235)$ . In Table V, we give the



TABLE V:  $B \rightarrow A$  form factors at maximally recoil, i.e.  $q^2 = 0$ . Results in the first line of each form factor are calculated using  $\theta_K = 45^\circ$ ,  $\theta_{1P_1} = 10^\circ$  or  $\theta_{3P_1} = 38^\circ$ , while the second line corresponds to the angle  $\theta_K = -45^\circ$ ,  $\theta_{1P_1} = 45^\circ$  or  $\theta_{3P_1} = 50^\circ$ . The errors are from: decay constants of  $B_{(s)}$  meson and shape parameter  $\omega_b$ ; Gegenbauer moments in axial-vectors' LCDAs.

	$B \rightarrow K_1(1270)$	$B \rightarrow h_1(1170)$	$B_s \rightarrow K_1(1270)$	$B \rightarrow h_1(1380)$	$B_s \rightarrow h_1(1170)$	$B_s \rightarrow h_1(1380)$
$A$	$-0.05^{+0.01+0.05}_{-0.01-0.05}$	$0.13^{+0.03+0.02}_{-0.02-0.02}$	$-0.05^{+0.01+0.04}_{-0.01-0.04}$	$0.07^{+0.01+0.01}_{-0.01-0.01}$	$0.07^{+0.01+0.00}_{-0.01-0.03}$	$-0.17^{+0.03+0.02}_{-0.03-0.02}$
	$0.33^{+0.07+0.05}_{-0.06-0.05}$	$0.14^{+0.03+0.02}_{-0.03-0.02}$	$-0.11^{+0.02+0.04}_{-0.02-0.04}$	$-0.02^{+0.00+0.00}_{-0.01-0.00}$	$-0.03^{+0.01+0.04}_{-0.01-0.04}$	$-0.19^{+0.03+0.02}_{-0.03-0.02}$
$V_0$	$0.11^{+0.02+1.10}_{-0.02-0.10}$	$0.29^{+0.06+0.02}_{-0.05-0.02}$	$-0.12^{+0.02+0.09}_{-0.02-0.09}$	$0.16^{+0.03+0.01}_{-0.03-0.02}$	$0.16^{+0.03+0.01}_{-0.03-0.01}$	$-0.40^{+0.06+0.03}_{-0.07-0.03}$
	$0.60^{+0.12+0.10}_{-0.11-0.10}$	$0.32^{+0.06+0.03}_{-0.06-0.03}$	$0.11^{+0.03+0.09}_{-0.02-0.09}$	$-0.05^{+0.01+0.00}_{-0.01-0.00}$	$-0.08^{+0.01+0.01}_{-0.01-0.01}$	$-0.43^{+0.07+0.03}_{-0.08-0.03}$
$V_1$	$-0.09^{+0.02+0.08}_{-0.02-0.08}$	$0.22^{+0.04+0.03}_{-0.04-0.03}$	$-0.09^{+0.01+0.07}_{-0.01-0.07}$	$0.12^{+0.03+0.02}_{-0.02-0.02}$	$0.12^{+0.02+0.01}_{-0.02-0.02}$	$-0.31^{+0.05+0.04}_{-0.07-0.04}$
	$0.57^{+0.12+0.08}_{-0.10-0.08}$	$0.24^{+0.05+0.03}_{-0.04-0.03}$	$-0.20^{+0.04+0.07}_{-0.04-0.07}$	$-0.04^{+0.01+0.01}_{-0.01-0.01}$	$-0.05^{+0.01+0.01}_{-0.01-0.01}$	$-0.34^{+0.05+0.04}_{-0.06-0.04}$
$V_2$	$-0.10^{+0.01+0.02}_{-0.02-0.02}$	$0.03^{+0.01+0.01}_{-0.01-0.01}$	$-0.01^{+0.00+0.02}_{-0.00-0.02}$	$0.01^{+0.00+0.01}_{-0.00-0.01}$	$0.02^{+0.00+0.00}_{-0.00-0.00}$	$-0.02^{+0.00+0.01}_{-0.00-0.01}$
	$0.11^{+0.02+0.02}_{-0.02-0.02}$	$0.04^{+0.01+0.01}_{-0.01-0.01}$	$-0.17^{+0.03+0.02}_{-0.04-0.02}$	$-0.004^{+0.001+0.001}_{-0.001-0.001}$	$-0.01^{+0.00+0.00}_{-0.00-0.00}$	$-0.02^{+0.00+0.01}_{-0.00-0.01}$
$T_1(T_2)$	$-0.06^{+0.01+0.07}_{-0.03-0.07}$	$0.18^{+0.04+0.02}_{-0.03-0.02}$	$-0.08^{+0.01+0.06}_{-0.01-0.06}$	$0.10^{+0.02+0.01}_{-0.02-0.01}$	$0.10^{+0.02+0.01}_{-0.02-0.01}$	$-0.25^{+0.04+0.03}_{-0.05-0.03}$
	$0.45^{+0.10+0.07}_{-0.08-0.07}$	$0.20^{+0.04+0.02}_{-0.03-0.02}$	$-0.12^{+0.02+0.06}_{-0.03-0.06}$	$-0.04^{+0.06+0.04}_{-0.01-0.00}$	$-0.04^{+0.00+0.01}_{-0.00-0.01}$	$-0.27^{+0.04+0.03}_{-0.05-0.03}$
$T_3$	$-0.11^{+0.02+0.03}_{-0.03-0.03}$	$0.05^{+0.01+0.01}_{-0.01-0.01}$	$-0.02^{+0.00+0.02}_{-0.00-0.02}$	$0.02^{+0.00+0.01}_{-0.00-0.01}$	$0.03^{+0.01+0.01}_{-0.01-0.01}$	$-0.05^{+0.01+0.02}_{-0.00-0.02}$
	$0.17^{+0.04+0.03}_{-0.03-0.03}$	$0.06^{+0.01+0.01}_{-0.01-0.01}$	$-0.19^{+0.04+0.02}_{-0.05-0.02}$	$-0.01^{+0.00+0.00}_{-0.00-0.00}$	$-0.01^{+0.00+0.00}_{-0.00-0.00}$	$-0.05^{+0.01+0.02}_{-0.01-0.02}$
	$B \rightarrow K_1(1400)$	$B \rightarrow f_1(1285)$	$B_s \rightarrow K_1(1400)$	$B \rightarrow f_1(1420)$	$B_s \rightarrow f_1(1420)$	$B_s \rightarrow f_1(1285)$
$A$	$0.05^{+0.01+0.05}_{-0.01-0.05}$	$0.19^{+0.04+0.02}_{-0.03-0.02}$	$0.12^{+0.03+0.04}_{-0.02-0.04}$	$-0.01^{+0.00+0.00}_{-0.00-0.00}$	$-0.24^{+0.04+0.03}_{-0.04-0.03}$	$-0.01^{+0.00+0.00}_{-0.00-0.00}$
	$0.34^{+0.07+0.05}_{-0.06-0.05}$	$0.18^{+0.04+0.02}_{-0.03-0.02}$	$-0.05^{+0.01+0.04}_{-0.01-0.04}$	$-0.05^{+0.01+0.01}_{-0.01-0.01}$	$-0.23^{+0.04+0.03}_{-0.04-0.03}$	$-0.06^{+0.01+0.00}_{-0.01-0.00}$
$V_0$	$-0.12^{+0.02+0.11}_{-0.03-0.11}$	$0.26^{+0.05+0.06}_{-0.05-0.06}$	$-0.14^{+0.03+0.10}_{-0.04-0.10}$	$-0.01^{+0.00+0.01}_{-0.00-0.01}$	$-0.34^{+0.05+0.08}_{-0.06-0.08}$	$-0.01^{+0.00+0.00}_{-0.00-0.00}$
	$0.64^{+0.13+0.11}_{-0.11-0.11}$	$0.25^{+0.05+0.06}_{-0.04-0.06}$	$-0.12^{+0.02+0.10}_{-0.02-0.10}$	$-0.07^{+0.01+0.02}_{-0.01-0.02}$	$-0.33^{+0.05+0.08}_{-0.06-0.08}$	$-0.08^{+0.01+0.01}_{-0.01-0.01}$
$V_1$	$0.09^{+0.02+0.09}_{-0.02-0.09}$	$0.32^{+0.07+0.04}_{-0.06-0.04}$	$0.24^{+0.05+0.08}_{-0.04-0.08}$	$-0.02^{+0.00+0.00}_{-0.00-0.01}$	$-0.44^{+0.07+0.05}_{-0.08-0.05}$	$-0.02^{+0.00+0.00}_{-0.00-0.00}$
	$0.62^{+0.13+0.09}_{-0.11-0.09}$	$0.32^{+0.07+0.04}_{-0.06-0.04}$	$-0.09^{+0.01+0.08}_{-0.01-0.08}$	$-0.09^{+0.02+0.01}_{-0.02-0.01}$	$-0.43^{+0.07+0.05}_{-0.08-0.05}$	$-0.10^{+0.02+0.01}_{-0.02-0.01}$
$V_2$	$0.10^{+0.02+0.02}_{-0.02-0.02}$	$0.10^{+0.02+0.00}_{-0.02-0.00}$	$0.20^{+0.05+0.02}_{-0.04-0.02}$	$-0.01^{+0.00+0.00}_{-0.00-0.00}$	$-0.11^{+0.02+0.04}_{-0.02-0.04}$	$-0.01^{+0.00+0.00}_{-0.00-0.00}$
	$0.10^{+0.02+0.02}_{-0.02-0.02}$	$0.10^{+0.02+0.00}_{-0.02-0.00}$	$-0.00^{+0.00+0.02}_{-0.00-0.02}$	$-0.02^{+0.00+0.02}_{-0.01-0.02}$	$-0.11^{+0.02+0.04}_{-0.02-0.04}$	$-0.03^{+0.00+0.00}_{-0.01-0.00}$
$T_1(T_2)$	$0.06^{+0.02+0.07}_{-0.01-0.07}$	$0.26^{+0.05+0.03}_{-0.05-0.03}$	$0.14^{+0.03+0.06}_{-0.03-0.06}$	$-0.01^{+0.00+0.00}_{-0.00-0.00}$	$-0.33^{+0.05+0.04}_{-0.06-0.04}$	$-0.01^{+0.00+0.00}_{-0.00-0.00}$
	$0.48^{+0.10+0.07}_{-0.09-0.07}$	$0.25^{+0.05+0.03}_{-0.05-0.03}$	$-0.08^{+0.01+0.06}_{-0.01-0.06}$	$-0.07^{+0.01+0.01}_{-0.02-0.01}$	$-0.32^{+0.05+0.04}_{-0.06-0.04}$	$-0.08^{+0.01+0.01}_{-0.01-0.01}$
$T_3$	$0.13^{+0.03+0.03}_{-0.02-0.03}$	$0.14^{+0.03+0.04}_{-0.03-0.04}$	$0.24^{+0.06+0.02}_{-0.05-0.02}$	$-0.01^{+0.00+0.00}_{-0.00-0.00}$	$-0.16^{+0.03+0.00}_{-0.03-0.00}$	$-0.01^{+0.00+0.00}_{-0.00-0.00}$
	$0.15^{+0.03+0.03}_{-0.03-0.03}$	$0.13^{+0.03+0.04}_{-0.02-0.04}$	$-0.01^{+0.01+0.02}_{-0.00-0.02}$	$-0.03^{+0.01+0.00}_{-0.01-0.00}$	$-0.15^{+0.02+0.00}_{-0.03-0.00}$	$-0.04^{+0.01+0.00}_{-0.01-0.00}$
This work	$B \rightarrow b_1$	$B \rightarrow a_1$	LFQM[6, 7]	$B \rightarrow b_1(K_{1B})$	$B \rightarrow a_1(K_{1A})$	
$A$	$0.19^{+0.04+0.03}_{-0.03-0.02}$	$0.26^{+0.06+0.03}_{-0.05-0.03}$	$A$	$0.10 (0.11)$	$0.25(0.26)$	
$V_0$	$0.45^{+0.09+0.04}_{-0.08-0.04}$	$0.34^{+0.07+0.08}_{-0.06-0.08}$	$V_0$	$0.39(0.41)$	$0.13(0.14)$	
$V_1$	$0.33^{+0.07+0.04}_{-0.06-0.04}$	$0.43^{+0.09+0.05}_{-0.08-0.05}$	$V_1$	$0.18(0.19)$	$0.37(0.39)$	
$V_2$	$0.03^{+0.01+0.01}_{-0.00-0.01}$	$0.14^{+0.03+0.00}_{-0.03-0.00}$	$V_2$	$-0.03(-0.05)$	$0.18(0.17)$	
$T_1(T_2)$	$0.27^{+0.06+0.03}_{-0.05-0.03}$	$0.34^{+0.07+0.05}_{-0.06-0.05}$	$T_1(T_2)$	$-(0.13)$	$-(0.11)$	
$T_3$	$0.06^{+0.01+0.02}_{-0.01-0.02}$	$0.19^{+0.04+0.01}_{-0.03-0.01}$	$T_3$	$-(-0.07)$	$-(0.19)$	

TABLE VI: Distinct contributions to form factor  $T_1$  from various distribution amplitudes.

	$B \rightarrow \rho$	$B \rightarrow a_1(1260)$	$B \rightarrow b_1(1235)$
$\phi^T$	0.086	0.142	0.080
$\phi^a$	0.047	0.086	0.086
$\phi^v$	0.063	0.115	0.100
total	0.196	0.343	0.266

numerical results for  $B \rightarrow A$  form factors, in which we have used minus values for decay constants of  $^1P_1$  mesons<sup>3</sup>. The errors are from: decay constants of  $B_{(s)}$  mesons and shape parameters  $\omega_b$ ; Gegenbauer moments in axial-vectors' LCDAs. In the calculation, we use the mass of the two physical states  $K_1(1270)$ ,  $K_1(1400)$  as that of two spin states  $K_{1A}$ ,  $K_{1B}$  for simplicity and similar for the branching ratios which are given in the following. That only involves a slight difference to the form factors. As the quark contents (to be precise the mixing angles) of the axial-vectors  $K_1(f_1, h_1)$  have not been uniquely determined, we give two different kinds of results for form factors as in Ref. [37]: the results in the first line are calculated using  $\theta_K = 45^\circ$  while the second line corresponds to the angle  $\theta_K = -45^\circ$ . This is also done for the results involving the flavor-singlet and flavor-octet mesons: the results in the first line are calculated using  $\theta_{1P_1} = 10^\circ$ ,  $\theta_{3P_1} = 38^\circ$ ; while the second line corresponds to the angle  $\theta_{1P_1} = 45^\circ$ ,  $\theta_{3P_1} = 50^\circ$ .

A number of remarks on  $B \rightarrow A$  form factors are in order.

1. Form factors are strongly dependent on mixing angles. Many of them even are different by order of magnitude, because the mixing angles describe directly the inner quark contents of the meson. The large difference of form factors surely will induce large differences in branching ratios, which we will see later.
2. We give a comparison of the  $B \rightarrow \rho$ ,  $B \rightarrow a_1(1260)$  and  $B \rightarrow b_1(1235)$  form factors. Form factors  $V_0$ ,  $V_1$ ,  $T_1$  for  $B \rightarrow A$  transition are larger than the corresponding  $B \rightarrow V$  ones. It seems that the form factor  $A^{B \rightarrow (a_1, b_1)}$  is somewhat equal to or even smaller than  $V^{B \rightarrow \rho}$ . But actually that is artificial: as in Eq. (50), the pre-factor is  $m_B + m_V$  while for  $B \rightarrow A$  form factor  $A$ , the factor becomes  $m_B - m_A$ . We take  $T_1$  as an example to explain the reason

---

<sup>3</sup> Decay constants given in QCD sum rules [36, 37] are both positive for two kinds of axial-vectors and we find that this will give negative values for  $B \rightarrow ^1P_1$  form factors, like in [41]. For non-strange  $^1P_1$  mesons, this minus sign will not give any differences as it can not be observed experimentally. But we should point out the minus sign will affect the mixing between  $K_{1A}$  and  $K_{1B}$  by changing the mixing angle  $\theta$  to  $-\theta$ .

for the large  $B \rightarrow A$  form factors. In table VI, we give contributions from three kinds of LCDAs:  $\phi^T$ ,  $\phi^v$  and  $\phi^a$ . The contribution from  $\phi^T$  is larger for  $B \rightarrow a_1$ , than the other two transitions only because the axial-vector  $a_1$  decay constant is larger. Furthermore, larger axial vector meson mass implies larger contribution from twist-3 distribution amplitudes  $\phi^v$ ,  $\phi^a$  for both of  $T_1^{B \rightarrow b_1}$  and  $T_1^{B \rightarrow a_1}$ .

3. In our calculation for form factors involving  $f_1$  mesons, we have used the mixing angle between the octet and singlet:  $\theta = 38^\circ(50^\circ)$  which is very close to the ideal mixing angle  $\theta = 35.3^\circ$ . That implies that the lighter meson  $f_1(1285)$  is almost made up of  $\frac{\bar{u}u + \bar{d}d}{\sqrt{2}}$  while the heavier meson  $f_1(1420)$  is dominated by the  $\bar{s}s$  component. Thus  $B \rightarrow f_1(1420)$  and  $B_s \rightarrow f_1(1285)$  form factors are suppressed by the flavor structure and are numerically small. The form factors involving  $h_1$  are similar if the mixing angle is taken as  $45^\circ$ .
4. From the table V, we can see that the form factor  $T_1^{B \rightarrow a_1}$  is almost equal to  $T_1^{B \rightarrow b_1}$ . In the flavor SU(3) symmetry limit,  $B \rightarrow K_{1A}$  and  $B \rightarrow K_{1B}$  form factors are also almost equal with each other. But the physical states  $K_1(1270)$  and  $K_1(1400)$  are mixtures of  $B \rightarrow K_{1A,1B}$ . With the mixing angle  $\theta_K = \pm 45^\circ$ , the  $B_{d,s} \rightarrow K_1(1270)(K_1(1400))$  form factors are either enhanced by a factor  $\sqrt{2}$  or highly suppressed. This feature will definitely affect branching ratios which will be discussed later.

Up to now, there are not too many experimental constraints on  $B \rightarrow A$  form factors. However there are lots of studies using some non-perturbative methods: quark meson model [42], ISGW [43, 44], QCD sum rules and light-cone sum rules [38, 45, 46] and light-front quark model [6, 7]. Results in LFQM are also given in table V to make a comparison. These two approaches are very different in the treatment of dynamics of transition form factors, but at first we will analyze differences caused by non-perturbative inputs. For  $B \rightarrow a_1$  and  $B \rightarrow K_{1A}$  form factors, most of our results (except  $V_0$  and  $T_{1,2}$ ) are slightly larger than or almost equal with these of evaluated in LFQM, as slightly larger decay constants for  $a_1$  and  $K_{1A}$  are used:  $f_{a_1} = 203$  MeV and  $f_{K_{1A}} = 186$  MeV. The form factor  $V_0$  is calculated by the relation  $2m_A V_0 = (m_B - m_A)V_1 - (m_B + m_A)V_2$ . Small differences in  $V_1$  and  $V_2$  have induced a large difference in  $V_0$ , which could be reduced in future studies using more precise hadronic inputs. We have found there are large differences in  $B \rightarrow^1 P_1$  transition form factors. As the decay constant of  $b_1$  is zero in isospin limit, thus in LFQM the shape parameter  $\omega$  can not be directly determined and Cheng and Chua used the same value with that of  $a_1$  [6]. It is also similar for  $K_{1B}$ : they used the same shape parameter with that of  $K_{1A}$  which predicts  $f_{K_{1B}} = 11$  MeV. Compared with the QCD sum rule results  $f_{K_{1B}} = f_{K_{1B}}^T \times a_0^{\parallel}$  given

in table II and III, we can see: although they are consistent within large theoretical errors, there are still large differences in the central value. Thus our predictions for  $B \rightarrow {}^1P_1$  form factors (central values) are larger than those in LFQM. We have to confess that the differences in decays constants are not responsible for all differences in form factors. That may arise from further differences in the dynamics. Compared with the recent light-cone sum rules results [46]:

$$V_0^{Ba_1}(0) = 0.303_{-0.035}^{+0.022}, \quad V_0^{BK_{1A}}(0) = 0.316_{-0.042}^{+0.048}, \quad (57)$$

$$V_0^{Bb_1}(0) = -0.356_{-0.033}^{+0.039}, \quad V_0^{BK_{1B}}(0) = -0.360_{-0.028}^{+0.030}, \quad (58)$$

where uncertainties are from Borel window and input parameters, we can see that they are well consistent with our calculations in pQCD approach. As mentioned in Ref. [41], the Babar measurement of  $\bar{B}^0 \rightarrow a_1^+ \pi^-$  [47] favors  $V_0^{B \rightarrow a_1}(0) \simeq 0.30$  and this is very close to our result:  $V_0^{B \rightarrow a_1}(0) = 0.34$ . It is also noted that there are large uncertainties in our numerical results, especially due to large uncertainties of hadronic parameters, such as large Gegenbauer moments uncertainties shown in table III.

#### IV. CALCULATION OF RADIATIVE DECAY $B \rightarrow V\gamma$

##### A. The factorization formulae for decay amplitude

For convenience, we define a common factor  $F$  which appears in many diagrams by:

$$F = \frac{em_B^5 C_F}{\pi}. \quad (59)$$

As we have mentioned in the above section, we have to use the amplitudes with distinct chiralities. The explicit factorization formulae for the left-handed and right-handed photon from operator  $O_{7\gamma}$  depicted in Fig. 1 are given by:

$$\begin{aligned} \mathcal{M}_{7\gamma}^L &= 4r_b F \int_0^1 dx_1 dx_2 \int_0^\infty b_1 db_1 b_2 db_2 \phi_B(x_1, b_1) \left\{ C_{7\gamma}(t_a) E_e(t_a) \right. \\ &\quad \times \left[ (1+x_2) \phi_V^T(x_2) + r_V (1-2x_2) (\phi_V^v(x_2) + \phi_V^a(x_2)) \right] h_e(x_1 x_2, x_2, b_1, b_2) \\ &\quad \left. + r_V \left[ \phi_V^v(x_2) + \phi_V^a(x_2) \right] C_{7\gamma}(t'_a) E'_e(t'_a) h_e(x_1 x_2, x_1, b_2, b_1) \right\}, \quad (60) \end{aligned}$$

$$\mathcal{M}_{7\gamma}^R = -\frac{r_D}{r_b} \mathcal{M}_{7\gamma}^L, \quad (61)$$

where the left-helicity amplitude is from the  $m_b$  term in the effective Hamiltonian and the right-helicity amplitude is from the  $m_D$  term which is obviously highly suppressed. This  $O_{7\gamma}$  contribution

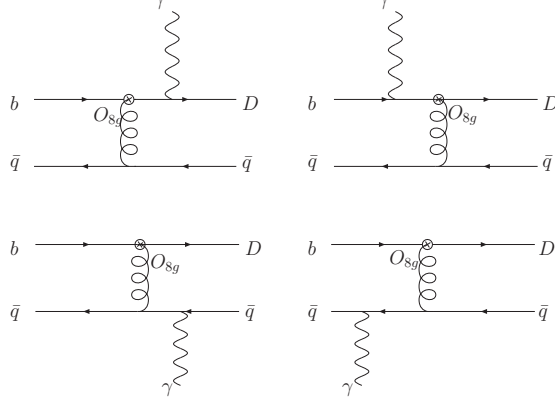


FIG. 3: Feynman diagrams of the chromo-magnetic penguin operator  $O_{8g}$

is the dominant one characterizing by the form factor  $T_1(T_2)$ . The formulas in eq.(60,61) are the same as that in eq.(54) times the Wilson coefficient  $C_7$ .

In pQCD approach, a hard gluon is required to kick the soft spectator in the  $B$  meson to turn into an energetic collinear anti-quark. This gluon could be generated from QCD interaction Hamiltonian or from the  $O_{8g}$  operator. In Fig. 3, we give the four diagrams from  $O_{8g}$  operator given in the effective Hamiltonian. The factorization formulae for the first two diagrams in Fig. 3 are

$$\begin{aligned} \mathcal{M}_{8g}^{L(a)} &= 2r_b F \int_0^1 dx_1 dx_2 \int_0^\infty b_1 db_1 b_2 db_2 \phi_B(x_1, b_1) \left\{ Q_D C_{8g}(t_b) E_e(t_b) \right. \\ &\quad \times \left[ (2x_2 - x_1) \phi_V^T(x_2) - 3x_2 r_V (\phi_V^v(x_2) + \phi_V^a(x_2)) \right] h_e(x_1 x_2, x_2 - 1, b_1, b_2) \\ &\quad \left. + \left[ x_1 \phi_V^T(x_2) + x_2 r_V (\phi_V^v(x_2) + \phi_V^a(x_2)) \right] Q_b C_{8g}(t'_b) E'_e(t'_b) h_e(x_1 x_2, 1 + x_1, b_2, b_1) \right\}, \end{aligned} \quad (62)$$

$$\mathcal{M}_{8g}^{R(a)} = -\frac{r_D}{r_b} \mathcal{M}_{8g}^{L(a)}. \quad (63)$$

If we consider the last two diagrams in Fig. 3, there will be more sources to generate the right-handed photon in addition to the  $m_D$  term in the effective electro-weak Hamiltonian. The third diagram can give a small contribution which is from the higher twist component:

$$\begin{aligned} \mathcal{M}_{8g}^{L(b)}(Q_q) &= 2r_b Q_q F \int_0^1 dx_1 dx_2 \int_0^\infty b_1 db_1 b_2 db_2 \phi_B(x_1, b_1) \left\{ C_{8g}(t_c) E_e(t_c) \right. \\ &\quad \times \left[ (2 + x_2 - x_1) \phi_V^T(x_2) + 3x_2 r_V (\phi_V^v(x_2) + \phi_V^a(x_2)) \right] h_e(x_1 - x_2, -x_2, b_1, b_2) \\ &\quad \left. + \left[ x_2 r_2 (\phi_V^v(x_2) + \phi_V^a(x_2)) - x_1 \phi_V^T(x_2) \right] C_{8g}(t'_c) E'_e(t'_c) h_e(x_1 - x_2, x_1, b_2, b_1) \right\} \\ &\quad - 2r_D Q_q F \int_0^1 dx_1 dx_2 \int_0^\infty b_1 db_1 b_2 db_2 \phi_B(x_1, b_1) C_{8g}(t_c) E_e(t_c) \\ &\quad \times \left[ 3x_2 r_V (\phi_V^v(x_2) - \phi_V^a(x_2)) \right] h_e(x_1 - x_2, -x_2, b_1, b_2), \end{aligned} \quad (64)$$

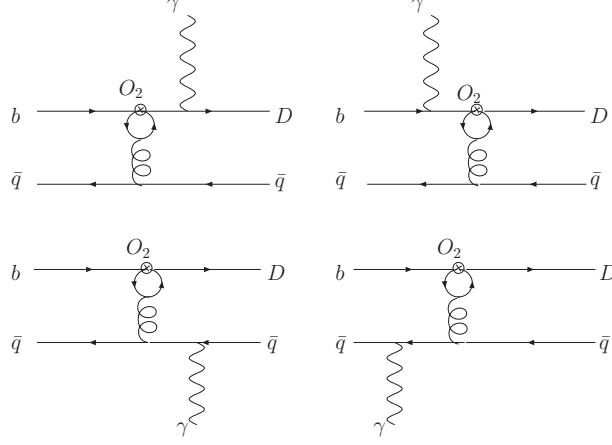


FIG. 4: Feynman diagrams in which the operator  $O_2$  is inserted in the loop with a photon emitted from the external quark line

$$\begin{aligned}
\mathcal{M}_{8g}^{R(b)}(Q_q) = & -2r_D Q_q F \int_0^1 dx_1 dx_2 \int_0^\infty db_1 db_2 db_2 \phi_B(x_1, b_1) \left\{ C_{8g}(t_c) E_e(t_c) \right. \\
& \times \left[ (2 + x_2 - x_1) \phi_V^T(x_2) + 3x_2 r_V (\phi_V^v(x_2) + \phi_V^a(x_2)) \right] h_e(x_1 - x_2, -x_2, b_1, b_2) \\
& + \left. \left[ x_2 r_V (\phi_V^v(x_2) + \phi_V^a(x_2)) - x_1 \phi_V^T(x_2) \right] C_{8g}(t'_c) E'_e(t'_c) h_e(x_1 - x_2, x_1, b_2, b_1) \right\} \\
& + 2r_b Q_q F \int_0^1 dx_1 dx_2 \int_0^\infty db_1 db_2 db_2 \phi_B(x_1, b_1) C_{8g}(t_c) E_e(t_c) \\
& \times \left[ 3x_2 r_V (\phi_V^v(x_2) - \phi_V^a(x_2)) \right] h_e(x_1 - x_2, -x_2, b_1, b_2). \tag{65}
\end{aligned}$$

Next we want to mention some higher order corrections as usual which may give important contributions: charm and up quark loop ( $\mathcal{O}(\alpha_s)$ ) contributions in Fig. 4, Fig. 5 and Fig. 6. It should be pointed out that these contributions are not related to next-to-leading order corrections in pQCD approach, while next-to-leading order corrections to the exclusive processes  $\pi\gamma^* \rightarrow \gamma$  in pQCD approach have been investigated in Ref. [12].

We use the subtitle “quark line photon emission” to denote that a photon is emitted through the external quark lines as in Fig.4. We define the  $c$  and  $u$  loop function in order that the  $b \rightarrow Dg$  vertex can be expressed as  $\bar{D}\gamma^\mu(1 - \gamma^5)I_{\mu\nu}^a A^{a\nu}b$ . It has the gauge invariant form [48] as follows:

$$\begin{aligned}
I_{\mu\nu}^a = & \frac{gT^a}{2\pi^2} (k^2 g_{\mu\nu} - k_\mu k_\nu) \int_0^1 dx x(1-x) \left[ 1 + \log \left( \frac{m_i^2 - x(1-x)k^2}{t^2} \right) \right] \\
= & -\frac{gT^a}{8\pi^2} (k^2 g_{\mu\nu} - k_\mu k_\nu) \left[ G(m_i^2, k^2, t) - \frac{2}{3} \right], \tag{66}
\end{aligned}$$

where  $k$  is the gluon momentum and  $m_i$  is the loop internal quark mass.  $G$  is the function from

the loop integration:

$$\begin{aligned}
G(m_i^2, k^2, t) = & \theta(-k^2) \frac{2}{3} \left[ \frac{5}{3} + \frac{4m_i^2}{k^2} - \ln \frac{m_i^2}{t^2} + \left( 1 + \frac{2m_i^2}{k^2} \right) \sqrt{1 - \frac{4m_i^2}{k^2}} \ln \frac{\sqrt{1 - 4m_i^2/k^2} - 1}{\sqrt{1 - 4m_i^2/k^2} + 1} \right] \\
& + \theta(k^2) \theta(4m_i^2 - k^2) \frac{2}{3} \left[ \frac{5}{3} + \frac{4m_i^2}{k^2} - \ln \frac{m_i^2}{t^2} \right. \\
& \left. - 2 \left( 1 + \frac{2m_i^2}{k^2} \right) \sqrt{\frac{4m_i^2}{k^2} - 1} \arctan \left( \frac{1}{\sqrt{4m_i^2/k^2 - 1}} \right) \right] \\
& + \theta(k^2 - 4m_i^2) \frac{2}{3} \left[ \frac{5}{3} + \frac{4m_i^2}{k^2} - \ln \frac{m_i^2}{t^2} \right. \\
& \left. + \left( 1 + \frac{2m_i^2}{k^2} \right) \sqrt{1 - \frac{4m_i^2}{k^2}} \left( \ln \frac{1 - \sqrt{1 - 4m_i^2/k^2}}{1 + \sqrt{1 - 4m_i^2/k^2}} + i\pi \right) \right]. \tag{67}
\end{aligned}$$

The loop function  $G$  has the dependence of gluon momentum square of  $k^2$ . But there is no singularity when we take the limit of  $k \rightarrow 0$ , so we can neglect  $k_T$  components of  $k^2$  in the loop function  $G$ . Using this effective vertex, the factorization formulae for the first two diagrams of Fig.4 is calculated as:

$$\begin{aligned}
M_{1i}^{L(a)} = & -Q_D F \int_0^1 dx_1 dx_2 \int b_1 db_1 b_2 db_2 \phi_B(x_1, b_1) C_2(t_b) E_e(t_b) \left[ G(m_i^2, -x_1 x_2 m_B^2, t_b) - \frac{2}{3} \right] \\
& \times \left[ x_2^2 r_V (\phi_V^v(x_2) + \phi_V^a(x_2)) + 3x_1 x_2 \phi_V^T(x_2) \right] h_e(x_1 x_2, x_2 - 1, b_1, b_2), \tag{68}
\end{aligned}$$

$$\begin{aligned}
M_{1i}^{R(a)} = & -Q_b F \int_0^1 dx_1 dx_2 \int b_1 db_1 b_2 db_2 \phi_B(x_1, b_1) C_2(t'_b) E'_e(t'_b) \left[ G(m_i^2, -x_1 x_2 m_B^2, t'_b) - \frac{2}{3} \right] \\
& \times x_1 x_2 r_V (\phi_V^a(x_2) - \phi_V^v(x_2)) h_e(x_1 x_2, 1 + x_1, b_2, b_1), \tag{69}
\end{aligned}$$

where  $Q_D = -\frac{1}{3}$ . For the other two diagrams of Fig.4, the factorization formulas are

$$\begin{aligned}
\mathcal{M}_{1i}^{L(b)}(Q_q) = & Q_q F \int_0^1 dx_1 dx_2 \int_0^\infty b_1 db_1 b_2 db_2 \phi_B(x_1, b_1) \left\{ C_2(t_c) E_e(t_c) \right. \\
& \times \left[ x_2 r_V (1 + 2x_2) [\phi_V^v(x_2) + \phi_V^a(x_2)] + 3(x_2 - x_1) \phi_V^T(x_2) \right] \\
& \times \left[ G(m_i^2, -(x_1 - x_2) m_B^2, t_c) - \frac{2}{3} \right] h_e(x_1 - x_2, -x_2, b_1, b_2) \\
& + \left[ x_2 r_V (\phi_V^v(x_2) + \phi_V^a(x_2)) - x_1 \phi_V^T(x_2) \right] \left[ G(m_i^2, -(x_1 - x_2) m_B^2, t'_c) - \frac{2}{3} \right] \\
& \left. \times C_2(t'_c) E'_e(t'_c) h_e(x_1 - x_2, x_1, b_2, b_1) \right\}, \tag{70}
\end{aligned}$$

$$\begin{aligned}
\mathcal{M}_{1i}^{R(b)}(Q_q) = & Q_q F \int_0^1 dx_1 dx_2 \int_0^\infty b_1 db_1 b_2 db_2 \phi_B(x_1, b_1) C_2(t_c) E_e(t_c) h_e(x_1 - x_2, -x_2, b_1, b_2) \\
& \times \left[ G(m_i^2, -(x_1 - x_2) m_B^2, t_c) - \frac{2}{3} \right] \times (2 + x_2) x_2 r_V \left[ \phi_V^v(x_2) - \phi_V^a(x_2) \right]. \tag{71}
\end{aligned}$$

In Fig. 5, we give the diagrams in which a photon emitted from the internal loop quark line. The sum of the effective vertex  $b \rightarrow D\gamma g^*$  in Fig.5 has been derived by [49, 50]:

$$I = \bar{D} \gamma^\rho (1 - \gamma_5) T^a b I_{\mu\nu\rho} A^\mu A^{a\nu}, \tag{72}$$

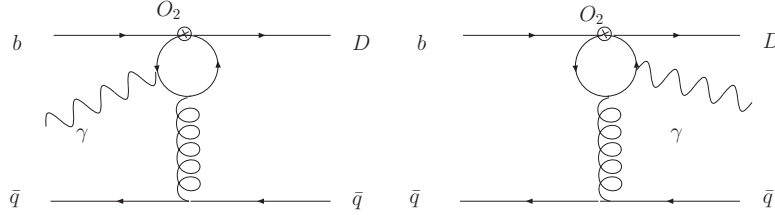


FIG. 5: Feynman diagrams in which the operator  $O_2$  is inserted in the loop with both of the photon and the virtual gluon emitted from the internal quark line.

with the tensor structure given by

$$I_{\mu\nu\rho} = A_4 [(q \cdot k)\epsilon_{\mu\nu\rho\sigma}(q - k)^\sigma + \epsilon_{\nu\rho\sigma\tau}q^\sigma k^\tau k_\mu - \epsilon_{\mu\rho\sigma\tau}q^\sigma k^\tau q_\nu] + A_5 [\epsilon_{\mu\rho\sigma\tau}q^\sigma k^\tau k_\nu - k^2\epsilon_{\mu\nu\rho\sigma}q^\sigma], \quad (73)$$

and

$$A_4 = \frac{4ieg}{3\pi^2} \int_0^1 dx \int_0^{1-x} dy \frac{xy}{x(1-x)k^2 + 2xyq \cdot k - m_i^2 + i\epsilon}, \quad (74)$$

$$A_5 = -\frac{4ieg}{3\pi^2} \int_0^1 dx \int_0^{1-x} dy \frac{x(1-x)}{x(1-x)k^2 + 2xyq \cdot k - m_i^2 + i\epsilon}, \quad (75)$$

where  $q$  is the momentum of the photon  $q = P_B - P_V$ , and  $k$  is the momentum of the gluon. Then the amplitudes can be expressed as follows:

$$\begin{aligned} \mathcal{M}_{2i}^L &= -\frac{8}{3}F \int_0^1 dx \int_0^{1-x} dy \int_0^1 dx_1 dx_2 \int b_1 db_1 \phi_B(x_1, b_1) C_2(t_d) \alpha_s(t_d) \exp[-S_B(t_d)] \\ &\times \frac{h'_e}{xyx_2 m_B^2 - m_i^2} \times \left\{ xyx_2 [(1-x_2)r_V(\phi_V^v(x_2) + \phi_V^a(x_2)) - (1+2x_1)\phi_V^T(x_2)] \right. \\ &\left. + x(1-x) [x_2^2 r_V(\phi_V^v(x_2) + \phi_V^a(x_2)) + 3x_1 x_2 \phi_V^T(x_2)] \right\}, \quad (76) \end{aligned}$$

$$\begin{aligned} \mathcal{M}_{2i}^R &= \frac{8}{3}F \int_0^1 dx \int_0^{1-x} dy \int_0^1 dx_1 dx_2 \int b_1 db_1 \phi_B(x_1, b_1) C_2(t_d) \alpha_s(t_d) \exp[-S_B(t_d)] \\ &\times \frac{h'_e}{xyx_2 m_B^2 - m_i^2} \times xyx_2^2 r_V [\phi_V^v(x_2) - \phi_V^a(x_2)], \quad (77) \end{aligned}$$

where the function  $h'_e$  is defined by:

$$h'_e \equiv K_0(\sqrt{x_1 x_2} m_B b_1) - \left[ \theta(B^2) K_0(b_1 \sqrt{|B^2|}) + \theta(-B^2) i \frac{\pi}{2} H_0(b_1 \sqrt{|B^2|}) \right], \quad (78)$$

with

$$B^2 = x_1 x_2 m_B^2 - \frac{y}{1-x} x_2 m_B^2 + \frac{m_i^2}{x(1-x)}. \quad (79)$$

Diagrams in Fig. 6 in which the photon is emitted from the external loop and the gluon is emitted from QCD interaction Hamiltonian do not give any contribution to  $B \rightarrow V\gamma$ . The



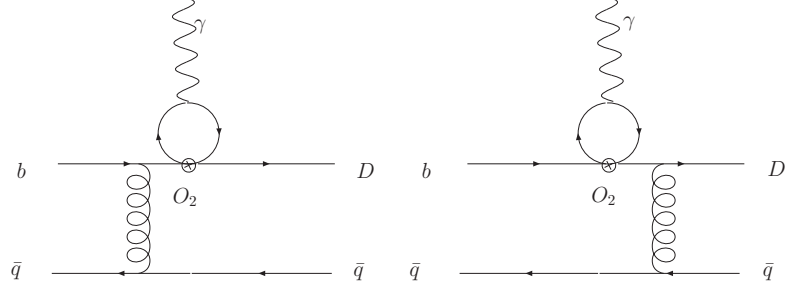


FIG. 6: Feynman diagrams in which the operator  $O_2$  is inserted in the loop with a photon emitted from the internal quark line

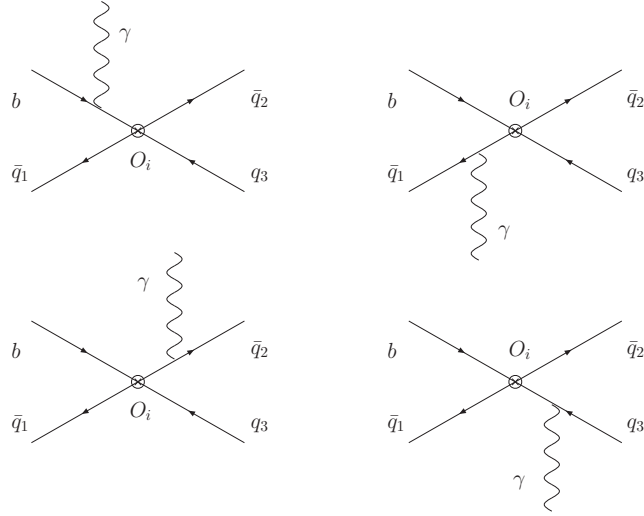


FIG. 7: Feynman diagrams for annihilation topologies

reason is as follows. Similar with  $b \rightarrow Dg$ , the vertex for  $b \rightarrow D\gamma$  can also be expressed as  $\bar{D}\gamma^\mu A^\nu(1 - \gamma^5)(k^2 g_{\mu\nu} - k_\mu k_\nu)b$  only with a different coefficient. For an on-shell photon, the following conditions are required:  $k^2 = 0$  and  $\epsilon \cdot k = 0$ , thus the contribution from diagrams in Fig. 6 vanishes in  $b \rightarrow s(d)\gamma$  decays. But it should be noted that these diagrams can give a non-zero contribution to  $b \rightarrow s(d)\gamma^* \rightarrow s(d)l^+l^-$ .

In annihilation diagrams, there are three different kinds of operators in the  $\otimes$  depicted in Fig. 7. In the following, we use  $LL$  to denote the left-handed current between  $b$  and  $\bar{q}$  quark and the left-handed current between the final state two quarks;  $LR$  denotes the left-handed current between  $b$  and  $\bar{q}$  quark and the right-handed current between the final state two quarks; we use  $SP$  to denote the  $(S - P)(S + P)$  current which is from the Fierz transformation of  $(V - A)(V + A)$  operators.

The factorization formulae for these diagrams are given by:

$$\begin{aligned}\mathcal{M}_{ann}^{L(a,LL)}(a_i, Q_{q_1}) &= \mathcal{M}_{ann}^{L(a,LR)}(a_i, Q_{q_1}) \\ &= F \frac{3\sqrt{6}Q_{q_1}r_V f_V \pi}{2m_B^2} \int_0^1 dx_1 \int_0^\infty b_1 db_1 a_i(t'_e) E_a(t'_e) \phi_B(x_1, b_1) K_0(\sqrt{x_1} m_B b_1),\end{aligned}\quad (80)$$

$$\begin{aligned}\mathcal{M}_{ann}^{R(a,LL)}(a_i, Q_{q_1}) &= \mathcal{M}_{ann}^{R(a,LR)}(a_i, Q_{q_1}) \\ &= -F \frac{3\sqrt{6}Q_b r_V f_V \pi}{2m_B^2} \int_0^1 dx_1 \int_0^\infty b_1 db_1 a_i(t_e) E_a(t_e) \phi_B(x_1, b_1) K_0(\sqrt{1+x_1} m_B b_1),\end{aligned}\quad (81)$$

$$\begin{aligned}\mathcal{M}_{ann}^{L(b,LL)}(a_i, Q_{q_2}, Q_{q_3}) &= \mathcal{M}_{ann}^{R(b,LR)}(a_i, Q_{q_2}, Q_{q_3}) \\ &= -F \frac{3\sqrt{6}r_V f_B \pi}{2m_B^2} \int_0^1 dx_2 \int b_2 db_2 \left[ \phi_V^v(x_2) + \phi_V^a(x_2) \right] \\ &\quad \times \left\{ Q_{q_2} a_i(t_f) E'_a(t_f) i \frac{\pi}{2} H_0^{(1)}(\sqrt{1-x_2} m_B b_2) \right. \\ &\quad \left. - x_2 Q_{q_3} a_i(t'_f) E'_a(t'_f) i \frac{\pi}{2} H_0^{(1)}(\sqrt{x_2} m_B b_2) \right\},\end{aligned}\quad (82)$$

$$\begin{aligned}\mathcal{M}_{ann}^{R(b,LL)}(a_i, Q_{q_2}, Q_{q_3}) &= \mathcal{M}_{ann}^{L(b,LR)}(a_i, Q_{q_2}, Q_{q_3}) \\ &= -F \frac{3\sqrt{6}r_V f_B \pi}{2m_B^2} \int_0^1 dx_2 \int b_2 db_2 \\ &\quad \times \left\{ (1-x_2) \left[ \phi_V^v(x_2) - \phi_V^a(x_2) \right] Q_{q_2} a_i(t_f) E'_a(t_f) i \frac{\pi}{2} H_0^{(1)}(\sqrt{1-x_2} m_B b_2) \right. \\ &\quad \left. - \left[ \phi_V^v(x_2) - \phi_V^a(x_2) \right] Q_{q_3} a_i(t'_f) E'_a(t'_f) i \frac{\pi}{2} H_0^{(1)}(\sqrt{x_2} m_B b_2) \right\},\end{aligned}\quad (83)$$

$$\begin{aligned}\mathcal{M}_{ann}^{L(SP)}(a_i) &= F \frac{3\sqrt{6}f_B \pi}{m_B^2} \int_0^1 dx_2 \int b_2 db_2 \phi_V^T(x_2) \\ &\quad \times \left\{ Q_{q_2} a_i(t_f) E'_a(t_f) i \frac{\pi}{2} H_0^{(1)}(\sqrt{1-x_2} m_B b_2) + Q_{q_3} a_i(t'_f) E'_a(t'_f) i \frac{\pi}{2} H_0^{(1)}(\sqrt{x_2} m_B b_2) \right\}.\end{aligned}\quad (84)$$

Finally, there is another kind of contribution from  $O_{7\gamma}$ : the neutral vector meson  $\bar{q}q$  is generated by a photon as depicted in Fig. 8. Although these diagrams are suppressed by the electromagnetic coupling constant, the enhancement factor  $m_B/\Lambda_{QCD}$  can make it important in some cases [51]. We include these diagrams in our calculation. The first two diagrams of Fig. 8 are equal to each other, so are the last two diagrams. The factorization formulae are given by:

$$\begin{aligned}\mathcal{M}_{en}^L(Q_q) &= -F \frac{3\sqrt{6}\alpha_{em} Q_q Q_b r_b f_V}{m_B m_V} \int_0^1 dx_1 \int_0^\infty b_1 db_1 \phi_B(x_1, b_1) \\ &\quad \times \left\{ C_{7\gamma}(t_e) E_a(t_e) K_0(\sqrt{1+x_1} m_B b_1) + C_{7\gamma}(t'_e) E_a(t'_e) K_0(\sqrt{x_1} m_B b_1) \right\},\end{aligned}\quad (85)$$

$$\mathcal{M}_{en}^R(Q_q) = -\frac{r_D}{r_b} \mathcal{M}_{en}^L(Q_q).\quad (86)$$

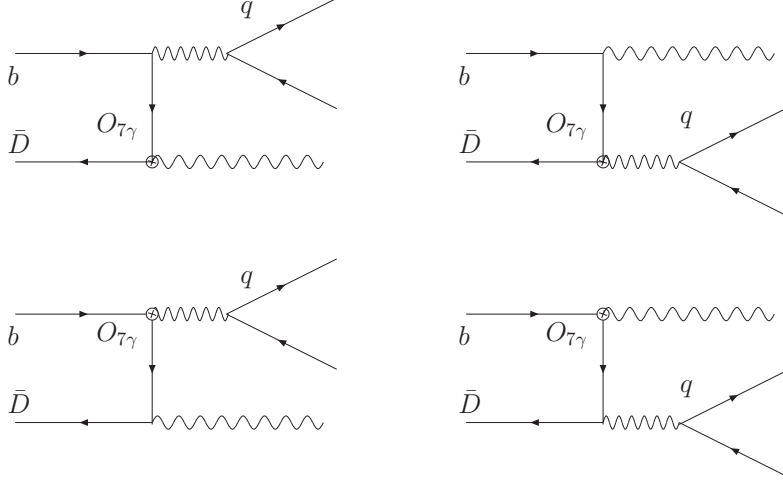


FIG. 8: Feynman diagrams with double-photon contributions

### B. Numerical results of Branching ratios

With those decay amplitude formulas for different Feynman diagrams in the last subsection, it is easy to get the total decay amplitude for each channel of  $B \rightarrow V\gamma$ :  $B^- \rightarrow \rho^-\gamma$ ,  $B^0 \rightarrow \rho^0\gamma$ ,  $B^0 \rightarrow \omega\gamma$ ,  $B^- \rightarrow K^{*-}\gamma$ ,  $B^0 \rightarrow \phi\gamma$ ,  $B^0 \rightarrow K^{*0}\gamma$ ,  $B_s^0 \rightarrow K^{*0}\gamma$ ,  $B_s^0 \rightarrow \rho^0\gamma$ ,  $B_s^0 \rightarrow \omega\gamma$ , and  $B_s^0 \rightarrow \phi\gamma$ . The explicit expressions are shown in Appendix B. The CP-averaged decay width is then

$$\Gamma(B \rightarrow V\gamma) = \frac{|\mathcal{A}(\bar{B} \rightarrow V\gamma)|^2 + |\mathcal{A}(B \rightarrow \bar{V}\gamma)|^2}{32\pi m_B} (1 - r_V^2)^3, \quad (87)$$

where the summation on polarizations is implemented.

For CKM matrix elements, we use the same values as in Ref. [19]:

$$\begin{aligned} |V_{ud}| &= 0.974, & |V_{us}| &= 0.226, & |V_{ub}| &= (3.68_{-0.08}^{+0.11}) \times 10^{-3}, \\ |V_{td}| &= (8.20_{-0.27}^{+0.59}) \times 10^{-3}, & |V_{ts}| &= 40.96 \times 10^{-3}, & |V_{tb}| &= 1.0, \\ \alpha &= (99_{-9.4}^{+4})^\circ, & \gamma &= (59.0_{-3.7}^{+9.7})^\circ, & \arg[-V_{ts}V_{tb}^*] &= 1.0^\circ, \end{aligned} \quad (88)$$

where we have adopted the updated results from [52] and drop the (small) errors on  $V_{ud}$ ,  $V_{us}$ ,  $V_{ts}$  and  $V_{tb}$ . The CKM factors mostly give an overall factor to branching ratios. However, the CKM angles do give large uncertainties to branching ratios of some decay modes and to all the non-zero CP asymmetries which will be discussed in the following subsection.

CP-averaged branching ratios of  $B \rightarrow V\gamma$  decays are listed in table VII. The first error in these entries arises from the input hadronic parameters, which is dominated by  $B(B_s)$ -meson decay constants (taken as  $f_B = (0.19 \pm 0.02)$  GeV and  $f_{B_s} = (0.23 \pm 0.02)$  GeV) and  $B(B_s)$  meson wave function shape parameters (taken as  $\omega_B = (0.40 \pm 0.05)$  GeV and  $\omega_{B_s} = (0.50 \pm 0.05)$  GeV). The second error is from the hard scale  $t$ , defined in Eqs. (A1) – (A8) in Appendix A, which

TABLE VII:  $CP$ -averaged branching ratios ( $\times 10^{-6}$ ) of  $B \rightarrow V\gamma$  decays obtained in pQCD approach (This work); the errors for these entries correspond to uncertainties in input hadronic quantities, from the scale-dependence, and CKM matrix elements, respectively. For comparison, we also listed the current experimental measurements [3, 69, 70, 71] and theoretical estimates of branching ratios recently given in Ref. [31] (QCDF) and in Ref. [64] (SCET).

Modes	QCDF	SCET	This work	Exp.
$B^- \rightarrow K^{*-}\gamma$	$53.3 \pm 13.5 \pm 5.8$	$46 \pm 12 \pm 4 \pm 2 \pm 1$	$35.8^{+17.6+5.4+1.1}_{-12.8-4.0-1.1}$	$40.3 \pm 2.6$ [HFAG]
$\bar{B}^0 \rightarrow \bar{K}^{*0}\gamma$	$54.2 \pm 13.2 \pm 6.7$	$43 \pm 11 \pm 4 \pm 2 \pm 1$	$38.1^{+17.3+5.5+1.1}_{-12.7-3.8-1.1}$	$40.1 \pm 2.0$ [HFAG]
$\bar{B}_s^0 \rightarrow \phi\gamma$	$39.4 \pm 10.7 \pm 5.3$	$43 \pm 11 \pm 3 \pm 3 \pm 1$	$35.8^{+13.7+4.9+1.1}_{-10.3-3.5-1.1}$	$57^{+18+12}_{-15-11}$ [Belle]
Modes	QCDF	This work	Exp.	
$B^- \rightarrow \rho^-\gamma$	$1.16 \pm 0.22 \pm 0.13$	$1.15^{+0.57+0.18+0.17}_{-0.39-0.11-0.09}$	$1.10^{+0.37}_{-0.33} \pm 0.09$ [BaBar]	$0.55^{+0.42+0.09}_{-0.36-0.08}$ [Belle]
$\bar{B}^0 \rightarrow \rho^0\gamma$	$0.55 \pm 0.11 \pm 0.07$	$0.57^{+0.26+0.09+0.08}_{-0.19-0.06-0.04}$	$0.79^{+0.22}_{-0.20} \pm 0.06$ [BaBar]	$1.25^{+0.37+0.07}_{-0.33-0.06}$ [Belle]
$\bar{B}^0 \rightarrow \omega\gamma$	$0.44 \pm 0.09 \pm 0.05$	$0.51^{+0.23+0.08+0.08}_{-0.17-0.05-0.03}$	$0.40^{+0.24}_{-0.20} \pm 0.05$ [BaBar]	$0.56^{+0.34+0.05}_{-0.27-0.10}$ [Belle]
$\bar{B}_s^0 \rightarrow K^{*0}\gamma$	$1.26 \pm 0.25 \pm 0.18$	$1.11^{+0.42+0.15+0.16}_{-0.32-0.12-0.07}$	—	
$\bar{B}^0 \rightarrow \phi\gamma$	—	$(7.5^{+2.8+2.1+1.1}_{-2.1-0.9-0.5}) \times 10^{-6}$	$< 0.85$ [HFAG]	
$\bar{B}_s^0 \rightarrow \rho^0\gamma$	—	$(1.7^{+0.4+0.1+0.0}_{-0.4-0.1-0.1}) \times 10^{-3}$	—	
$\bar{B}_s^0 \rightarrow \omega\gamma$	—	$(1.8^{+0.4+0.1+0.1}_{-0.4-0.2-0.1}) \times 10^{-4}$	—	

we vary from  $0.75t$  to  $1.25t$  (not changing  $1/b_i$ ), and from  $\Lambda_{QCD}^{(5)} = 0.25 \pm 0.05$  GeV. This scale-dependence characterize the size of next-to-leading order contributions in pQCD approach. A part of this perturbative improvement coming from next-to-leading order Wilson coefficients is already available [22]. However, the complete next-to-leading order corrections to hard spectator kernels are still missing. The third error is the combined uncertainties in CKM matrix elements and angles of the unitarity triangle. It is clear that the largest uncertainty here is the first one from the input hadronic parameters.

These ten  $B \rightarrow V\gamma$  decay channels can be divided into three different types:  $b \rightarrow s$  transitions,  $b \rightarrow d$  transitions and purely annihilation decays. The first type contains  $\bar{B}^0 \rightarrow \bar{K}^{*0}\gamma$ ,  $B^- \rightarrow K^{*-}\gamma$  and  $\bar{B}_s \rightarrow \phi\gamma$ . Among these decays, the dominant contribution from  $O_{7\gamma}$ , is proportional to  $V_{tb}V_{ts}^* \sim \lambda^2$ . This contribution can be related to the form factor  $T_1^{B \rightarrow V}$ . In the flavor SU(3) symmetry limit, form factors for these three channels should be equal which could also relates the three decays. We do obtain similar branching ratios for this kind decays only with small deviations. The penguin contribution in  $b \rightarrow d\gamma$  processes is proportional to  $V_{tb}V_{td}^* \sim \lambda^3$ , which is expected

to be suppressed by one order magnitude relative to the  $b \rightarrow s$  transitions. In our calculation, branching ratio results for pure annihilation processes are mainly from two-photon diagrams in Fig. 8. Thus  $\mathcal{BR}(B \rightarrow \phi\gamma)$  is surely consistent with Ref. [51]. This feature can also certainly interpret the large differences between  $\bar{B}_s \rightarrow \rho^0\gamma$  and  $\bar{B}_s \rightarrow \omega\gamma$ . This contribution is proportional to the charge of the constitute quark. This factor is  $\frac{2}{3} - \frac{-1}{3}$  for  $\rho^0$  while  $\frac{2}{3} + \frac{-1}{3}$  for  $\omega$ . Thus the branching ratio of  $B_s \rightarrow \rho^0\gamma$  is one order in magnitude larger than that of  $(B_s \rightarrow \omega\gamma)$ .

In the literature, there are many studies concentrating on  $B \rightarrow V\gamma$  [16, 17, 18, 53, 54, 55, 56, 57, 58, 59, 60, 61, 62, 63, 64]. Recently, a comprehensive study [31] using QCDF method and QCD sum rules appears. In that paper, the authors used QCDF approach to calculate all  $B \rightarrow V\gamma$  approach and included some power corrections: weak annihilation contributions, the soft-gluon emission from quark (charm and light-quark) loops and long distance photon emission from the soft quarks. In Table VII, we quote them to make a comparison. Their uncertainties come from form factors, the renormalization scale, the soft-gluon terms, the CKM parameters, decay constants, Gegenbauer moments, the first inverse moments of  $B(B_s)$  mesons and quark masses, etc. Their results for branching ratios of  $B^- \rightarrow K^{*-}\gamma$  and  $\bar{B}^0 \rightarrow \bar{K}^{*0}\gamma$  are about (20–50)% larger than our predictions. The main reason is differences in form factors  $T_1$ : they used  $T_1^{B \rightarrow K^*} = 0.31 \pm 0.04$  while our calculation gives a smaller  $T_1 = 0.23_{-0.04}^{+0.05}$ . The smaller form factor is also preferred by recent Lattice QCD result:  $T_1^{B \rightarrow K^*} = 0.24 \pm 0.03_{-0.01}^{+0.04}$ . Although the difference is not too large, it can already induce a sizable difference to branching ratios.  $b \rightarrow d$  transitions and  $\bar{B}_s \rightarrow \phi\gamma$  are well consistent with each other, as the effective form factors used in Ref. [31] are smaller and almost equal to our results. Very recently, the authors in Ref. [64] used the more theoretical approach SCET to investigate the three  $b \rightarrow s$  decays channels:  $B^- \rightarrow K^{*-}\gamma$ ,  $\bar{B}^0 \rightarrow \bar{K}^{*0}\gamma$  and  $\bar{B}_s \rightarrow \phi\gamma$ . After integrating out the hard scale  $m_b$  which results in SCET<sub>I</sub>, contributions to  $B \rightarrow V\gamma$  decay amplitudes can be divided into two different groups: contributions from operators  $J_A$  and  $J_B$ . The  $B$ -type operator is power suppressed in SCET<sub>I</sub> but it can give leading power contributions when matching onto SCET<sub>II</sub> as  $A$ -type operator receives power suppressions. When performing the matching from SCET<sub>I</sub> to SCET<sub>II</sub>, we have to be cautious about the  $A$ -type operator as this term suffers from the end-point singularities. Thus one has to leave it as a non-perturbative free parameter determined from experiments or some non-perturbative QCD approaches, but recent studies using zero-bin subtractions show that this term can also factorized in rapidity space [65]. In Ref. [64], the authors calculated the two-loop corrections ( $\alpha_s^2$ ) to short-distance coefficients of the  $A$ -type operator (called vertex functions) determined from QCD to SCET<sub>I</sub> matching and utilized the physical  $B \rightarrow V$  form factor  $T_1$  to extract the soft form factor in SCET. While for the  $B$ -

type operator which can be factorized into convolutions of LCDAs and hard kernels, both of the Wilson coefficient and jet function have been calculated up to one loop order. Short-distance Wilson coefficients for the  $B$ -type operator are extracted at the scale  $m_b$  and have been evolved down the intermediate scale  $\mu \sim 1.5$  GeV using renormalization group equations. With these results, the authors find: compared with the leading order contribution, the order  $\alpha_s$  corrections from vertex corrections and hard spectator scattering can be as large as 10% and both of them also provide imaginary amplitudes about 5% in magnitude; the order  $\alpha_s^2$  corrections are not too large. We quote their final results for branching ratios in table VII and they are also consistent with ours.

The three experimental collaborations, BaBar [66], Belle [67] and CLEO [68], have reported their measurements on  $\mathcal{BR}(B \rightarrow K^*\gamma)$ . Since all of these results are well consistent with each other, we quote the averaging results from Heavy Flavor Averaging Group (HFAG) [3] in table VII. We also include the very recent result on  $\mathcal{BR}(\bar{B}_s^0 \rightarrow \phi\gamma)$  [69]. All of them agree with our calculations. On the  $b \rightarrow d$  transition, branching ratios of some channels have been given by the BaBar [70] and Belle [71] collaboration. We find that our results agree well with BaBar's results but not with Belle's central value results. In flavor SU(3) symmetry limit, the relation  $\mathcal{BR}(B^- \rightarrow \rho^-\gamma) = 2\mathcal{BR}(\bar{B}^0 \rightarrow \rho^0\gamma) = \mathcal{BR}(\bar{B}^0 \rightarrow \omega\gamma)$  should be held. The small deviation in our calculation is caused by the SU(3) symmetry breaking effect. Since the electro-magnetic penguin operator  $O_{7\gamma}$  gives the dominant contribution, it is difficult to understand the results from Belle collaboration: why is the branching ratio of  $\bar{B}^0 \rightarrow \rho^0\gamma$  larger than  $B^- \rightarrow \rho^-\gamma$ . But before we conclude it is the signal for non-standard model scenarios, it is necessary to re-examine this channel on the experimental side. All other decay modes, including  $\bar{B}_s$  decays and annihilation type decays, have not been experimentally measured.

### C. CP asymmetry studies

The direct CP-asymmetry in  $\bar{B} \rightarrow V\gamma$  is defined by:

$$A_{\text{CP}}^{\text{dir}} \equiv \frac{\mathcal{BR}(\bar{B} \rightarrow \bar{V}\gamma) - \mathcal{BR}(B \rightarrow V\gamma)}{\mathcal{BR}(\bar{B} \rightarrow \bar{V}\gamma) + \mathcal{BR}(B \rightarrow V\gamma)} = \frac{|\mathcal{A}(\bar{B} \rightarrow \bar{V}\gamma)|^2 - |\mathcal{A}(B \rightarrow V\gamma)|^2}{|\mathcal{A}(\bar{B} \rightarrow \bar{V}\gamma)|^2 + |\mathcal{A}(B \rightarrow V\gamma)|^2}. \quad (89)$$

In order to give a non-zero direct CP asymmetry, we need two kinds of contributions with different strong phases and different weak phases. The magnitude of the CP asymmetry also depends on relative sizes of the two different amplitudes: if one amplitude is much larger than the other one, we can only get a small CP asymmetry. Since there is only penguin contribution in  $\bar{B}^0 \rightarrow \phi\gamma$

process, the direct CP asymmetry is zero. In other  $B \rightarrow V\gamma$  decays, there are contributions from the penguin operator and two kinds of tree operators (proportional to  $V_{cb}V_{cd,cs}^*$  and  $V_{ub}V_{ud,us}^*$ ). Taking these amplitudes into account, we obtain the numerical results for direct CP asymmetries (in %) in other  $B \rightarrow V\gamma$  decays as:

$$A_{\text{CP}}^{\text{dir}}(B^- \rightarrow \rho^- \gamma) = 12.8_{-0.3}^{+0.8+2.9+0.8}, \quad (90)$$

$$A_{\text{CP}}^{\text{dir}}(\bar{B}^0 \rightarrow \rho^0 \gamma) = 12.4_{-0.4}^{+0.2+1.8+0.5}, \quad (91)$$

$$A_{\text{CP}}^{\text{dir}}(B^- \rightarrow K^{*-} \gamma) = -0.4 \pm 0.0 \pm 0.1 \pm 0.0, \quad (92)$$

$$A_{\text{CP}}^{\text{dir}}(\bar{B}^0 \rightarrow \bar{K}^{*0} \gamma) = -0.3_{-0.0}^{+0.0+0.0+0.0}, \quad (93)$$

$$A_{\text{CP}}^{\text{dir}}(\bar{B}^0 \rightarrow \omega \gamma) = 12.1_{-0.2}^{+0.0+1.8+0.5}, \quad (94)$$

$$A_{\text{CP}}^{\text{dir}}(\bar{B}_s^0 \rightarrow \rho^0 \gamma) = -0.1_{-0.0}^{+0.0+0.3+0.0}, \quad (95)$$

$$A_{\text{CP}}^{\text{dir}}(\bar{B}_s^0 \rightarrow K^{*0} \gamma) = 12.7_{-0.5}^{+0.1+1.6+0.5}, \quad (96)$$

$$A_{\text{CP}}^{\text{dir}}(\bar{B}_s^0 \rightarrow \omega \gamma) = -0.3_{-0.0}^{+0.0+0.9+0.0}, \quad (97)$$

$$A_{\text{CP}}^{\text{dir}}(\bar{B}_s^0 \rightarrow \phi \gamma) = -0.3_{-0.0}^{+0.0+0.0+0.0}, \quad (98)$$

where the three kinds of errors are given as that of the branching ratios case. It is easy to see that theoretical uncertainties here are much smaller than branching ratios in table VII, especially the first one from hadronic input parameters, since they are mostly canceled in eq.(89). In the three  $b \rightarrow s$  channels  $B^- \rightarrow K^{*-} \gamma$ ,  $\bar{B}^0 \rightarrow \bar{K}^{*0} \gamma$  and  $\bar{B}_s \rightarrow \phi \gamma$ , CKM matrix element for the magnetic penguin operator is  $V_{tb}V_{ts}^* \sim \lambda^2$ , while the tree operator is either proportional to  $V_{cb}V_{cs}^* \sim \lambda^2$  or  $V_{ub}V_{us}^* \sim \lambda^4$ . The CKM matrix element in the first tree operator is almost parallel to the penguin operator. This kind of contribution has a same weak phase with the penguin contribution. The second tree operator is small in magnitude. Thus we expect small CP asymmetries in these channels. Experimentally, both BaBar and Belle collaboration give their combined measurements of the two  $B \rightarrow K^* \gamma$  channels [72]:

$$A_{\text{CP}}^{\text{dir}}(B \rightarrow K^* \gamma) = \begin{cases} -1.5 \pm 4.4 \pm 1.2, & [\text{Belle}], \\ -1.3 \pm 3.6 \pm 1.0, & [\text{BaBar}]. \end{cases} \quad (99)$$

Although the central value of CP asymmetry is larger than the one in our calculation in eq.(92,93), it is still consistent with zero.

In annihilation-type decays  $B_s \rightarrow \rho^0(\omega)\gamma$ , the tree amplitude is also suppressed by CKM matrix elements, thus the CP asymmetry is small too. In  $b \rightarrow d$  transitions  $B^- \rightarrow \rho^{*-} \gamma$ ,  $\bar{B}^0 \rightarrow \rho^0(\omega)\gamma$  and  $\bar{B}_s \rightarrow K^{*0} \gamma$ , the CKM matrix element for the magnetic penguin operator is  $V_{tb}V_{td}^* \sim \lambda^3$ , while

the tree operator is either proportional to  $V_{cb}V_{cd}^* \sim \lambda^3$  or  $V_{ub}V_{ud}^* \sim \lambda^3$ . Then tree contribution is not suppressed and can be comparative with the penguin contribution. Thus we expect relatively large CP asymmetries in these four processes, which are also shown in the above.

Restricting the final vector state  $V$  to have definite CP-parity, the time-dependent decay width for the  $B^0 \rightarrow f$  decay is:

$$\Gamma(B^0(t) \rightarrow f) = e^{-\Gamma t} \bar{\Gamma}(B \rightarrow f) \left[ \cosh\left(\frac{\Delta\Gamma t}{2}\right) + H_f \sinh\left(\frac{\Delta\Gamma t}{2}\right) - A_{\text{CP}}^{\text{dir}} \cos(\Delta m t) - S_f \sin(\Delta m t) \right], \quad (100)$$

where  $\Delta m = m_H - m_L > 0$ ,  $\bar{\Gamma}$  is the average decay width, and  $\Delta\Gamma = \Gamma_H - \Gamma_L$  is the difference of decay widths for the heavier and lighter  $B^0$  mass eigenstates. The time dependent decay width  $\Gamma(\bar{B}^0(t) \rightarrow f)$  is obtained from the above expression by flipping the signs of the  $\cos(\Delta m t)$  and  $\sin(\Delta m t)$  terms. In the  $B_d$  system,  $\Delta\Gamma$  is small and can be neglected. In the  $B_s$  system, we expect a much larger decay width difference  $(\Delta\Gamma/\Gamma)_{B_s} = -0.127 \pm 0.024$  [73] within the standard model, while experimentally  $(\Delta\Gamma/\Gamma)_{B_s} = -0.33_{-0.11}^{+0.09}$  [3], so that both  $S_f$  and  $H_f$ , can be extracted from the time dependent decays of  $B_s$  mesons. The definition of the various quantities in the above equation are as follows:

$$S_f(V\gamma) = \frac{2 \text{Im} \left( \frac{q}{p} (\mathcal{A}_L^* \bar{\mathcal{A}}_L + \mathcal{A}_R^* \bar{\mathcal{A}}_R) \right)}{|\mathcal{A}_L|^2 + |\mathcal{A}_R|^2 + |\bar{\mathcal{A}}_L|^2 + |\bar{\mathcal{A}}_R|^2}, \quad (101)$$

$$H_f(V\gamma) = \frac{2 \text{Re} \left( \frac{q}{p} (\mathcal{A}_L^* \bar{\mathcal{A}}_L + \mathcal{A}_R^* \bar{\mathcal{A}}_R) \right)}{|\mathcal{A}_L|^2 + |\mathcal{A}_R|^2 + |\bar{\mathcal{A}}_L|^2 + |\bar{\mathcal{A}}_R|^2}, \quad (102)$$

where  $\bar{A}$  and  $A$  denote the amplitudes for the  $\bar{B}$  and  $B$  meson decays.  $q/p$  is given in terms of the  $B_q^0$ - $\bar{B}_q^0$  mixing matrix  $M_{12}$ ,

$$\frac{q}{p} = \sqrt{\frac{M_{12}^*}{M_{12}}} = e^{i\phi_q} \quad (103)$$

with

$$\phi_d \equiv -\arg[(V_{td}^* V_{tb})^2] = -2\beta, \quad \phi_s \equiv -\arg[(V_{ts}^* V_{tb})^2] = 2\epsilon. \quad (104)$$

where the convention  $\arg[V_{cb}] = \arg[V_{cs}] = 0$  is adopted.

In  $b \rightarrow D\gamma$  ( $D = d, s$ ) processes, the dominant contribution to decay amplitudes comes from the chiral-odd dipole operator  $O_7$ . As only left-handed quarks participate in the weak interaction, an effective operator of this type necessitates, a helicity flip on one of the external quark lines, which results in a factor  $m_b$  (and a left-handed photon) in  $b_R \rightarrow D_L\gamma_L$  and a factor  $m_D$  (and a right-handed photon) in  $b_L \rightarrow D_R\gamma_R$ . Hence, the emission of right-handed photon is suppressed



TABLE VIII: Mixing-induced CP-asymmetry parameters (in percentage) of  $B \rightarrow V\gamma$  decays obtained in pQCD approach. The errors are the same with table VII. The  $H_f$  parameter in  $B_d^0$  decays could hardly be measured as the decay width difference is small.

Modes	$S_f$	$H_f$
$\bar{B}^0 \rightarrow \bar{K}^{*0}\gamma$	$-4.0^{+0.1+0.3+0.1}_{-0.0-0.2-0.1}$	$4.1^{+0.0+0.2+0.1}_{-0.1-0.3-0.1}$
$\bar{B}_s^0 \rightarrow \phi\gamma$	$0.2^{+0.0+0.0+0.0}_{-0.0-0.0-0.0}$	$5.5^{+0.1+0.4+0.0}_{-0.2-0.4-0.0}$
$\bar{B}^0 \rightarrow \rho^0\gamma$	$0.8^{+0.1+0.0+0.0}_{-0.1-0.2-0.1}$	$0.4^{+0.3+0.5+0.1}_{-0.1-0.3-0.1}$
$\bar{B}^0 \rightarrow \omega\gamma$	$0.4^{+0.0+0.2+0.0}_{-0.1-0.2-0.0}$	$0.5^{+0.1+0.4+0.1}_{-0.0-0.3-0.0}$
$\bar{B}_s^0 \rightarrow K^{*0}\gamma$	$0.7^{+0.0+0.4+0.1}_{-0.1-0.2-0.1}$	$-0.3^{+0.1+0.3+0.1}_{-0.2-0.3-0.0}$

by a factor  $m_D/m_b$ . In the  $b \rightarrow D\gamma$  process, the emitted photon is predominantly left-handed, and right-handed in  $\bar{b}$  decays. This leads to very small predictions of  $S_f$  and  $H_f$ . The mixing-induced CP asymmetry variables are calculated and summarized in table VIII.  $\bar{B}^0 \rightarrow \bar{K}^{*0}\gamma$  has been treated as an effective flavor eigenstate. Apparently, the numerical results agree with our expectations. On the experimental side, the mixing-induced CP asymmetries have been measured by Belle and BaBar as follows [74, 75, 76]:

$$S_f(B \rightarrow K^*\gamma \rightarrow K_S\pi^0\gamma) = \begin{cases} -0.79^{+0.63}_{-0.50} \pm 0.10, & [\text{Belle}], \\ -0.08 \pm 0.31 \pm 0.05, & [\text{BaBar}], \end{cases} \quad (105)$$

$$S_f(\bar{B}^0 \rightarrow \rho^0\gamma) = -0.83 \pm 0.65 \pm 0.18. \quad (106)$$

They are consistent with zero since there are large uncertainties in these results. The theoretical results agree with the experimental data taking the experimental uncertainty into account. But as this parameter could be a good probe to detect the non-standard scenarios, more studies, including both of the precise experimental studies and the theoretical studies, are strongly deserving.

#### D. Isospin asymmetry and U-spin asymmetry

Apart from branching ratios and CP asymmetry variables, we will also consider some ratios of branching fractions defined below. In the evaluations for branching fractions, there are many uncertainties, especially from hadronic input parameters, which can blur our predictions, but we can improve the accuracy of our predictions by using ratios of branching fractions. Many uncertainties, such as those from decay constants, will cancel in these parameters. The most important ratios

are the parameters characterizing isospin asymmetries which are defined by:

$$A(\rho, \omega) = \frac{\bar{\Gamma}(B^0 \rightarrow \omega\gamma)}{\bar{\Gamma}(B^0 \rightarrow \rho^0\gamma)} - 1, \quad (107)$$

$$A_I(\rho) = \frac{2\bar{\Gamma}(\bar{B}^0 \rightarrow \rho^0\gamma)}{\bar{\Gamma}(\bar{B}^\pm \rightarrow \rho^\pm\gamma)} - 1, \quad (108)$$

$$A_I(K^*) = \frac{\bar{\Gamma}(\bar{B}^0 \rightarrow K^{*0}\gamma) - \bar{\Gamma}(B^\pm \rightarrow K^{*\pm}\gamma)}{\bar{\Gamma}(\bar{B}^0 \rightarrow K^{*0}\gamma) + \bar{\Gamma}(B^\pm \rightarrow K^{*\pm}\gamma)}, \quad (109)$$

where the partial decay rates are CP-averaged.

In the flavor SU(3) symmetry limit and if we neglect diagrams which are proportional to the quark charge, all of these three parameters should be equal to 0. The  $\omega$  meson decay constant is smaller than that for  $\rho^0$  meson, the  $\bar{u}u$  component contributes with a different sign and the electromagnetic diagrams with two photons are different in the charge factor. These differences make  $A(\rho, \omega)$  deviate from 0 (smaller than 0). The origins for deviations for  $A_I(\rho)$  and  $A_I(K^*)$  from 0 are similar: the spectator quarks are different and annihilation diagrams are also different. Taking on all those power suppressed contributions, our predictions are

$$A(\rho, \omega) = -0.11_{-0.00-0.00-0.00}^{+0.01+0.01+0.00}, \quad (110)$$

$$A_I(\rho) = 0.06_{-0.03-0.01-0.02}^{+0.03+0.01+0.04}, \quad (111)$$

$$A_I(K^*) = 0.06_{-0.01-0.00-0.00}^{+0.02+0.01+0.00}. \quad (112)$$

As we expected, theoretical uncertainties due to the hadronic parameters are indeed smaller due to cancelations. Using experimental results listed in table VII, we can calculate the isospin asymmetry parameters from experiments

$$A(\rho, \omega) = \begin{cases} -0.49_{-0.30}^{+0.34} & [\text{BaBar}], \\ -0.55_{-0.27}^{+0.27} & [\text{Belle}], \end{cases} \quad (113)$$

$$A_I(\rho) = \begin{cases} -0.54_{-0.67}^{+0.65} & [\text{BaBar}], \\ 3.89_{-4.04}^{+3.60} & [\text{Belle}], \end{cases} \quad (114)$$

$$A_I(K^*) = 0.03 \pm 0.04, \quad (115)$$

where we have assumed all the uncertainties are not correlated by adding them quadratically. From the experimental results, except  $A_I(K^*)$ , we find that there are large differences between the results from the two collaborations. Our results are consistent with them, since the error bars in the experiments are too large. We wish a more precise measurement on these parameters in the future.

Apart from the isospin symmetry, U-spin symmetry is another kind symmetry which is well held in strong interactions. U-spin can connect two different kinds of weak decays [77, 78, 79]:  $b \rightarrow s$  ( $\Delta S = 1$ ) and  $b \rightarrow d$  by exchange of  $d \leftrightarrow s$ . The decay amplitudes of  $b \rightarrow s$  process can be expressed as:

$$\mathcal{A}(B \rightarrow f) = V_{ub}^* V_{us} \mathcal{A}_u + V_{cb}^* V_{cs} \mathcal{A}_c, \quad (116)$$

$$\mathcal{A}(\bar{B} \rightarrow \bar{f}) = V_{ub} V_{us}^* \mathcal{A}_u + V_{cb} V_{cs}^* \mathcal{A}_c, \quad (117)$$

while the decay amplitudes of  $UB \rightarrow Uf$  are

$$\mathcal{A}(UB \rightarrow Uf) = V_{ub}^* V_{ud} U \mathcal{A}_u + V_{cb}^* V_{cd} U \mathcal{A}_c, \quad (118)$$

$$\mathcal{A}(U\bar{B} \rightarrow U\bar{f}) = V_{ub} V_{ud}^* U \mathcal{A}_u + V_{cb} V_{cd}^* U \mathcal{A}_c. \quad (119)$$

Using the relation  $\mathcal{A}_u = U \mathcal{A}_u$  and  $\mathcal{A}_c = U \mathcal{A}_c$  in U-spin symmetry limit and the CKM unitarity relation

$$\text{Im}(V_{ub}^* V_{us} V_{cd} V_{cs}^*) = -\text{Im}(V_{ub}^* V_{ud} V_{cd} V_{cd}^*), \quad (120)$$

we obtain

$$|\mathcal{A}(B \rightarrow f)|^2 - |\mathcal{A}(\bar{B} \rightarrow \bar{f})|^2 = -|\mathcal{A}(UB \rightarrow Uf)|^2 + |\mathcal{A}(U\bar{B} \rightarrow U\bar{f})|^2. \quad (121)$$

This equation relates the differences of partial decay widths. The following radiative  $B$  decays can be related to each other by this symmetry:  $B^- \rightarrow \rho^- \gamma$  and  $B^- \rightarrow K^{*-} \gamma$ ;  $\bar{B}^0 \rightarrow \bar{K}^{*0} \gamma$  and  $\bar{B}_s^0 \rightarrow K^{*0} \gamma$ . As an example, we define the following parameter to test U-spin symmetry breaking:

$$\Delta \equiv A_{CP}(B^- \rightarrow K^{*-} \gamma) - A_{CP}(B^- \rightarrow \rho^- \gamma) \times \frac{\mathcal{BR}(B^- \rightarrow \rho^- \gamma)}{\mathcal{BR}(B^- \rightarrow K^{*-} \gamma)}. \quad (122)$$

In our pQCD calculation, we find

$$\Delta = (-8.4_{-0.8-2.3-0.6}^{+0.4+1.3+0.3}) \times 10^{-3}. \quad (123)$$

This result is close to 0. The U spin symmetry seems quite good here. But the most important reason is the small CP asymmetry in  $B^- \rightarrow K^{*-} \gamma$  and the small ratio  $\frac{\mathcal{BR}(B^- \rightarrow \rho^- \gamma)}{\mathcal{BR}(B^- \rightarrow K^{*-} \gamma)}$ . The absolute value for the  $b \rightarrow s$  channel's CP asymmetry is small. This direct CP asymmetry may be dramatically enhanced by some new physics with a different weak phase. The precise measurement of CP asymmetries can at least give a constraint on the non-standard model scenario parameters.

## V. CALCULATION OF $B \rightarrow A(1^3P_1)\gamma$ AND $A(1^1P_1)\gamma$ DECAYS

The factorization formulae for  $B \rightarrow A\gamma$  is more complicated than  $B \rightarrow V\gamma$  because of the mixing between different mesons:  $K_{1A}$  and  $K_{1B}$ ;  $f_1$  and  $f_8$ ;  $h_1$  and  $h_8$ . The real physical states  $K_1(1270)$  and  $K_1(1400)$  are mixtures of the  $K_{1A}$  and  $K_{1B}$  states with the mixing angle  $\theta_K$ :

$$|K_1(1270)\rangle = |K_{1A}\rangle\sin\theta_K + |K_{1B}\rangle\cos\theta_K, \quad (124)$$

$$|K_1(1400)\rangle = |K_{1A}\rangle\cos\theta_K - |K_{1B}\rangle\sin\theta_K. \quad (125)$$

In flavor SU(3) symmetry limit, these mesons can not mix with each other; but since  $s$  quark is heavier than the  $u, d$  quarks,  $K_1(1270)$  and  $K_1(1400)$  are not purely  $1^3P_1$  or  $1^1P_1$  states. In general, the mixing angle can be determined by experimental data. The partial decay rate for  $\tau^- \rightarrow K_1\nu_\tau$  is given by:

$$\Gamma(\tau^- \rightarrow K_1\nu_\tau) = \frac{m_\tau^3}{16\pi} G_F^2 |V_{us}|^2 f_A^2 \left(1 - \frac{m_A^2}{m_\tau^2}\right)^2 \left(1 + \frac{2m_A^2}{m_\tau^2}\right), \quad (126)$$

with the measured results for branching fractions [30]:

$$\mathcal{BR}(\tau^- \rightarrow K_1(1270)\nu_\tau) = (4.7 \pm 1.1) \times 10^{-3}, \quad \mathcal{BR}(\tau^- \rightarrow K_1(1400)\nu_\tau) = (1.7 \pm 2.6) \times 10^{-3}. \quad (127)$$

We can straightforward obtain the longitudinal decay constant (in MeV):

$$|f_{K_1(1270)}| = 169_{-21}^{+19}; \quad |f_{K_1(1400)}| = 125_{-125}^{+74}. \quad (128)$$

In principle, one can combine the decay constants for  $K_{1A}$ ,  $K_{1B}$  evaluated in QCD sum rules with the above results to determine the mixing angle  $\theta_K$ . But since there are large uncertainties in Eq. (128), the constraint on the mixing angle is expected to be rather smooth:

$$-143^\circ < \theta_K < -120^\circ, \quad \text{or} \quad -49^\circ < \theta_K < -27^\circ, \quad \text{or} \quad 37^\circ < \theta_K < 60^\circ, \quad \text{or} \quad 131^\circ < \theta_K < 153^\circ. \quad (129)$$

where we have taken the uncertainties from the branching ratios in Eq.(127) and the first Gegenbauer moment  $a_1^K$  into account but neglected the mass differences as usual. For simplicity, we use two reference values in Ref. [37]

$$\theta_K = \pm 45^\circ. \quad (130)$$

Besides, the flavor-octet and the flavor-singlet can also mix with each other:

$$|f_1(1285)\rangle = |f_1\rangle\cos\theta_{3P_1} + |f_8\rangle\sin\theta_{3P_1}, \quad |f_1(1420)\rangle = -|f_1\rangle\sin\theta_{3P_1} + |f_8\rangle\cos\theta_{3P_1}, \quad (131)$$

$$|h_1(1170)\rangle = |h_1\rangle\cos\theta_{1P_1} + |h_8\rangle\sin\theta_{1P_1}, \quad |h_1(1380)\rangle = -|h_1\rangle\sin\theta_{1P_1} + |h_8\rangle\cos\theta_{1P_1}. \quad (132)$$

The reference points are chosen as:  $\theta_{3P_1} = 38^\circ$  or  $\theta_{3P_1} = 50^\circ$ ;  $\theta_{1P_1} = 10^\circ$  or  $\theta_{1P_1} = 45^\circ$  [37]. We should point out that if the mixing angle is  $\theta = 35.3^\circ$ , the mixing is ideal:  $f_1(1285)$  is made up of  $\frac{\bar{u}u+\bar{d}d}{\sqrt{2}}$  while  $f_1(1420)$  is composed of  $\bar{s}s$ . Thus some of the form factors are very small which will of course give small production rates of this meson.

Apart from these differences, the expression for  $B \rightarrow A\gamma$  is different from  $B \rightarrow V\gamma$  in more aspects. Since the twist-2 LCDA  $\phi_{||}$  is normalized to  $a_0^{||}$ , we should replace the decay constant  $f_V$  by  $f_A a_0^{||}$  in the first two annihilation diagrams. As there is no overlap between an axial-vector meson and a photon (wrong parity), there is no contribution from the two photon electromagnetic operator diagrams in Fig. 8. Regardless of these differences, the factorization formulae for  $B \rightarrow A\gamma$  decays can be obtained from the corresponding  $B \rightarrow V\gamma$  ones using the replacement in Eq. (39) if the electroweak current is  $\sigma_{\mu\nu}(1 + \gamma_5)$  or  $\gamma_\mu(1 - \gamma_5)$  type. If the current is  $\sigma_{\mu\nu}(1 - \gamma_5)$ , we should add an additional minus sign. In annihilation diagrams, if the electroweak current is  $LL$  or  $SP$  in the lower two diagrams, we need replace the distribution amplitudes as in Eq. (39); while we add a minus sign if the current is  $LR$ . We show the formulas in Appendix C.

Branching ratios (in unit of  $10^{-6}$ ) and direct CP asymmetries (in %) for  $B \rightarrow (a_1, b_1)\gamma$  processes are calculated straightforward as follows:

$$\mathcal{BR}(B^- \rightarrow a_1^-(1260)\gamma) = 3.0_{-1.1-0.3-0.2-0.7}^{+1.6+0.4+0.4+0.8}, \quad (133)$$

$$\mathcal{BR}(\bar{B}^0 \rightarrow a_1^0(1260)\gamma) = 1.5_{-0.5-0.2-0.1-0.4}^{+0.7+0.2+0.2+0.4}, \quad (134)$$

$$\mathcal{BR}(\bar{B}_s \rightarrow a_1^0(1260)\gamma) = (2.1_{-0.5-0.1-0.1-0.0}^{+0.6+0.3+0.1+0.0}) \times 10^{-4}, \quad (135)$$

$$\mathcal{BR}(B^- \rightarrow b_1^-(1235)\gamma) = 2.0_{-0.7-0.3-0.1-0.5}^{+1.0+0.4+0.3+0.6}, \quad (136)$$

$$\mathcal{BR}(\bar{B}^0 \rightarrow b_1^0(1235)\gamma) = 1.1_{-0.3-0.1-0.1-0.2}^{+0.5+0.2+0.2+0.3}, \quad (137)$$

$$\mathcal{BR}(\bar{B}_s \rightarrow b_1^0(1235)\gamma) = (5.4_{-0.9-2.5-0.2-1.8}^{+1.0+6.4+0.3+2.1}) \times 10^{-5}, \quad (138)$$

$$A_{CP}^{dir}(B^- \rightarrow a_1^-(1260)\gamma) = 11.2_{-0.5-2.4-0.8-1.3}^{+2.3+3.0+0.9+2.7}, \quad (139)$$

$$A_{CP}^{dir}(\bar{B}^0 \rightarrow a_1^0(1260)\gamma) = 3.8_{-0.5-0.5-0.3-0.7}^{+0.3+0.3+0.2+0.4}, \quad (140)$$

$$A_{CP}^{dir}(\bar{B}_s \rightarrow a_1^0(1260)\gamma) = 0.8_{-0.1-1.5-0.0-0.0}^{+0.1+0.8+0.1+0.0}, \quad (141)$$

$$A_{CP}^{dir}(B^- \rightarrow b_1^-(1235)\gamma) = 16.0_{-0.5-2.7-1.1-0.7}^{+1.3+4.2+0.7+1.7}, \quad (142)$$

$$A_{CP}^{dir}(\bar{B}^0 \rightarrow b_1^0(1235)\gamma) = 11.0_{-0.3-2.5-0.7-0.2}^{+0.2+1.9+0.5+0.3}, \quad (143)$$

$$A_{CP}^{dir}(\bar{B}_s \rightarrow b_1^0(1235)\gamma) = -0.5_{-0.0-1.5-0.0-0.0}^{+0.0+2.7+0.0+0.0}, \quad (144)$$

while we give branching ratios and CP asymmetries for  $B \rightarrow K_1(f_1, h_1)\gamma$  in table IX and X, respectively. The errors for these entries correspond to uncertainties in the input hadronic quantities,

TABLE IX:  $CP$ -averaged branching ratios ( $\times 10^{-6}$ ) of  $B \rightarrow A\gamma$  decays obtained in pQCD approach using two different mixing angles; the errors for these entries correspond to uncertainties in the input hadronic quantities, from the scale-dependence, and CKM matrix elements, the Gegenbauer moments of the axial-vector mesons respectively.

Modes	$\theta_K = 45^\circ$	$\theta_K = -45^\circ$	Exp.
$B^- \rightarrow K_1^-(1270)\gamma$	$134^{+68+21+4+41}_{-49-18-4-38}$	$1.4^{+1.2+0.3+0.0+5.0}_{-0.7-0.6-0.0-2.0}$	$42.8 \pm 9.4 \pm 4.3$ [21]
$\bar{B}^0 \rightarrow \bar{K}_1^0(1270)\gamma$	$141^{+64+19+4+45}_{-48-18-4-41}$	$1.4^{+0.9+0.3+0.0+5.4}_{-0.6-0.5-0.0-1.9}$	
$B^- \rightarrow K_1^-(1400)\gamma$	$1.4^{+1.2+0.3+0.0+5.0}_{-0.7-0.6-0.0-2.0}$	$134^{+68+21+4+41}_{-49-18-4-38}$	$< 14.4$
$\bar{B}^0 \rightarrow \bar{K}_1^0(1400)\gamma$	$1.4^{+0.9+0.3+0.0+5.4}_{-0.6-0.5-0.0-1.9}$	$141^{+64+19+4+45}_{-48-18-4-41}$	
$\bar{B}_s \rightarrow K_1^0(1270)\gamma$	$0.19^{+0.07+0.02+0.02+0.34}_{-0.06-0.03-0.01-0.22}$	$0.38^{+0.24+0.09+0.07+0.44}_{-0.15-0.07-0.03-0.32}$	
$\bar{B}_s \rightarrow K_1^0(1400)\gamma$	$0.38^{+0.24+0.09+0.07+0.44}_{-0.15-0.07-0.03-0.32}$	$0.19^{+0.07+0.02+0.02+0.34}_{-0.06-0.03-0.01-0.22}$	
Modes	$\theta_{3P_1} = 38^\circ$	$\theta_{3P_1} = 50^\circ$	
$\bar{B}^0 \rightarrow f_1(1285)\gamma$	$1.7^{+0.8+0.2+0.2+0.5}_{-0.6-0.2-0.1-0.4}$	$1.6^{+0.7+0.2+0.2+0.4}_{-0.5-0.2-0.1-0.4}$	
$\bar{B}^0 \rightarrow f_1(1420)\gamma$	$(4.9^{+2.3+0.6+0.7+3.9}_{-1.7-1.1-0.3-2.7}) \times 10^{-3}$	$0.11^{+0.05+0.01+0.02+0.04}_{-0.04-0.02-0.01-0.04}$	
$\bar{B}_s^0 \rightarrow f_1(1285)\gamma$	$0.11^{+0.05+0.01+0.00+0.03}_{-0.04-0.01-0.00-0.03}$	$3.8^{+1.6+0.4+0.1+0.7}_{-1.2-0.4-0.1-0.7}$	
$\bar{B}_s^0 \rightarrow f_1(1420)\gamma$	$61.9^{+24.5+5.5+1.8+17.4}_{-18.9-6.0-1.8-15.5}$	$58.2^{+22.9+5.1+1.6+16.7}_{-17.7-5.6-1.7-14.8}$	
Modes	$\theta_{1P_1} = 10^\circ$	$\theta_{1P_1} = 45^\circ$	
$\bar{B}^0 \rightarrow h_1(1170)\gamma$	$0.99^{+0.43+0.16+0.14+0.24}_{-0.33-0.13-0.06-0.21}$	$1.24^{+0.55+0.20+0.18+0.31}_{-0.41-0.16-0.08-0.27}$	
$\bar{B}^0 \rightarrow h_1(1380)\gamma$	$0.28^{+0.12+0.05+0.04+0.07}_{-0.09-0.04-0.02-0.06}$	$(2.0^{+0.8+0.3+0.3+0.3}_{-0.7-0.3-0.1-0.3}) \times 10^{-2}$	
$\bar{B}_s^0 \rightarrow h_1(1170)\gamma$	$7.9^{+2.9+1.0+0.2+1.8}_{-2.2-0.7-0.2-1.6}$	$2.3^{+0.9+0.3+0.1+0.7}_{-0.7-0.3-0.1-0.6}$	
$\bar{B}_s^0 \rightarrow h_1(1380)\gamma$	$44.4^{+16.8+5.6+1.3+11.0}_{-12.8-4.1-1.3-9.7}$	$50.0^{+18.8+6.3+1.5+12.2}_{-14.3-4.5-1.5-10.7}$	

the scale-dependence, CKM matrix elements, and the Gegenbauer moments of the axial-vector mesons. It is noted that theoretical uncertainties for branching ratios are quite large. The branching fractions of  $B \rightarrow a_1(1260)(b_1(1235))\gamma$  are larger than that of  $B \rightarrow \rho\gamma$ , as we have shown that  $B \rightarrow A$  form factors are larger. As we have mentioned in the above, there are some ambiguities in the quark content of  $B \rightarrow K_1(f_1, h_1)\gamma$ : these mesons are mixtures but the mixing angles are not uniquely determined. The reference points for the mixing angles are two-fold, thus we give two different kinds of results collected in these two tables. The branching ratios and CP asymmetries are very sensitive to the mixing angles, which is not quite constrained.

Experimentalist gave results for  $B^- \rightarrow K_1^-(1270)\gamma$  [21] shown also in table IX. Compared with it, our result for  $B^- \rightarrow K_1^-(1270)\gamma$ , is about 3 times larger, when  $\theta_K = 45^\circ$ ; or very smaller than the experimental results, when  $\theta_K = -45^\circ$ . In Fig. 9, we show the strong dependence of the branching

TABLE X: Direct CP asymmetries of  $B \rightarrow A\gamma$  decays obtained in pQCD approach using two different mixing angles; the errors for these entries correspond to uncertainties in the input hadronic quantities, from the scale-dependence, and CKM matrix elements, respectively.

Modes	$\theta_K = 45^\circ$	$\theta_K = -45^\circ$
$B^- \rightarrow K_1^-(1270)\gamma$	$-0.6^{+0.0+0.2+0.0+0.1}_{-0.0-0.1-0.0-0.1}$	$-3.8^{+0.7+1.1+1.8+4.0}_{-1.3-0.3-0.3-13.0}$
$\bar{B}^0 \rightarrow \bar{K}_1^0(1270)\gamma$	$-0.2 \pm 0.0 \pm 0.0 \pm 0.0 \pm 0.0$	$0.1^{+0.0+0.1+0.0+2.2}_{-0.1-0.3-0.0-0.4}$
$B^- \rightarrow K_1^-(1400)\gamma$	$-3.8^{+0.7+1.1+1.8+4.0}_{-1.3-0.3-0.3-13.0}$	$-0.6^{+0.0+0.2+0.0+0.1}_{-0.0-0.1-0.0-0.1}$
$\bar{B}^0 \rightarrow \bar{K}_1^0(1400)\gamma$	$0.1^{+0.0+0.1+0.0+2.2}_{-0.1-0.3-0.0-0.4}$	$-0.2 \pm 0.0 \pm 0.0 \pm 0.0 \pm 0.0$
$\bar{B}_s \rightarrow K_1^0(1270)\gamma$	$-8.4^{+0.0+0.5+0.4+5.1}_{-2.9-3.4-0.4-11.2}$	$-3.1^{+3.9+4.0+0.8+8.6}_{-0.1-3.1-0.6-14.1}$
$\bar{B}_s \rightarrow K_1^0(1400)\gamma$	$-3.1^{+3.9+4.0+0.8+8.6}_{-0.1-3.1-0.6-14.1}$	$-8.4^{+0.0+0.5+0.4+5.1}_{-2.9-3.4-0.4-11.2}$
Modes	$\theta_{3P_1} = 38^\circ$	$\theta_{3P_1} = 50^\circ$
$\bar{B}^0 \rightarrow f_1(1285)\gamma$	$3.4^{+0.6+0.8+0.2+0.7}_{-0.1-0.5-0.2-0.1}$	$3.4^{+0.7+0.8+0.2+0.8}_{-0.1-0.4-0.2-0.1}$
$\bar{B}^0 \rightarrow f_1(1420)\gamma$	$7.1^{+0.0+0.7+0.3+0.0}_{-3.1-7.7-0.5-2.3}$	$4.1^{+0.1+0.5+0.2+0.1}_{-0.3-1.9-0.3-0.4}$
$\bar{B}_s^0 \rightarrow f_1(1285)\gamma$	$-0.1^{+0.3+0.1+0.0+0.1}_{-0.0-0.1-0.0-0.2}$	$-0.2^{+0.1+0.0+0.0+0.0}_{-0.0-0.1-0.0-0.0}$
$\bar{B}_s^0 \rightarrow f_1(1420)\gamma$	$-0.2 \pm 0.0 \pm 0.0 \pm 0.0 \pm 0.0$	$-0.2 \pm 0.0 \pm 0.0 \pm 0.0 \pm 0.0$
Modes	$\theta_{1P_1} = 10^\circ$	$\theta_{1P_1} = 45^\circ$
$\bar{B}^0 \rightarrow h_1(1170)\gamma$	$10.2^{+0.0+1.4+0.4+0.0}_{-0.9-2.5-0.7-0.4}$	$10.1^{+0.1+1.7+0.4+0.2}_{-0.5-2.3-0.7-0.3}$
$\bar{B}^0 \rightarrow h_1(1380)\gamma$	$9.8^{+0.8+2.4+0.4+1.1}_{-0.0-2.0-0.7-0.0}$	$11.3^{+0.0+0.0+0.5+0.0}_{-5.1-4.2-0.7-3.5}$
$\bar{B}_s^0 \rightarrow h_1(1170)\gamma$	$-0.2 \pm 0.0 \pm 0.0 \pm 0.0 \pm 0.0$	$-0.1^{+0.0+0.0+0.0+0.0}_{-0.0-0.1-0.0-0.0}$
$\bar{B}_s^0 \rightarrow h_1(1380)\gamma$	$-0.2 \pm 0.0 \pm 0.0 \pm 0.0 \pm 0.0$	$-0.2 \pm 0.0 \pm 0.0 \pm 0.0 \pm 0.0$

ratio on the mixing angle. At  $\theta_K = 45^\circ$ , the  $B^- \rightarrow K_1^-(1270)\gamma$  receives almost a maximal branching ratio. The current  $B^- \rightarrow K_1^-(1270)\gamma$  experiment implies our chosen two reference points of the mixing angle are not favored. From this Fig. 9, we could read out the experimental constrained mixing angle value, which are also two fold. However large hadronic uncertainties and the missing next-to-leading order corrections [80] plus the still large experimental error bars make this constraint not very effective. Except for these two processes, other decay modes have not been measured. Here we refrain from a direct comparison with the previous studies on  $B \rightarrow A\gamma$  [7, 38, 81, 82, 83, 84], as the analysis is similar in  $B \rightarrow A$  form factors which has been performed in section III.

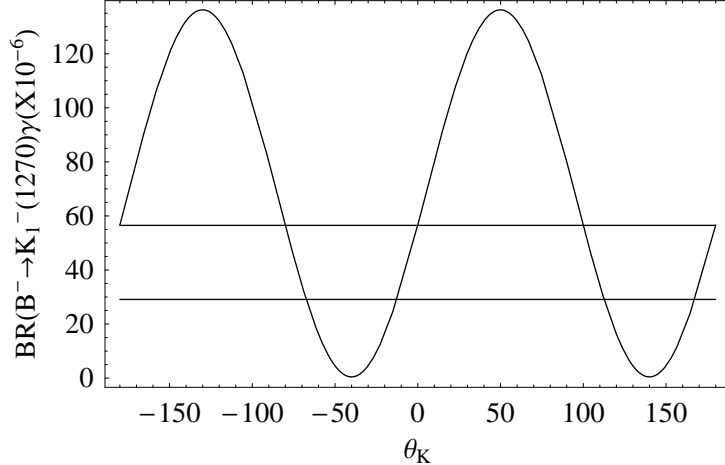


FIG. 9: The  $\theta_K$  dependence of the  $B^- \rightarrow K_1^-(1270)\gamma$  branching ratio. The region between the two horizontal lines are allowed by the experimental  $1\sigma$  bound, where we add the statistic and the systematic uncertainties linearly:  $29.1 < \mathcal{BR} < 56.5$ .

## VI. SUMMARY

pQCD approach is based on  $k_T$  factorization where we keep the transverse momentum of valence quarks in the meson, to smear the endpoint singularity.  $k_T$  resummation of double logarithms results in the Sudakov factor. Resummation of double logarithms from the threshold region leads to the jet function. Sudakov factor and jet function can suppress the contribution from the large  $b$  region and small  $x$  region, respectively. This makes the pQCD approach self-consistent. Inspired by the success of pQCD approach in non-leptonic B decays [85], we give a comprehensive study on the charmless  $B_{(s)} \rightarrow V(A)\gamma$  decays in pQCD approach.

Semi-leptonic and radiative decays are somewhat simpler than non-leptonic decays as only one hadronic meson involved in the final state. In this case, the dominant amplitude can be parameterized in form factors. In order to make precise prediction and extract CKM matrix elements, we have to know the behavior of form factors. In pQCD approach, the final state meson moves nearly on the light-cone and a hard-gluon-exchange is required. Thus the dominant contribution is from the hard region which can be factorized. In section III, we have used the same input hadronic parameters with Ref. [19] and updated all the  $B \rightarrow V$  decay form factors in pQCD approach. Compared with the results evaluated from other approaches, we find: despite of a number of theoretical differences in different approaches, all the numerical results of the form factors are surprisingly consistent with each other.

The 10  $B \rightarrow V\gamma$  decay channels can be divided into three categories based on their dominant quark transition  $b \rightarrow s$ ,  $b \rightarrow d$  and the annihilation topology. Our prediction on the first category



of decays  $\mathcal{BR}(B \rightarrow K^*\gamma)$  is consistent with the averaged value from experiments. On the  $b \rightarrow d$  transition, branching ratios have been given by BaBar and Belle collaborations with still large error bars. We find our results are well consistent with BaBar's results but a little far from the Belle's central value results in some channels. We also give our predictions on the purely annihilation type decays with very small branching ratios in SM. In three  $b \rightarrow s$  transitions  $B^- \rightarrow K^{*-}\gamma$ ,  $\bar{B}^0 \rightarrow \bar{K}^{*0}\gamma$  and  $\bar{B}_s \rightarrow \phi\gamma$ , the direct CP asymmetry is small, since the tree contribution is suppressed by the CKM matrix element. In the  $b \rightarrow d$  transitions  $B^- \rightarrow \rho^-\gamma$ ,  $\bar{B}^0 \rightarrow \bar{\rho}^0(\omega)\gamma$  and  $\bar{B}_s \rightarrow K^{*0}\gamma$ , the tree contribution can be comparable with the penguin contribution. Thus we obtain large CP asymmetries in these four processes. In SM, the two quantities  $S_f$  and  $H_f$  in time-dependent decay are expected to be rather small. This is due to the fact that the dominant contribution to decay amplitudes comes from the chiral-odd dipole operator  $O_7$ . Except for a few decays discussed in the above, all other decay modes including  $\bar{B}_s$  decays and annihilation type decays, remain essentially unexplored. We wish a wealth of measurements at the  $B$  factories and other experiments in the future.

In section III, we also study  $B \rightarrow A$  form factors. As the quark contents (to be precise the mixing angle) for the axial-vectors have not been uniquely determined, we give two different kinds of results for the form factors according to different mixing angles. For the axial-vector mesons  $f_1$ , we have used the mixing angle between the octet and singlet:  $\theta = 38^\circ(50^\circ)$  which is close to the ideal mixing angle  $\theta = 35.3^\circ$ . With this mixing angle, one can easily check that the lighter meson  $f_1(1285)$  is made almost up of  $\frac{\bar{u}u + \bar{d}d}{\sqrt{2}}$  while the heavier meson  $f_1(1420)$  is composed of  $\bar{s}s$ . Thus partial decay widths of  $B \rightarrow f_1(1420)\gamma$  and  $B_s \rightarrow f_1(1285)\gamma$  are suppressed by the flavor structure. In Fig. 9, we show the strong dependence of the  $B^- \rightarrow K_1^-(1270)\gamma$  decay branching ratio on the mixing angle  $\theta_K$ . Our calculation can be used to constrain this mixing angle using experimental measurements provided with well understood hadronic inputs. The study of higher resonance production in  $B$  decays can help us to uncover the mysterious structure of these excited states.

### Acknowledgements

This work is partly supported by National Science Foundation of China under the Grant No. 10475085 and 10625525. We would like to acknowledge S.-Y. Li, Y. Li, Y.-L. Shen, X.-X. Wang, Y.-M. Wang, K.-C. Yang, M.-Z. Yang and H. Zou for valuable discussions.

## APPENDIX A: PQCD FUNCTIONS

In this appendix, we group the functions which appear in the factorization formulae. The hard scales are chosen as

$$t_a = \max\{\sqrt{x_2}m_B, 1/b_1, 1/b_2\}, \quad t'_a = \max\{\sqrt{x_1}m_B, 1/b_1, 1/b_2\}, \quad (\text{A1})$$

$$t_b = \max\{\sqrt{x_1x_2}m_B, \sqrt{(1-x_2)}m_B, 1/b_1, 1/b_2\}, \quad (\text{A2})$$

$$t'_b = \max\{\sqrt{x_1x_2}m_B, \sqrt{1+x_1}m_B, 1/b_1, 1/b_2\}, \quad (\text{A3})$$

$$t_c = \max\{\sqrt{|x_1-x_2|}m_B, \sqrt{x_2}m_B, 1/b_1, 1/b_2\}, \quad (\text{A4})$$

$$t'_c = \max\{\sqrt{|x_1-x_2|}m_B, \sqrt{x_1}m_B, 1/b_1, 1/b_2\}, \quad (\text{A5})$$

$$t_d = \max\{\sqrt{x_1x_2}m_B, \sqrt{|B^2|}, 1/b_1\}, \quad (\text{A6})$$

$$t_e = \max\{\sqrt{1+x_1}m_B, 1/b_1\}, \quad t'_e = \max\{\sqrt{x_1}m_B, 1/b_1\}, \quad (\text{A7})$$

$$t_f = \max\{\sqrt{1-x_2}m_B, 1/b_2\}, \quad t'_f = \max\{\sqrt{x_2}m_B, 1/b_2\}. \quad (\text{A8})$$

The functions  $h_i$  in decay amplitudes are from the propagators of virtual quark and gluon and are defined by:

$$\begin{aligned} h_e(A, B, b_1, b_2) = & \left[ \theta(A)K_0(\sqrt{A}m_Bb_1) + \theta(-A)i\frac{\pi}{2}H_0(\sqrt{-A}m_Bb_1) \right] \\ & \times \left\{ \theta(b_1 - b_2) \left[ \theta(B)K_0(\sqrt{B}m_Bb_1)I_0(\sqrt{B}m_Bb_2) \right. \right. \\ & \left. \left. + \theta(-B)i\frac{\pi}{2}H_0^{(1)}(\sqrt{-B}m_Bb_1)J_0(\sqrt{-B}m_Bb_2) \right] + (b_1 \leftrightarrow b_2) \right\}, \quad (\text{A9}) \end{aligned}$$

where  $H_0^{(1)}(z) = J_0(z) + iY_0(z)$ .

The Sudakov factor from threshold resummation is universal, independent of flavors of internal quarks, twists, and the specific processes. To simplify the analysis, the following parametrization has been used [26]:

$$S_t(x) = \frac{2^{1+2c}\Gamma(3/2+c)}{\sqrt{\pi}\Gamma(1+c)} [x(1-x)]^c, \quad (\text{A10})$$

with  $c = 0.4$ . This parametrization, symmetric under the interchange of  $x$  and  $1-x$ , is convenient for evaluation of the amplitudes. It is obvious that the threshold resummation modifies the end-point behavior of the meson distribution amplitudes, rendering them vanish faster at  $x \rightarrow 0$ .

The evolution factors  $E_e^{(l)}$  and  $E_a^{(l)}$  are given by

$$E_e(t) = \alpha_s(t)S_t(x_2) \exp[-S_B(t) - S_2(t)], \quad E'_e(t) = \alpha_s(t)S_t(x_1) \exp[-S_B(t) - S_2(t)], \quad (\text{A11})$$

$$E_a(t) = S_t(x_1) \exp[-S_B(t)], \quad E'_a(t) = S_t(x_2) \exp[-S_2(t)], \quad (\text{A12})$$

in which the Sudakov exponents are defined as

$$S_B(t) = s\left(x_1 \frac{m_B}{\sqrt{2}}, b_1\right) + \frac{5}{3} \int_{1/b_1}^t \frac{d\bar{\mu}}{\bar{\mu}} \gamma_q(\alpha_s(\bar{\mu})), \quad (\text{A13})$$

$$S_2(t) = s\left(x_2 \frac{m_B}{\sqrt{2}}, b_2\right) + s\left((1-x_2) \frac{m_B}{\sqrt{2}}, b_2\right) + 2 \int_{1/b_2}^t \frac{d\bar{\mu}}{\bar{\mu}} \gamma_q(\alpha_s(\bar{\mu})), \quad (\text{A14})$$

with the quark anomalous dimension  $\gamma_q = -\alpha_s/\pi$ . The explicit form for the function  $s(Q, b)$  is:

$$\begin{aligned} s(Q, b) = & \frac{A^{(1)}}{2\beta_1} \hat{q} \ln\left(\frac{\hat{q}}{\hat{b}}\right) - \frac{A^{(1)}}{2\beta_1} (\hat{q} - \hat{b}) + \frac{A^{(2)}}{4\beta_1^2} \left(\frac{\hat{q}}{\hat{b}} - 1\right) - \left[\frac{A^{(2)}}{4\beta_1^2} - \frac{A^{(1)}}{4\beta_1} \ln\left(\frac{e^{2\gamma_E-1}}{2}\right)\right] \ln\left(\frac{\hat{q}}{\hat{b}}\right) \\ & + \frac{A^{(1)}\beta_2}{4\beta_1^3} \hat{q} \left[\frac{\ln(2\hat{q}) + 1}{\hat{q}} - \frac{\ln(2\hat{b}) + 1}{\hat{b}}\right] + \frac{A^{(1)}\beta_2}{8\beta_1^3} [\ln^2(2\hat{q}) - \ln^2(2\hat{b})], \end{aligned} \quad (\text{A15})$$

where the variables are defined by

$$\hat{q} \equiv \ln[Q/(\sqrt{2}\Lambda)], \quad \hat{b} \equiv \ln[1/(b\Lambda)], \quad (\text{A16})$$

and the coefficients  $A^{(i)}$  and  $\beta_i$  are

$$\begin{aligned} \beta_1 = \frac{33 - 2n_f}{12}, \quad \beta_2 = \frac{153 - 19n_f}{24}, \\ A^{(1)} = \frac{4}{3}, \quad A^{(2)} = \frac{67}{9} - \frac{\pi^2}{3} - \frac{10}{27}n_f + \frac{8}{3}\beta_1 \ln\left(\frac{1}{2}e^{\gamma_E}\right), \end{aligned} \quad (\text{A17})$$

$n_f$  is the number of the quark flavors and  $\gamma_E$  is the Euler constant. We will use the one-loop running coupling constant, i.e. we pick up only the four terms in the first line of the expression for the function  $s(Q, b)$ .

## APPENDIX B: ANALYTIC FORMULAE FOR THE $B \rightarrow V\gamma$ DECAY AMPLITUDES

The analytic formulae for  $B^- \rightarrow \rho^- \gamma$  is:

$$\begin{aligned} \mathcal{A}^i(B^- \rightarrow \rho^- \gamma) = & \frac{G_F}{\sqrt{2}} V_{ub} V_{ud}^* \left\{ \mathcal{M}_{1u}^{i(a)} + \mathcal{M}_{1u}^{i(b)}(Q_u) + \mathcal{M}_{2u}^i + \mathcal{M}_{ann}^{i(a,LL)}(a_1, Q_u) + \mathcal{M}_{ann}^{i(b,LL)}(a_1, Q_d, Q_u) \right\} \\ & + \frac{G_F}{\sqrt{2}} V_{cb} V_{cd}^* \left\{ \mathcal{M}_{1c}^{i(a)} + \mathcal{M}_{1c}^{i(b)}(Q_u) + \mathcal{M}_{2c}^i \right\} \\ & - \frac{G_F}{\sqrt{2}} V_{tb} V_{td}^* \left\{ \mathcal{M}_{7\gamma}^i + \mathcal{M}_{8g}^{i(a)} + \mathcal{M}_{8g}^{i(b)}(Q_u) + \mathcal{M}_{ann}^{i(a,LL)}(a_4 + a_{10}, Q_u) \right. \\ & \left. + \mathcal{M}_{ann}^{i(b,LL)}(a_4 + a_{10}, Q_d, Q_u) + \mathcal{M}_{ann}^{i(SP)}(a_6 + a_8, Q_d, Q_u) \right\}, \end{aligned} \quad (\text{B1})$$

while the expression for  $B^- \rightarrow K^{*-}\gamma$  is basically the same except with the only difference in the CKM matrix elements:  $V_{qd} \rightarrow V_{qs}$ . The formulas for other channels are

$$\begin{aligned}
\sqrt{2}\mathcal{A}^i(\bar{B}^0 \rightarrow \rho^0\gamma) = & \frac{G_F}{\sqrt{2}}V_{ub}V_{ud}^* \left\{ \mathcal{M}_{ann}^{i(a,LL)}(a_2, Q_d) + \mathcal{M}_{ann}^{i(b,LL)}(a_2, Q_u, Q_u) - \mathcal{M}_{1u}^{i(a)} - \mathcal{M}_{1u}^{i(b)}(Q_d) - \mathcal{M}_{2u}^i \right\} \\
& + \frac{G_F}{\sqrt{2}}V_{cb}V_{cd}^* \left\{ -\mathcal{M}_{1c}^{i(a)} - \mathcal{M}_{1c}^{i(b)}(Q_d) - \mathcal{M}_{2c}^i \right\} - \frac{G_F}{\sqrt{2}}V_{tb}V_{td}^* \left\{ -\mathcal{M}_{7\gamma}^i - \mathcal{M}_{8g}^{i(a)} \right. \\
& - \mathcal{M}_{8g}^{i(b)}(Q_d) + \mathcal{M}_{ann}^{i(a,LL)}(-a_4 + \frac{3}{2}a_7 + \frac{3}{2}a_9 + \frac{1}{2}a_{10}, Q_d) \\
& + \mathcal{M}_{ann}^{i(b,LL)}(a_3 + a_9, Q_u, Q_u) + \mathcal{M}_{ann}^{i(b,LR)}(a_5 + a_7, Q_u, Q_u) \\
& + \mathcal{M}_{ann}^{i(b,LL)}(-a_3 - a_4 + \frac{1}{2}a_9 + \frac{1}{2}a_{10}, Q_d, Q_d) + \mathcal{M}_{ann}^{i(b,LR)}(-a_5 + \frac{1}{2}a_7, Q_d, Q_d) \\
& \left. + \mathcal{M}_{ann}^{i(SP)}(-a_6 + \frac{1}{2}a_8, Q_d, Q_d) + \mathcal{M}_{en}^i(Q_u - Q_d) \right\}, \tag{B2}
\end{aligned}$$

$$\begin{aligned}
\sqrt{2}\mathcal{A}^i(\bar{B}^0 \rightarrow \omega\gamma) = & \frac{G_F}{\sqrt{2}}V_{ub}V_{ud}^* \left\{ \mathcal{M}_{ann}^{i(a,LL)}(a_2, Q_d) + \mathcal{M}_{ann}^{i(b,LL)}(a_2, Q_u, Q_u) + \mathcal{M}_{1u}^{i(a)} + \mathcal{M}_{1u}^{i(b)}(Q_d) + \mathcal{M}_{2u}^i \right\} \\
& + \frac{G_F}{\sqrt{2}}V_{cb}V_{cd}^* \left\{ \mathcal{M}_{1c}^{i(a)} + \mathcal{M}_{1c}^{i(b)}(Q_d) + \mathcal{M}_{2c}^i \right\} - \frac{G_F}{\sqrt{2}}V_{tb}V_{td}^* \left\{ \mathcal{M}_{7\gamma}^i + \mathcal{M}_{8g}^{i(a)} \right. \\
& + \mathcal{M}_{8g}^{i(b)}(Q_d) + \mathcal{M}_{ann}^{i(a,LL)}(2a_3 + a_4 + 2a_5 + \frac{1}{2}a_7 + \frac{1}{2}a_9 - \frac{1}{2}a_{10}, Q_d) \\
& + \mathcal{M}_{ann}^{i(b,LL)}(a_3 + a_9, Q_u, Q_u) + \mathcal{M}_{ann}^{i(b,LR)}(a_5 + a_7, Q_u, Q_u) \\
& + \mathcal{M}_{ann}^{i(b,LL)}(a_3 + a_4 - \frac{1}{2}a_9 - \frac{1}{2}a_{10}, Q_d, Q_d) + \mathcal{M}_{ann}^{i(b,LR)}(a_5 - \frac{1}{2}a_7, Q_d, Q_d) \\
& \left. + \mathcal{M}_{ann}^{i(SP)}(a_6 - \frac{1}{2}a_8, Q_d, Q_d) + \mathcal{M}_{en}^i(Q_u + Q_d) \right\}, \tag{B3}
\end{aligned}$$

$$\begin{aligned}
\mathcal{A}^i(\bar{B}^0 \rightarrow \bar{K}^{*0}\gamma) = & \frac{G_F}{\sqrt{2}}V_{ub}V_{us}^* \left\{ \mathcal{M}_{1u}^{i(a)} + \mathcal{M}_{1u}^{i(b)}(Q_d) + \mathcal{M}_{2u}^i \right\} \\
& + \frac{G_F}{\sqrt{2}}V_{cb}V_{cs}^* \left\{ \mathcal{M}_{1c}^{i(a)} + \mathcal{M}_{1c}^{i(b)}(Q_d) + \mathcal{M}_{2c}^i \right\} \\
& - \frac{G_F}{\sqrt{2}}V_{tb}V_{ts}^* \left\{ \mathcal{M}_{7\gamma}^i + \mathcal{M}_{8g}^{i(a)} + \mathcal{M}_{8g}^{i(b)}(Q_d) + \mathcal{M}_{ann}^{i(a,LL)}(a_4 - \frac{1}{2}a_{10}, Q_d) \right. \\
& \left. + \mathcal{M}_{ann}^{i(b,LL)}(a_4 - \frac{1}{2}a_{10}, Q_s, Q_d) + \mathcal{M}_{ann}^{i(SP)}(a_6 - \frac{1}{2}a_8, Q_s, Q_d) \right\}. \tag{B4}
\end{aligned}$$

The expression for  $\bar{B}_s \rightarrow K^{*0}\gamma$  can be obtained by replacing  $V_{qs}$  by  $V_{qd}$  from  $\bar{B}^0 \rightarrow \bar{K}^{*0}\gamma$ .

The formulas for the  $B_s \rightarrow \phi\gamma$  decay are

$$\begin{aligned}
\mathcal{A}^i(\bar{B}_s \rightarrow \phi\gamma) = & \frac{G_F}{\sqrt{2}} V_{ub} V_{us}^* \left\{ \mathcal{M}_{1u}^{i(a)} + \mathcal{M}_{1u}^{i(b)}(Q_s) + \mathcal{M}_{2u}^i \right\} \\
& + \frac{G_F}{\sqrt{2}} V_{cb} V_{cs}^* \left\{ \mathcal{M}_{1c}^{i(a)} + \mathcal{M}_{1c}^{i(b)}(Q_s) + \mathcal{M}_{2c}^i \right\} \\
& - \frac{G_F}{\sqrt{2}} V_{tb} V_{ts}^* \left\{ \mathcal{M}_{7\gamma}^i + \mathcal{M}_{8g}^{i(a)} + \mathcal{M}_{8g}^{i(b)}(Q_s) \right. \\
& + \mathcal{M}_{ann}^{i(a,LL)}(a_3 + a_4 + a_5 - \frac{1}{2}a_7 - \frac{1}{2}a_9 - \frac{1}{2}a_{10}, Q_s) \\
& + \mathcal{M}_{ann}^{i(b,LL)}(a_3 + a_4 - \frac{1}{2}a_9 - \frac{1}{2}a_{10}, Q_s, Q_s) + \mathcal{M}_{ann}^{i(b,LR)}(a_5 - \frac{1}{2}a_7, Q_s, Q_s) \\
& \left. + \mathcal{M}_{ann}^{i(SP)}(a_6 - \frac{1}{2}a_8, Q_s, Q_s) + \mathcal{M}_{en}^i(Q_s) \right\}. \tag{B5}
\end{aligned}$$

For the annihilation type decays, we have

$$\begin{aligned}
\mathcal{A}^i(\bar{B}^0 \rightarrow \phi\gamma) = & -\frac{G_F}{\sqrt{2}} V_{tb} V_{td}^* \left\{ \mathcal{M}_{ann}^{i(a,LL)}(a_3 + a_5 - \frac{1}{2}a_7 - \frac{1}{2}a_9, Q_s) + \mathcal{M}_{en}^i(Q_s) \right. \\
& \left. + \mathcal{M}_{ann}^{i(b,LL)}(a_3 - \frac{1}{2}a_9, Q_s, Q_s) + \mathcal{M}_{ann}^{i(b,LR)}(a_5 - \frac{1}{2}a_7, Q_s, Q_s) \right\}, \tag{B6}
\end{aligned}$$

$$\begin{aligned}
\sqrt{2}\mathcal{A}^i(\bar{B}_s \rightarrow \rho^0\gamma) = & \frac{G_F}{\sqrt{2}} V_{ub} V_{us}^* \left\{ \mathcal{M}_{ann}^{i(a,LL)}(a_2, Q_s) + \mathcal{M}_{ann}^{i(b,LL)}(a_2, Q_u, Q_u) \right\} \\
& - \frac{G_F}{\sqrt{2}} V_{tb} V_{ts}^* \left\{ \mathcal{M}_{ann}^{i(a,LL)}(\frac{3}{2}a_7 + \frac{3}{2}a_9, Q_s) + \mathcal{M}_{en}^i(Q_u - Q_d) \right. \\
& + \mathcal{M}_{ann}^{i(b,LL)}(a_3 + a_9, Q_u, Q_u) + \mathcal{M}_{ann}^{i(b,LR)}(a_5 + a_7, Q_u, Q_u) \\
& \left. + \mathcal{M}_{ann}^{i(b,LL)}(-a_3 + \frac{1}{2}a_9, Q_d, Q_d) + \mathcal{M}_{ann}^{i(b,LR)}(-a_5 + \frac{1}{2}a_7, Q_d, Q_d) \right\}, \tag{B7}
\end{aligned}$$

$$\begin{aligned}
\sqrt{2}\mathcal{A}^i(\bar{B}_s \rightarrow \omega\gamma) = & \frac{G_F}{\sqrt{2}} V_{ub} V_{us}^* \left\{ \mathcal{M}_{ann}^{i(a,LL)}(a_2, Q_s) + \mathcal{M}_{ann}^{i(b,LL)}(a_2, Q_u, Q_u) \right\} \\
& - \frac{G_F}{\sqrt{2}} V_{tb} V_{ts}^* \left\{ \mathcal{M}_{ann}^{i(a,LL)}(2a_3 + 2a_5 + \frac{1}{2}a_7 + \frac{1}{2}a_9, Q_s) + \mathcal{M}_{en}^i(Q_u + Q_d) \right. \\
& + \mathcal{M}_{ann}^{i(b,LL)}(a_3 + a_9, Q_u, Q_u) + \mathcal{M}_{ann}^{i(b,LR)}(a_5 + a_7, Q_u, Q_u) \\
& \left. + \mathcal{M}_{ann}^{i(b,LL)}(a_3 - \frac{1}{2}a_9, Q_d, Q_d) + \mathcal{M}_{ann}^{i(b,LR)}(a_5 - \frac{1}{2}a_7, Q_d, Q_d) \right\}. \tag{B8}
\end{aligned}$$

### APPENDIX C: ANALYTIC FORMULAE FOR THE $B \rightarrow A\gamma$ DECAY AMPLITUDES

The expression for  $B \rightarrow^1 P_1\gamma$  is different from  $B \rightarrow V\gamma$  in various aspects. The first two annihilation diagrams vanish for neutral axial vector mesons (not including  $K_{1B}$ ). There is not any two-photon diagram contribution in  $B \rightarrow A\gamma$  decays. The explicit formula for the  $B^- \rightarrow b_1^-(1235)\gamma$

decay amplitude is

$$\begin{aligned}
A^i(B^- \rightarrow b_1^-(1235)\gamma) &= \frac{G_F}{\sqrt{2}} V_{ub} V_{ud}^* \left\{ \mathcal{M}_{1u}^{i(a)} + \mathcal{M}_{1u}^{i(b)}(Q_u) + \mathcal{M}_{2u}^i + \mathcal{M}_{ann}^{i(b,LL)}(a_1, Q_d, Q_u) \right\} \\
&+ \frac{G_F}{\sqrt{2}} V_{cb} V_{cd}^* \left\{ \mathcal{M}_{1c}^{i(a)} + \mathcal{M}_{1c}^{i(b)}(Q_u) + \mathcal{M}_{2c}^i \right\} \\
&- \frac{G_F}{\sqrt{2}} V_{tb} V_{td}^* \left\{ \mathcal{M}_{7\gamma}^i + \mathcal{M}_{8g}^{i(a)} + \mathcal{M}_{8g}^{i(b)}(Q_u) \right. \\
&\quad \left. + \mathcal{M}_{ann}^{i(b,LL)}(a_4 + a_{10}, Q_d, Q_u) + \mathcal{M}_{ann}^{i(SP)}(a_6 + a_8, Q_d, Q_u) \right\}, \quad (C1)
\end{aligned}$$

while the expression for U-spin related process  $B^- \rightarrow K_{1B}^- \gamma$  is basically the same except with the only difference in the CKMmatrix elements:  $V_{qd} \rightarrow V_{qs}$ . The formulas for the neutral decays modes are

$$\begin{aligned}
\sqrt{2} A^i(\bar{B}^0 \rightarrow b_1^0(1235)\gamma) &= \frac{G_F}{\sqrt{2}} V_{ub} V_{ud}^* \left\{ \mathcal{M}_{ann}^{i(b,LL)}(a_2, Q_u, Q_u) - \mathcal{M}_{1u}^{i(a)} - \mathcal{M}_{1u}^{i(b)}(Q_d) - \mathcal{M}_{2u}^i \right\} \\
&+ \frac{G_F}{\sqrt{2}} V_{cb} V_{cd}^* \left\{ -\mathcal{M}_{1c}^{i(a)} - \mathcal{M}_{1c}^{i(b)}(Q_d) - \mathcal{M}_{2c}^i \right\} - \frac{G_F}{\sqrt{2}} V_{tb} V_{td}^* \left\{ -\mathcal{M}_{7\gamma}^i \right. \\
&- \mathcal{M}_{8g}^{i(b)}(Q_d) + \mathcal{M}_{ann}^{i(b,LL)}(a_3 + a_9, Q_u, Q_u) + \mathcal{M}_{ann}^{i(b,LR)}(a_5 + a_7, Q_u, Q_u) \\
&+ \mathcal{M}_{ann}^{i(b,LL)}(-a_3 - a_4 + \frac{1}{2}a_9 + \frac{1}{2}a_{10}, Q_d, Q_d) - \mathcal{M}_{8g}^{i(a)} \\
&\left. + \mathcal{M}_{ann}^{i(b,LR)}(-a_5 + \frac{1}{2}a_7, Q_d, Q_d) + \mathcal{M}_{ann}^{i(SP)}(-a_6 + \frac{1}{2}a_8, Q_d, Q_d) \right\}, \quad (C2)
\end{aligned}$$

$$\begin{aligned}
A^i(\bar{B}^0 \rightarrow \bar{K}_{1B}^0 \gamma) &= \frac{G_F}{\sqrt{2}} V_{ub} V_{us}^* \left\{ \mathcal{M}_{1u}^{i(a)} + \mathcal{M}_{1u}^{i(b)}(Q_d) + \mathcal{M}_{2u}^i \right\} \\
&+ \frac{G_F}{\sqrt{2}} V_{cb} V_{cs}^* \left\{ \mathcal{M}_{1c}^{i(a)} + \mathcal{M}_{1c}^{i(b)}(Q_d) + \mathcal{M}_{2c}^i \right\} \\
&- \frac{G_F}{\sqrt{2}} V_{tb} V_{ts}^* \left\{ \mathcal{M}_{7\gamma}^i + \mathcal{M}_{8g}^{i(a)} + \mathcal{M}_{8g}^{i(b)}(Q_d) + \mathcal{M}_{ann}^{i(a,LL)}(a_4 - \frac{1}{2}a_{10}, Q_d) \right. \\
&\left. + \mathcal{M}_{ann}^{i(b,LL)}(a_4 - \frac{1}{2}a_{10}, Q_s, Q_d) + \mathcal{M}_{ann}^{i(SP)}(a_6 - \frac{1}{2}a_8, Q_s, Q_d) \right\}, \quad (C3)
\end{aligned}$$

and the expression for  $\bar{B}_s \rightarrow K_{1B}^0 \gamma$  can be obtained by replacing  $V_{qs}$  by  $V_{qd}$ .

The decay amplitudes involving  $h_1(1170)$  and  $h_1(1380)$  can obtained as

$$A^i(B \rightarrow h_1(1170)\gamma) = A^i(B \rightarrow h_1\gamma)\cos\theta_{1P_1} + A^i(B \rightarrow h_8\gamma)\sin\theta_{1P_1}, \quad (C4)$$

$$A^i(B \rightarrow h_1(1380)\gamma) = -A^i(B \rightarrow h_1\gamma)\sin\theta_{1P_1} + A^i(B \rightarrow h_8\gamma)\cos\theta_{1P_1}, \quad (C5)$$

where  $B$  denotes  $\bar{B}^0$  or  $\bar{B}_s^0$  with

$$\begin{aligned}
\sqrt{2}\mathcal{A}^i(\bar{B}^0 \rightarrow h_8\gamma) &= \frac{G_F}{\sqrt{2}}V_{ub}V_{ud}^*\frac{1}{\sqrt{6}}\left\{\mathcal{M}_{ann}^{i(b,LL)}(a_2, Q_u, Q_u) + \mathcal{M}_{1u}^{i(a)} + \mathcal{M}_{1u}^{i(b)}(Q_d) + \mathcal{M}_{2u}^i\right\} \\
&+ \frac{G_F}{\sqrt{2}}V_{cb}V_{cd}^*\frac{1}{\sqrt{6}}\left\{\mathcal{M}_{1c}^{i(a)} + \mathcal{M}_{1c}^{i(b)}(Q_d) + \mathcal{M}_{2c}^i\right\} \\
&- \frac{G_F}{\sqrt{2}}V_{tb}V_{td}^*\frac{1}{\sqrt{6}}\left\{\mathcal{M}_{7\gamma}^i + \mathcal{M}_{8g}^{i(a)} + \mathcal{M}_{ann}^{i(SP)}(a_6 - \frac{1}{2}a_8, Q_d, Q_d)\right\} \\
&+ \mathcal{M}_{8g}^{i(b)}(Q_d) + \mathcal{M}_{ann}^{i(b,LL)}(a_3 + a_9, Q_u, Q_u) + \mathcal{M}_{ann}^{i(b,LR)}(a_5 + a_7, Q_u, Q_u) \\
&+ \mathcal{M}_{ann}^{i(b,LL)}(a_3 + a_4 - \frac{1}{2}a_9 - \frac{1}{2}a_{10}, Q_d, Q_d) + \mathcal{M}_{ann}^{i(b,LR)}(a_5 - \frac{1}{2}a_7, Q_d, Q_d) \\
&- 2\mathcal{M}_{ann}^{i(b,LL)}(a_3 - \frac{1}{2}a_9, Q_s, Q_s) - 2\mathcal{M}_{ann}^{i(b,LR)}(a_5 - \frac{1}{2}a_7, Q_s, Q_s)\left.\right\}, \quad (C6)
\end{aligned}$$

$$\begin{aligned}
\sqrt{2}\mathcal{A}^i(\bar{B}^0 \rightarrow h_1\gamma) &= \frac{G_F}{\sqrt{2}}V_{ub}V_{ud}^*\frac{1}{\sqrt{3}}\left\{\mathcal{M}_{ann}^{i(b,LL)}(a_2, Q_u, Q_u) + \mathcal{M}_{1u}^{i(a)} + \mathcal{M}_{1u}^{i(b)}(Q_d) + \mathcal{M}_{2u}^i\right\} \\
&+ \frac{G_F}{\sqrt{2}}V_{cb}V_{cd}^*\frac{1}{\sqrt{3}}\left\{\mathcal{M}_{1c}^{i(a)} + \mathcal{M}_{1c}^{i(b)}(Q_d) + \mathcal{M}_{2c}^i\right\} \\
&- \frac{G_F}{\sqrt{2}}V_{tb}V_{td}^*\frac{1}{\sqrt{3}}\left\{\mathcal{M}_{7\gamma}^i + \mathcal{M}_{8g}^{i(a)} + \mathcal{M}_{ann}^{i(SP)}(a_6 - \frac{1}{2}a_8, Q_d, Q_d)\right\} \\
&+ \mathcal{M}_{8g}^{i(b)}(Q_d) + \mathcal{M}_{ann}^{i(b,LL)}(a_3 + a_9, Q_u, Q_u) + \mathcal{M}_{ann}^{i(b,LR)}(a_5 + a_7, Q_u, Q_u) \\
&+ \mathcal{M}_{ann}^{i(b,LL)}(a_3 + a_4 - \frac{1}{2}a_9 - \frac{1}{2}a_{10}, Q_d, Q_d) + \mathcal{M}_{ann}^{i(b,LR)}(a_5 - \frac{1}{2}a_7, Q_d, Q_d) \\
&+ \mathcal{M}_{ann}^{i(b,LL)}(a_3 - \frac{1}{2}a_9, Q_s, Q_s) + \mathcal{M}_{ann}^{i(b,LR)}(a_5 - \frac{1}{2}a_7, Q_s, Q_s)\left.\right\}, \quad (C7)
\end{aligned}$$

$$\begin{aligned}
\mathcal{A}^i(\bar{B}_s \rightarrow h_8\gamma) &= \frac{G_F}{\sqrt{2}}V_{ub}V_{us}^*\frac{-2}{\sqrt{6}}\left\{\mathcal{M}_{1u}^{i(a)} + \mathcal{M}_{1u}^{i(b)}(Q_s) + \mathcal{M}_{2u}^i\right\} \\
&+ \frac{G_F}{\sqrt{2}}V_{cb}V_{cs}^*\frac{-2}{\sqrt{6}}\left\{\mathcal{M}_{1c}^{i(a)} + \mathcal{M}_{1c}^{i(b)}(Q_s) + \mathcal{M}_{2c}^i\right\} \\
&- \frac{G_F}{\sqrt{2}}V_{tb}V_{ts}^*\frac{-2}{\sqrt{6}}\left\{\mathcal{M}_{7\gamma}^i + \mathcal{M}_{8g}^{i(a)} + \mathcal{M}_{8g}^{i(b)}(Q_s) + \mathcal{M}_{ann}^{i(SP)}(a_6 - \frac{1}{2}a_8, Q_s, Q_s)\right. \\
&+ \mathcal{M}_{ann}^{i(b,LL)}(a_3 + a_4 - \frac{1}{2}a_9 - \frac{1}{2}a_{10}, Q_s, Q_s) + \mathcal{M}_{ann}^{i(b,LR)}(a_5 - \frac{1}{2}a_7, Q_s, Q_s)\left.\right\}, \\
&+ \frac{G_F}{\sqrt{2}}V_{ub}V_{us}^*\frac{1}{\sqrt{6}}\left\{\mathcal{M}_{ann}^{i(b,LL)}(a_2, Q_u, Q_u)\right\} \\
&- \frac{G_F}{\sqrt{2}}V_{tb}V_{ts}^*\frac{1}{\sqrt{6}}\left\{\mathcal{M}_{ann}^{i(b,LL)}(a_3 + a_9, Q_u, Q_u) + \mathcal{M}_{ann}^{i(b,LR)}(a_5 + a_7, Q_u, Q_u)\right. \\
&+ \mathcal{M}_{ann}^{i(b,LL)}(a_3 - \frac{1}{2}a_9, Q_d, Q_d) + \mathcal{M}_{ann}^{i(b,LR)}(a_5 - \frac{1}{2}a_7, Q_d, Q_d)\left.\right\}, \quad (C8)
\end{aligned}$$

$$\begin{aligned}
\mathcal{A}^i(\bar{B}_s \rightarrow h_1\gamma) &= \frac{G_F}{\sqrt{2}}V_{ub}V_{us}^* \frac{1}{\sqrt{3}} \left\{ \mathcal{M}_{1u}^{i(a)} + \mathcal{M}_{1u}^{i(b)}(Q_s) + \mathcal{M}_{2u}^i \right\} \\
&+ \frac{G_F}{\sqrt{2}}V_{cb}V_{cs}^* \frac{1}{\sqrt{3}} \left\{ \mathcal{M}_{1c}^{i(a)} + \mathcal{M}_{1c}^{i(b)}(Q_s) + \mathcal{M}_{2c}^i \right\} \\
&- \frac{G_F}{\sqrt{2}}V_{tb}V_{ts}^* \frac{1}{\sqrt{3}} \left\{ \mathcal{M}_{7\gamma}^i + \mathcal{M}_{8g}^{i(a)} + \mathcal{M}_{8g}^{i(b)}(Q_s) + \mathcal{M}_{ann}^{i(SP)}(a_6 - \frac{1}{2}a_8, Q_s, Q_s) \right. \\
&+ \mathcal{M}_{ann}^{i(b,LL)}(a_3 + a_4 - \frac{1}{2}a_9 - \frac{1}{2}a_{10}, Q_s, Q_s) + \mathcal{M}_{ann}^{i(b,LR)}(a_5 - \frac{1}{2}a_7, Q_s, Q_s) \left. \right\}, \\
&+ \frac{G_F}{\sqrt{2}}V_{ub}V_{us}^* \frac{1}{\sqrt{3}} \left\{ \mathcal{M}_{ann}^{i(b,LL)}(a_2, Q_u, Q_u) \right\} \\
&- \frac{G_F}{\sqrt{2}}V_{tb}V_{ts}^* \frac{1}{\sqrt{3}} \left\{ \mathcal{M}_{ann}^{i(b,LL)}(a_3 + a_9, Q_u, Q_u) + \mathcal{M}_{ann}^{i(b,LR)}(a_5 + a_7, Q_u, Q_u) \right. \\
&+ \mathcal{M}_{ann}^{i(b,LL)}(a_3 - \frac{1}{2}a_9, Q_d, Q_d) + \mathcal{M}_{ann}^{i(b,LR)}(a_5 - \frac{1}{2}a_7, Q_d, Q_d) \left. \right\}. \tag{C9}
\end{aligned}$$

The annihilation type decay amplitude is:

$$\begin{aligned}
\sqrt{2}\mathcal{A}^i(\bar{B}_s \rightarrow b_1^0(1235)\gamma) &= \frac{G_F}{\sqrt{2}}V_{ub}V_{us}^* \left\{ \mathcal{M}_{ann}^{i(b,LL)}(a_2, Q_u, Q_u) \right\} \\
&- \frac{G_F}{\sqrt{2}}V_{tb}V_{ts}^* \left\{ \mathcal{M}_{ann}^{i(b,LL)}(a_3 + a_9, Q_u, Q_u) + \mathcal{M}_{ann}^{i(b,LR)}(a_5 + a_7, Q_u, Q_u) \right. \\
&+ \mathcal{M}_{ann}^{i(b,LL)}(-a_3 + \frac{1}{2}a_9, Q_d, Q_d) + \mathcal{M}_{ann}^{i(b,LR)}(-a_5 + \frac{1}{2}a_7, Q_d, Q_d) \left. \right\} \tag{C10}
\end{aligned}$$

In the following, we will give the analytic factorization formulae for  $B \rightarrow^3 P_1\gamma$  which is similar with  $B \rightarrow V\gamma$  except for some differences in the flavor structure and zero contribution from the two-photon diagrams,

$$\begin{aligned}
\mathcal{A}^i(B^- \rightarrow a_1^-(1235)\gamma) &= \frac{G_F}{\sqrt{2}}V_{ub}V_{ud}^* \left\{ \mathcal{M}_{1u}^{i(a)} + \mathcal{M}_{1u}^{i(b)}(Q_u) + \mathcal{M}_{2u}^i + \mathcal{M}_{ann}^{i(a,LL)}(a_1, Q_u) \right. \\
&+ \mathcal{M}_{ann}^{i(b,LL)}(a_1, Q_d, Q_u) \left. \right\} + \frac{G_F}{\sqrt{2}}V_{cb}V_{cd}^* \left\{ \mathcal{M}_{1c}^{i(a)} + \mathcal{M}_{1c}^{i(b)}(Q_u) + \mathcal{M}_{2c}^i \right\} \\
&- \frac{G_F}{\sqrt{2}}V_{tb}V_{td}^* \left\{ \mathcal{M}_{7\gamma}^i + \mathcal{M}_{8g}^{i(a)} + \mathcal{M}_{8g}^{i(b)}(Q_u) + \mathcal{M}_{ann}^{i(a,LL)}(a_4 + a_{10}, Q_u) \right. \\
&+ \mathcal{M}_{ann}^{i(b,LL)}(a_4 + a_{10}, Q_d, Q_u) + \mathcal{M}_{ann}^{i(SP)}(a_6 + a_8, Q_d, Q_u) \left. \right\}, \tag{C11}
\end{aligned}$$

while the expression for  $B^- \rightarrow K_{1A}^-\gamma$  is the same except with the only difference in the CKM



matrix elements:  $V_{qd} \rightarrow V_{qs}$ . The formulas for other channels are

$$\begin{aligned}
\sqrt{2}\mathcal{A}^i(\bar{B}^0 \rightarrow a_1^0(1235)\gamma) &= \frac{G_F}{\sqrt{2}}V_{ub}V_{ud}^* \left\{ \mathcal{M}_{ann}^{i(a,LL)}(a_2, Q_d) + \mathcal{M}_{ann}^{i(b,LL)}(a_2, Q_u, Q_u) - \mathcal{M}_{1u}^{i(a)} \right. \\
&\quad \left. - \mathcal{M}_{1u}^{i(b)}(Q_d) - \mathcal{M}_{2u}^i \right\} + \frac{G_F}{\sqrt{2}}V_{cb}V_{cd}^* \left\{ -\mathcal{M}_{1c}^{i(a)} - \mathcal{M}_{1c}^{i(b)}(Q_d) - \mathcal{M}_{2c}^i \right\} \\
&\quad - \frac{G_F}{\sqrt{2}}V_{tb}V_{td}^* \left\{ -\mathcal{M}_{7\gamma}^i - \mathcal{M}_{8g}^{i(a)} \right. \\
&\quad \left. - \mathcal{M}_{8g}^{i(b)}(Q_d) + \mathcal{M}_{ann}^{i(a,LL)}(-a_4 + \frac{3}{2}a_7 + \frac{3}{2}a_9 + \frac{1}{2}a_{10}, Q_d) \right. \\
&\quad \left. + \mathcal{M}_{ann}^{i(b,LL)}(a_3 + a_9, Q_u, Q_u) + \mathcal{M}_{ann}^{i(b,LR)}(a_5 + a_7, Q_u, Q_u) \right. \\
&\quad \left. + \mathcal{M}_{ann}^{i(b,LL)}(-a_3 - a_4 + \frac{1}{2}a_9 + \frac{1}{2}a_{10}, Q_d, Q_d) \right. \\
&\quad \left. + \mathcal{M}_{ann}^{i(b,LR)}(-a_5 + \frac{1}{2}a_7, Q_d, Q_d) + \mathcal{M}_{ann}^{i(SP)}(-a_6 + \frac{1}{2}a_8, Q_d, Q_d) \right\}, \tag{C12}
\end{aligned}$$

$$\begin{aligned}
\mathcal{A}^i(\bar{B}^0 \rightarrow \bar{K}_{1A}^0\gamma) &= \frac{G_F}{\sqrt{2}}V_{ub}V_{us}^* \left\{ \mathcal{M}_{1u}^{i(a)} + \mathcal{M}_{1u}^{i(b)}(Q_d) + \mathcal{M}_{2u}^i \right\} \\
&\quad + \frac{G_F}{\sqrt{2}}V_{cb}V_{cs}^* \left\{ \mathcal{M}_{1c}^{i(a)} + \mathcal{M}_{1c}^{i(b)}(Q_d) + \mathcal{M}_{2c}^i \right\} \\
&\quad - \frac{G_F}{\sqrt{2}}V_{tb}V_{ts}^* \left\{ \mathcal{M}_{7\gamma}^i + \mathcal{M}_{8g}^{i(a)} + \mathcal{M}_{8g}^{i(b)}(Q_d) + \mathcal{M}_{ann}^{i(a,LL)}(a_4 - \frac{1}{2}a_{10}, Q_d) \right. \\
&\quad \left. + \mathcal{M}_{ann}^{i(b,LL)}(a_4 - \frac{1}{2}a_{10}, Q_s, Q_d) + \mathcal{M}_{ann}^{i(SP)}(a_6 - \frac{1}{2}a_8, Q_s, Q_d) \right\}, \tag{C13}
\end{aligned}$$

and the expression for  $\bar{B}_s \rightarrow K_{1A}^0\gamma$  can be obtained by replacing  $V_{qs}$  by  $V_{qd}$ .

The decay amplitudes involving  $f_1(1285)$  and  $f_1(1420)$  can be obtained as

$$A^i(B \rightarrow f_1(1285)\gamma) = A^i(B \rightarrow f_1\gamma)\cos\theta_{3P_1} + A^i(B \rightarrow f_8\gamma)\sin\theta_{3P_1}, \tag{C14}$$

$$A^i(B \rightarrow h_1(1420)\gamma) = -A^i(B \rightarrow f_1\gamma)\sin\theta_{3P_1} + A^i(B \rightarrow f_8\gamma)\cos\theta_{3P_1}, \tag{C15}$$

where  $B$  denotes  $\bar{B}^0$  or  $\bar{B}_s^0$  with

$$\begin{aligned}
\sqrt{2}\mathcal{A}^i(\bar{B}^0 \rightarrow f_8\gamma) &= \frac{G_F}{\sqrt{2}}V_{ub}V_{ud}^* \frac{1}{\sqrt{6}} \left\{ \mathcal{M}_{ann}^{i(a,LL)}(a_2, Q_d) + \mathcal{M}_{ann}^{i(b,LL)}(a_2, Q_u, Q_u) + \mathcal{M}_{1u}^{i(a)} \right. \\
&\quad \left. + \mathcal{M}_{1u}^{i(b)}(Q_d) + \mathcal{M}_{2u}^i \right\} + \frac{G_F}{\sqrt{2}}V_{cb}V_{cd}^* \frac{1}{\sqrt{6}} \left\{ \mathcal{M}_{1c}^{i(a)} + \mathcal{M}_{1c}^{i(b)}(Q_d) + \mathcal{M}_{2c}^i \right\} \\
&\quad - \frac{G_F}{\sqrt{2}}V_{tb}V_{td}^* \frac{1}{\sqrt{6}} \left\{ \mathcal{M}_{7\gamma}^i + \mathcal{M}_{8g}^{i(a)} + \mathcal{M}_{8g}^{i(b)}(Q_d) \right. \\
&\quad \left. + \mathcal{M}_{ann}^{i(a,LL)}(2a_3 + a_4 + 2a_5 + \frac{1}{2}a_7 + \frac{1}{2}a_9 - \frac{1}{2}a_{10}, Q_d) \right. \\
&\quad \left. + \mathcal{M}_{ann}^{i(b,LL)}(a_3 + a_9, Q_u, Q_u) + \mathcal{M}_{ann}^{i(b,LR)}(a_5 + a_7, Q_u, Q_u) \right. \\
&\quad \left. + \mathcal{M}_{ann}^{i(b,LL)}(a_3 + a_4 - \frac{1}{2}a_9 - \frac{1}{2}a_{10}, Q_d, Q_d) + \mathcal{M}_{ann}^{i(b,LR)}(a_5 - \frac{1}{2}a_7, Q_d, Q_d) \right. \\
&\quad \left. + \mathcal{M}_{ann}^{i(SP)}(a_6 - \frac{1}{2}a_8, Q_d, Q_d) - 2\mathcal{M}_{ann}^{i(a,LL)}(a_3 + a_5 - \frac{1}{2}a_7 - \frac{1}{2}a_9, Q_s) \right. \\
&\quad \left. - 2\mathcal{M}_{ann}^{i(b,LL)}(a_3 - \frac{1}{2}a_9, Q_s, Q_s) - 2\mathcal{M}_{ann}^{i(b,LR)}(a_5 - \frac{1}{2}a_7, Q_s, Q_s) \right\}, \tag{C16}
\end{aligned}$$

$$\begin{aligned}
\sqrt{2}\mathcal{A}^i(\bar{B}^0 \rightarrow f_1\gamma) = & \frac{G_F}{\sqrt{2}}V_{ub}V_{ud}^*\frac{1}{\sqrt{3}}\left\{\mathcal{M}_{ann}^{i(a,LL)}(a_2, Q_d) + \mathcal{M}_{ann}^{i(b,LL)}(a_2, Q_u, Q_u) + \mathcal{M}_{1u}^{i(a)}\right. \\
& + \mathcal{M}_{1u}^{i(b)}(Q_d) + \mathcal{M}_{2u}^i\left.\right\} + \frac{G_F}{\sqrt{2}}V_{cb}V_{cd}^*\frac{1}{\sqrt{3}}\left\{\mathcal{M}_{1c}^{i(a)} + \mathcal{M}_{1c}^{i(b)}(Q_d) + \mathcal{M}_{2c}^i\right\} \\
& - \frac{G_F}{\sqrt{2}}V_{tb}V_{td}^*\frac{1}{\sqrt{3}}\left\{\mathcal{M}_{7\gamma}^i + \mathcal{M}_{8g}^{i(a)}\right. \\
& + \mathcal{M}_{8g}^{i(b)}(Q_d) + \mathcal{M}_{ann}^{i(a,LL)}(2a_3 + a_4 + 2a_5 + \frac{1}{2}a_7 + \frac{1}{2}a_9 - \frac{1}{2}a_{10}, Q_d) \\
& + \mathcal{M}_{ann}^{i(b,LL)}(a_3 + a_9, Q_u, Q_u) + \mathcal{M}_{ann}^{i(b,LR)}(a_5 + a_7, Q_u, Q_u) \\
& + \mathcal{M}_{ann}^{i(b,LL)}(a_3 + a_4 - \frac{1}{2}a_9 - \frac{1}{2}a_{10}, Q_d, Q_d) + \mathcal{M}_{ann}^{i(b,LR)}(a_5 - \frac{1}{2}a_7, Q_d, Q_d) \\
& + \mathcal{M}_{ann}^{i(SP)}(a_6 - \frac{1}{2}a_8, Q_d, Q_d) + \mathcal{M}_{ann}^{i(a,LL)}(a_3 + a_5 - \frac{1}{2}a_7 - \frac{1}{2}a_9, Q_s) \\
& \left. + \mathcal{M}_{ann}^{i(b,LL)}(a_3 - \frac{1}{2}a_9, Q_s, Q_s) + \mathcal{M}_{ann}^{i(b,LR)}(a_5 - \frac{1}{2}a_7, Q_s, Q_s)\right\}, \quad (C17)
\end{aligned}$$

$$\begin{aligned}
\sqrt{2}\mathcal{A}^i(\bar{B}_s \rightarrow f_8\gamma) = & \frac{G_F}{\sqrt{2}}V_{ub}V_{us}^*\frac{1}{\sqrt{6}}\left\{\mathcal{M}_{ann}^{i(a,LL)}(a_2, Q_s) + \mathcal{M}_{ann}^{i(b,LL)}(a_2, Q_u, Q_u)\right\} \\
& - \frac{G_F}{\sqrt{2}}V_{tb}V_{ts}^*\frac{1}{\sqrt{6}}\left\{\mathcal{M}_{ann}^{i(a,LL)}(2a_3 + 2a_5 + \frac{1}{2}a_7 + \frac{1}{2}a_9, Q_s) \right. \\
& + \mathcal{M}_{ann}^{i(b,LL)}(a_3 + a_9, Q_u, Q_u) + \mathcal{M}_{ann}^{i(b,LR)}(a_5 + a_7, Q_u, Q_u) \\
& \left. + \mathcal{M}_{ann}^{i(b,LL)}(a_3 - \frac{1}{2}a_9, Q_d, Q_d) + \mathcal{M}_{ann}^{i(b,LR)}(a_5 - \frac{1}{2}a_7, Q_d, Q_d)\right\} \\
& + \frac{G_F}{\sqrt{2}}V_{ub}V_{us}^*\frac{-2}{\sqrt{6}}\left\{\mathcal{M}_{1u}^{i(a)} + \mathcal{M}_{1u}^{i(b)}(Q_s) + \mathcal{M}_{2u}^i\right\} \\
& + \frac{G_F}{\sqrt{2}}V_{cb}V_{cs}^*\frac{-2}{\sqrt{6}}\left\{\mathcal{M}_{1c}^{i(a)} + \mathcal{M}_{1c}^{i(b)}(Q_s) + \mathcal{M}_{2c}^i\right\} \\
& - \frac{G_F}{\sqrt{2}}V_{tb}V_{ts}^*\frac{-2}{\sqrt{6}}\left\{\mathcal{M}_{7\gamma}^i + \mathcal{M}_{8g}^{i(a)} + \mathcal{M}_{8g}^{i(b)}(Q_s) + \mathcal{M}_{ann}^{i(SP)}(a_6 - \frac{1}{2}a_8, Q_s, Q_s) \right. \\
& + \mathcal{M}_{ann}^{i(a,LL)}(a_3 + a_4 + a_5 - \frac{1}{2}a_7 - \frac{1}{2}a_9 - \frac{1}{2}a_{10}, Q_s) \quad (C18) \\
& \left. + \mathcal{M}_{ann}^{i(b,LL)}(a_3 + a_4 - \frac{1}{2}a_9 - \frac{1}{2}a_{10}, Q_s, Q_s) + \mathcal{M}_{ann}^{i(b,LR)}(a_5 - \frac{1}{2}a_7, Q_s, Q_s)\right\},
\end{aligned}$$

$$\begin{aligned}
\sqrt{2}\mathcal{A}^i(\bar{B}_s \rightarrow f_1\gamma) &= \frac{G_F}{\sqrt{2}}V_{ub}V_{us}^* \frac{1}{\sqrt{3}} \left\{ \mathcal{M}_{ann}^{i(a,LL)}(a_2, Q_s) + \mathcal{M}_{ann}^{i(b,LL)}(a_2, Q_u, Q_u) \right\} \\
&\quad - \frac{G_F}{\sqrt{2}}V_{tb}V_{ts}^* \frac{1}{\sqrt{3}} \left\{ \mathcal{M}_{ann}^{i(a,LL)}(2a_3 + 2a_5 + \frac{1}{2}a_7 + \frac{1}{2}a_9, Q_s) \right. \\
&\quad + \mathcal{M}_{ann}^{i(b,LL)}(a_3 + a_9, Q_u, Q_u) + \mathcal{M}_{ann}^{i(b,LR)}(a_5 + a_7, Q_u, Q_u) \\
&\quad + \mathcal{M}_{ann}^{i(b,LL)}(a_3 - \frac{1}{2}a_9, Q_d, Q_d) + \mathcal{M}_{ann}^{i(b,LR)}(a_5 - \frac{1}{2}a_7, Q_d, Q_d) \left. \right\} \\
&\quad + \frac{G_F}{\sqrt{2}}V_{ub}V_{us}^* \frac{1}{\sqrt{3}} \left\{ \mathcal{M}_{1u}^{i(a)} + \mathcal{M}_{1u}^{i(b)}(Q_s) + \mathcal{M}_{2u}^i \right\} \\
&\quad + \frac{G_F}{\sqrt{2}}V_{cb}V_{cs}^* \frac{1}{\sqrt{3}} \left\{ \mathcal{M}_{1c}^{i(a)} + \mathcal{M}_{1c}^{i(b)}(Q_s) + \mathcal{M}_{2c}^i \right\} \\
&\quad - \frac{G_F}{\sqrt{2}}V_{tb}V_{ts}^* \frac{1}{\sqrt{3}} \left\{ \mathcal{M}_{7\gamma}^i + \mathcal{M}_{8g}^{i(a)} + \mathcal{M}_{8g}^{i(b)}(Q_s) + \mathcal{M}_{ann}^{i(SP)}(a_6 - \frac{1}{2}a_8, Q_s, Q_s) \right. \\
&\quad + \mathcal{M}_{ann}^{i(a,LL)}(a_3 + a_4 + a_5 - \frac{1}{2}a_7 - \frac{1}{2}a_9 - \frac{1}{2}a_{10}, Q_s) \\
&\quad \left. + \mathcal{M}_{ann}^{i(b,LL)}(a_3 + a_4 - \frac{1}{2}a_9 - \frac{1}{2}a_{10}, Q_s, Q_s) + \mathcal{M}_{ann}^{i(b,LR)}(a_5 - \frac{1}{2}a_7, Q_s, Q_s) \right\}. \tag{C19}
\end{aligned}$$

For annihilation type decays, we have

$$\begin{aligned}
\sqrt{2}\mathcal{A}^i(\bar{B}_s \rightarrow a_1^0(1235)\gamma) &= \frac{G_F}{\sqrt{2}}V_{ub}V_{us}^* \left\{ \mathcal{M}_{ann}^{i(a,LL)}(a_2, Q_s) + \mathcal{M}_{ann}^{i(b,LL)}(a_2, Q_u, Q_u) \right\} \\
&\quad - \frac{G_F}{\sqrt{2}}V_{tb}V_{ts}^* \left\{ \mathcal{M}_{ann}^{i(a,LL)}(\frac{3}{2}a_7 + \frac{3}{2}a_9, Q_s) \right. \\
&\quad + \mathcal{M}_{ann}^{i(b,LL)}(a_3 + a_9, Q_u, Q_u) + \mathcal{M}_{ann}^{i(b,LR)}(a_5 + a_7, Q_u, Q_u) \\
&\quad \left. + \mathcal{M}_{ann}^{i(b,LL)}(-a_3 + \frac{1}{2}a_9, Q_d, Q_d) + \mathcal{M}_{ann}^{i(b,LR)}(-a_5 + \frac{1}{2}a_7, Q_d, Q_d) \right\}. \tag{C20}
\end{aligned}$$

Decay amplitudes of  $A^i(B \rightarrow K_1(1270)\gamma)$  and  $A^i(B \rightarrow K_1(1400)\gamma)$  (here  $B$  denotes  $\bar{B}_{u,d,s}$  and  $K_1$  denotes  $K_1^-(\bar{K}_1^0)$ ) can be obtained by:

$$A^i(B \rightarrow K_1(1270)\gamma) = \sin(\theta_K)A^i(B \rightarrow K_{1A}\gamma) + \cos(\theta_K)A^i(B \rightarrow K_{1B}\gamma), \tag{C21}$$

$$A^i(B \rightarrow K_1(1400)\gamma) = -\sin(\theta_K)A^i(B \rightarrow K_{1B}\gamma) + \cos(\theta_K)A^i(B \rightarrow K_{1A}\gamma). \tag{C22}$$

- 
- [1] For a review, see T. Hurth, Rev. Mod. Phys. **75**, 1159 (2003) [arXiv:hep-ph/0212304].
- [2] M. Misiak *et al.*, Phys. Rev. Lett. **98**, 022002 (2007) [arXiv:hep-ph/0609232].
- [3] E. Barberio *et al.* [Heavy Flavor Averaging Group (HFAG)], arXiv:hep-ex/0603003.
- [4] For a review on the present status, please see T. Hurth, Int. J. Mod. Phys. A **22**, 1781 (2007) [arXiv:hep-ph/0703226] and references therein.
- [5] L. Del Debbio, J. M. Flynn, L. Lellouch and J. Nieves [UKQCD Collaboration], Phys. Lett. B **416**, 392 (1998) [arXiv:hep-lat/9708008].

- [6] H. Y. Cheng, C. K. Chua and C. W. Hwang, Phys. Rev. D **69**, 074025 (2004) [arXiv:hep-ph/0310359].
- [7] H. Y. Cheng and C. K. Chua, Phys. Rev. D **69**, 094007 (2004) [arXiv:hep-ph/0401141].
- [8] P. Ball and R. Zwicky, Phys. Rev. D **71**, 014029 (2005) [arXiv:hep-ph/0412079].
- [9] M. Beneke, G. Buchalla, M. Neubert and C. T. Sachrajda, Phys. Rev. Lett. **83**, 1914 (1999) [arXiv:hep-ph/9905312].
- [10] C. W. Bauer, D. Pirjol and I. W. Stewart, Phys. Rev. Lett. **87**, 201806 (2001) [arXiv:hep-ph/0107002];  
C. W. Bauer, D. Pirjol and I. W. Stewart, Phys. Rev. D **65**, 054022 (2002) [arXiv:hep-ph/0109045].
- [11] Y. Y. Keum, H. n. Li and A. I. Sanda, Phys. Lett. B **504**, 6 (2001) [arXiv:hep-ph/0004004]; Phys. Rev. D **63**, 054008 (2001) [arXiv:hep-ph/0004173];  
C. D. Lu, K. Ukai and M. Z. Yang, Phys. Rev. D **63**, 074009 (2001) [arXiv:hep-ph/0004213].
- [12] S. Nandi and H. n. Li, Phys. Rev. D **76**, 034008 (2007) [arXiv:0704.3790 [hep-ph]].
- [13] B. H. Hong and C. D. Lu, Sci. China **G49**, 357 (2006) [arXiv:hep-ph/0505020].
- [14] H.-n Li, and S. Mishima, Phys. Rev. D **71**, 054025 (2005) [hep-ph/0411146]; H.-n. Li, Phys. Lett. B **622**, 63 (2005) [hep-ph/0411305].
- [15] A.V. Gritsan, Invited talk at 5th Flavor Physics and CP Violation Conference (FPCP 2007), Bled, Slovenia, 12-16 May 2007; arXiv:0706.2030 [hep-ex]
- [16] Y. Y. Keum, M. Matsumori and A. I. Sanda, Phys. Rev. D **72**, 014013 (2005) [arXiv:hep-ph/0406055].
- [17] C. D. Lu, M. Matsumori, A. I. Sanda and M. Z. Yang, Phys. Rev. D **72**, 094005 (2005) [Erratum-ibid. D **73**, 039902 (2006)] [arXiv:hep-ph/0508300].
- [18] Y. Li and C. D. Lu, Phys. Rev. D **74**, 097502 (2006) [arXiv:hep-ph/0605220].
- [19] A. Ali, G. Kramer, Y. Li, C. D. Lu, Y. L. Shen, W. Wang and Y. M. Wang, Phys. Rev. D **76**, 074018 (2007) [arXiv:hep-ph/0703162].  
C.D. Lu, Talk given at 4th International Workshop on the CKM Unitarity Triangle (CKM 2006), Nagoya, Japan, 12-16 Dec 2006 and talk given at 42nd Rencontres de Moriond on QCD and Hadronic Interactions, La Thuile, Italy, 17-24 Mar 2007, arXiv:0705.1782 [hep-ph]
- [20] T. Kurimoto, H. n. Li and A. I. Sanda, Phys. Rev. D **65**, 014007 (2002) [arXiv:hep-ph/0105003];  
C. D. Lu and M. Z. Yang, Eur. Phys. J. C **28**, 515 (2003) [arXiv:hep-ph/0212373].
- [21] K. Abe *et al.* [BELLE Collaboration], arXiv:hep-ex/0408138.
- [22] For a review, see G. Buchalla, A. J. Buras and M. E. Lautenbacher, Rev. Mod. Phys. **68**, 1125 (1996) [arXiv:hep-ph/9512380].
- [23] A. Ali, G. Kramer and C. D. Lu, Phys. Rev. D **58**, 094009 (1998) [arXiv:hep-ph/9804363].
- [24] H. n. Li and H. L. Yu, Phys. Rev. D **53**, 2480 (1996) [arXiv:hep-ph/9411308].
- [25] H. n. Li, Phys. Rev. D **66**, 094010 (2002) [arXiv:hep-ph/0102013].
- [26] H. n. Li and K. Ukai, Phys. Lett. B **555**, 197 (2003) [arXiv:hep-ph/0211272].
- [27] A. G. Grozin and M. Neubert, Phys. Rev. D **55**, 272 (1997) [arXiv:hep-ph/9607366].
- [28] M. Beneke and T. Feldmann, Nucl. Phys. B **592**, 3 (2001) [arXiv:hep-ph/0008255].
- [29] H. Kawamura, J. Kodaira, C. F. Qiao and K. Tanaka, Phys. Lett. B **523**, 111 (2001) [Erratum-ibid. B

- 536**, 344 (2002)] [arXiv:hep-ph/0109181].
- [30] W. M. Yao *et al.* [Particle Data Group], J. Phys. G **33**, 1 (2006).
- [31] P. Ball, G. W. Jones and R. Zwicky, Phys. Rev. D **75**, 054004 (2007) [arXiv:hep-ph/0612081].
- [32] V. M. Braun and A. Lenz, Phys. Rev. D **70**, 074020 (2004) [arXiv:hep-ph/0407282].
- [33] P. Ball and R. Zwicky, Phys. Lett. B **633**, 289 (2006) [arXiv:hep-ph/0510338].
- [34] P. Ball and R. Zwicky, JHEP **0604**, 046 (2006) [arXiv:hep-ph/0603232].
- [35] P. Ball and G. W. Jones, JHEP **0703**, 069 (2007) [arXiv:hep-ph/0702100].
- [36] K. C. Yang, JHEP **0510**, 108 (2005) [arXiv:hep-ph/0509337].
- [37] K. C. Yang, Nucl. Phys. B **776**, 187 (2007) [arXiv:0705.0692 [hep-ph]].
- [38] J. P. Lee, Phys. Rev. D **74**, 074001 (2006) [arXiv:hep-ph/0608087].
- [39] D. Becirevic, V. Lubicz and F. Mescia, Nucl. Phys. B **769**, 31 (2007) [arXiv:hep-ph/0611295].
- [40] C. D. Lu, W. Wang and Z. T. Wei, Phys. Rev. D **76**, 014013 (2007) [arXiv:hep-ph/0701265].
- [41] H. Y. Cheng and K. C. Yang, arXiv:0709.0137 [hep-ph].
- [42] A. Deandrea, R. Gatto, G. Nardulli and A. D. Polosa, Phys. Rev. D **59**, 074012 (1999) [arXiv:hep-ph/9811259].
- [43] D. Scora and N. Isgur, Phys. Rev. D **52**, 2783 (1995) [arXiv:hep-ph/9503486].
- [44] N. Isgur, D. Scora, B. Grinstein and M. B. Wise, Phys. Rev. D **39**, 799 (1989).
- [45] T. M. Aliev and M. Savci, Phys. Lett. B **456**, 256 (1999) [arXiv:hep-ph/9901395].
- [46] K. C. Yang, in preparation.
- [47] B. Aubert *et al.* [BABAR Collaboration], Phys. Rev. Lett. **98**, 181803 (2007) [arXiv:hep-ex/0612050].
- [48] M. Bander, D. Silverman and A. Soni, Phys. Rev. Lett. **43**, 242 (1979).
- [49] J. Liu and Y. P. Yao, Phys. Rev. D **42**, 1485 (1990).
- [50] H. Simma and D. Wyler, Nucl. Phys. B **344**, 283 (1990).
- [51] C. D. Lu, Y. L. Shen and W. Wang, Chin. Phys. Lett. **23**, 2684 (2006) [arXiv:hep-ph/0606092].
- [52] J. Charles *et al.* [CKMfitter Group], Eur. Phys. J. C **41**, 1 (2005) [arXiv:hep-ph/0406184].
- [53] H. n. Li and G. L. Lin, Phys. Rev. D **60**, 054001 (1999) [arXiv:hep-ph/9812508].
- [54] M. Beneke, T. Feldmann and D. Seidel, Eur. Phys. J. C **41**, 173 (2005) [arXiv:hep-ph/0412400].
- [55] S. W. Bosch and G. Buchalla, Nucl. Phys. B **621**, 459 (2002) [arXiv:hep-ph/0106081].
- [56] S. W. Bosch, arXiv:hep-ph/0208203.
- [57] T. Becher, R. J. Hill and M. Neubert, Phys. Rev. D **72**, 094017 (2005) [arXiv:hep-ph/0503263].
- [58] J. g. Chay and C. Kim, Phys. Rev. D **68**, 034013 (2003) [arXiv:hep-ph/0305033].
- [59] S. W. Bosch and G. Buchalla, JHEP **0501**, 035 (2005) [arXiv:hep-ph/0408231].
- [60] A. Ali and A. Y. Parkhomenko, Eur. Phys. J. C **23**, 89 (2002) [arXiv:hep-ph/0105302].
- [61] X. q. Li, G. r. Lu, R. m. Wang and Y. D. Yang, Eur. Phys. J. C **36**, 97 (2004) [arXiv:hep-ph/0305283].
- [62] A. Ali, E. Lunghi and A. Y. Parkhomenko, Phys. Lett. B **595**, 323 (2004) [arXiv:hep-ph/0405075].
- [63] A. Ali and A. Parkhomenko, arXiv:hep-ph/0610149.
- [64] A. Ali, B. D. Pecjak and C. Greub, arXiv:0709.4422 [hep-ph].

- [65] A. V. Manohar and I. W. Stewart, Phys. Rev. D **76**, 074002 (2007) [arXiv:hep-ph/0605001].
- [66] B. Aubert *et al.* [BABAR Collaboration], Phys. Rev. D **70**, 112006 (2004) [arXiv:hep-ex/0407003].
- [67] M. Nakao *et al.* [BELLE Collaboration], Phys. Rev. D **69**, 112001 (2004) [arXiv:hep-ex/0402042].
- [68] T. E. Coan *et al.* [CLEO Collaboration], Phys. Rev. Lett. **84**, 5283 (2000) [arXiv:hep-ex/9912057].
- [69] A. Drutskoy, arXiv:0710.1647 [hep-ex].
- [70] B. Aubert *et al.* [BABAR Collaboration], Phys. Rev. Lett. **98**, 151802 (2007) [arXiv:hep-ex/0612017].
- [71] K. Abe *et al.*, Phys. Rev. Lett. **96**, 221601 (2006) [arXiv:hep-ex/0506079].
- [72] M. Nakao, *et. al.*, Belle Collaboration, Phys. Rev. D **69**, 112001 (2004); B. Aubert, *et al.*, BaBar collaboration, Phys. Rev. D **70**, 112006 (2004)
- [73] M. Beneke, G. Buchalla, C. Greub, A. Lenz and U. Nierste, Phys. Lett. B **459**, 631 (1999) [arXiv:hep-ph/9808385]; A. Lenz and U. Nierste, JHEP **0706**, 072 (2007) [arXiv:hep-ph/0612167].
- [74] Y. Ushiroda *et al.*, Phys. Rev. Lett. **94**, 231601 (2005) [arXiv:hep-ex/0503008].
- [75] B. Aubert *et al.* [BABAR Collaboration], arXiv:0708.1614 [hep-ex].
- [76] Y. Ushiroda *et al.* [BELLE Collaboration], arXiv:0709.2769 [hep-ex].
- [77] J. M. Soares, Nucl. Phys. B **367**, 575 (1991).
- [78] M. Gronau, Phys. Lett. B **492**, 297 (2000) [arXiv:hep-ph/0008292].
- [79] T. Hurth and T. Mannel, Phys. Lett. B **511**, 196 (2001) [arXiv:hep-ph/0103331].
- [80] H. n. Li and S. Mishima, Phys. Rev. D **74**, 094020 (2006) [arXiv:hep-ph/0608277].
- [81] Y. J. Kwon and J. P. Lee, Phys. Rev. D **71**, 014009 (2005) [arXiv:hep-ph/0409133].
- [82] M. Jamil Aslam and Riazuddin, Phys. Rev. D **72**, 094019 (2005) [arXiv:hep-ph/0509082].
- [83] M. J. Aslam, Eur. Phys. J. C **49**, 651 (2007) [arXiv:hep-ph/0604025].
- [84] M. Jamil Aslam and Riazuddin, Phys. Rev. D **75**, 034004 (2007) [arXiv:hep-ph/0607114].
- [85] H. n. Li, Prog. Part. Nucl. Phys. **51**, 85 (2003) [arXiv:hep-ph/0303116];  
C. D. Lu, Mod. Phys. Lett. A **22**, 615 (2007) [arXiv:0706.0589 [hep-ph]].